APPLICATION OF CONJUGATED POLYMERS IN CHEMICAL AND BIOLOGICAL DETECTIONS

REN XINSHENG

NATIONAL UNIVERSITY OF SINGAPORE

2010

APPLICATION OF CONJUGATED POLYMERS IN CHEMICAL AND BIOLOGICAL DETECTIONS

REN XINSHENG

(B. SC., Shandong University, China)

A THESIS SUBMITTED

FOR THE DEGREE OF DOCTOR OF PHILOSOPHY

DEPARTMENT OF CHEMISTRY

NATIONAL UNIVERSITY OF SINGAPORE

2010

Acknowledgements

At this point of my academic career, there are many people I want to acknowledge.

First, I wish to express my gratitude to my supervisor, Dr. Xu Qing-Hua for his expert guidance, unselfish support and kind encouragement during these years.

I would also like to acknowledge the invaluable help from all the former and current members of Dr. Xu' group. The friendships from them make my memory of an enjoyable and unforgettable one.

I wish to express my heartful gratitude to my family, without their unconditional love and support, I could never have achieved this goal. I deeply thank my husband, Chen Haibin, for his love, support, patience, care, encouragement and understanding.

Last but not least, my acknowledgement goes to National University of Singapore for awarding me the research scholarship and for providing the facilities to carry out the research work reported herein.

Table of Contents

Summary

Conjugated polymers (CPs) are known to provide an advantage of collective optical response. Compared to small molecule counterparts, the electronic structure of the CPs coordinates the action of a large number of absorbing units. The excitation energy can migrate along the polymer backbone before transferring to the chromophore reporter and results in an amplification of fluorescent signals. CPs can be used as the optical platforms to develop highly sensitive chemical and biological sensors. Different schemes using conjugated polymers have been proposed to detect DNA, RNA, protein and metal ions.

CPs are also known to have large two-photon absorption cross-sections compared to the small molecule counterpart. In Chapter 2, we have investigated enhanced two-photon excitation fluorescence of drug molecule by FRET using two different conjugated polymers. CPs can be utilized to act as a two-photon excitation light harvesting complex and transfer the harvested energy to the drug molecules, which can significantly enhance the drug efficiency in two-photon excitation phototherapy.

In Chapter 3, by using CPs and a DNA intercalator, a scheme for label free DNA sequence detection was introduced. The detection sensitivity could be significantly improved through FRET from CPs, taking advantage of its collective optical response and optical amplification effects. The selectivity has also been significantly improved due to the addition of cationic conjugated polymers. The single nucleotide mismatch detection can be detected even at the room temperature.

In Chapter 4, a practical scheme for high sensitivity and selectivity mercury ions detection was presented by using a combination of oligonucleotides, DNA intercalators and CPs. The detection limit of sub-nM can be easily reached using this method. It works in a "mix-and-detect" manner and takes only a few minutes to complete the detection. This scheme could also be used as a two-photon sensor for detection of mercury ions deep into the biological environments with high sensitivity.

Most DNA based nanodevices were driven by DNA/RNA strands, acids/bases, enzymes and light. The visualization of the DNA conformational change is usually based on fluorescence signal change, in which the oligonucleotide needs to be labeled with fluorescent molecules. In Chapter 5, we developed a label free method using a water soluble polythiophene derivative PMNT to visualize the conformational switch of i-motif DNA driven by the environmental pH change. The DNA conformational switch was companied by a solution color change, which can be directly visualized by naked. The pH dependent fluorescence signal can undergo reversibly for many cycles. This i-DNA/PMNT complex could act as an environmentally friendly optical switch with a fast response.

The DNA cleavages catalyzed by nucleases are involved in many important biological processes such as replication, recombination and repair. Traditional methods have drawbacks such as being time-consuming, laborious and require substrate to be labeled. In Chapter 6, we demonstrated a label-free method for the S1 nuclease cleavage of single-stranded DNA based on CPs/DNA/intercalating dye system based on FRET. Nuclease assay based on FRET technique can provide us with a ratiometric fluorescence approach.

List of Publications

1. X.S. Ren, F. He and Q.-H. Xu, "Direct Visualization of Conformational Switch of i-Motif DNA with a Cationic Conjugated Polymer", Chemistry, an Asian Journal, 2010, 5(5), 1094-1098.

2. X.J. Zhang, X.S. Ren, Q.-H. Xu, K.P. Loh and Z.K. Chen, "One- and Two-Photon Turn-on Fluorescent Probe for Cysteine and Homocysteine with Large Emission Shift", Organic Letters, 2009, 11(6), 1257.

3. X.S. Ren and Q.-H. Xu, "Label Free DNA Sequence Detection with Enhanced Sensitivity and Selectivity using Cationic Conjugated Polymers and PicoGreen", Langmuir, 2009, 25(1), 43-47.

4. X.S. Ren and Q.-H. Xu, "Highly Sensitive and Selective Detection of Mercury Ions by Using Oligonucleotides, DNA Intercalators and Conjugated Polymers", Langmuir, 2009, 25(1), 29-31.

List of Tables

List of Figures

List of Schemes

Chapter 1

Introduction

1.1 Conjugated Polymers

Conjugated polymers (CPs) have emerged as one of the most important classes of transduction materials. They readily transform a chemical signal into an easily measured electrical or optical event. The discovery of conductive polymers garnered Heeger, Shirikawa, and MacDiarmid the Nobel Prize for Chemistry in 2000 (1, 2). These new materials contain a backbone with a continuous π-system. This kind of polymers have been widely used in light-emitting diodes (LEDs) (3-5), light-emitting electrochemical cells (LECs) (6-9), field effect transistors (FETs) (10), batteries (11, 12), biomaterials (13, 14), sensors (15, 16) etc. Some common conjugated polymer backbones are shown in Figure 1.1.

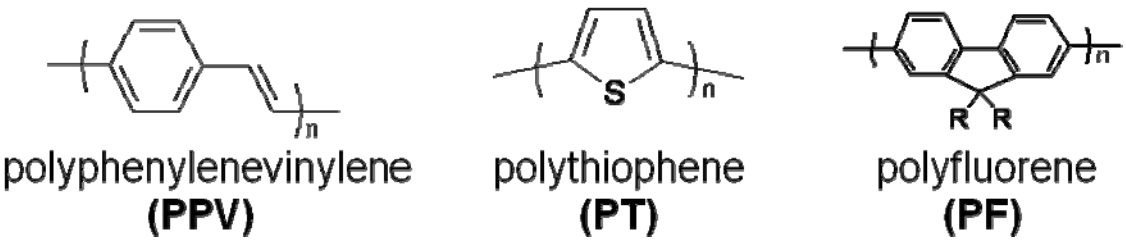

Figure 1.1 Backbone structures of several common conjugated polymers.

Conjugated polymers are characterized by a delocalized electronic structure and can be used as highly responsive optical reporters for chemical and biological targets (17-19). The backbone of CPs serves to hold a series of conjugated segments in close proximity. Thus, CPs are efficient for light harvesting and enable optical amplification via Förster resonance energy transfer (FRET) (17, 18, 20). A major advantage of these sensory materials is their ability to produce signal gained in response to interactions with analysts. This has led to them being referred to as amplifying fluorescent polymers. In analogy to microelectronic devices, the increased sensitivity (amplification) is derived from the ability of a conjugated polymer to serve as a highly efficient transport medium. But unlike a silicon circuit, which transports electrons or holes, amplifying fluorescent polymers transport excitation energy. The excitation energy is usually delocalized in conjugated polymers. These delocalized excited states are usually referred as excitons. Although structural disorder causes the effective localization length (conjugation length) to be significantly shorter than the actual chain length, excitons in conjugated polymers are highly mobile and can diffuse throughout an isolated polymer chain by mechanisms that involve both through space dipolar couplings and strong mixing of electronic states. Conjugated polymers also contain lots of π system and thus have good linear and nonlinear optical properties, which will be discussed later.

1.2 Conjugated Polymers as Light Harvesting Materials

Conjugated polymers are known to display capability of collective response, such as optical amplification through resonance energy transfer. The reason for such optical amplification is that conjugated polymers are long polymer chains made of many repetitive units. No matter where the polymer is excited, the excitation energy will

migrate along the polymer chain until it transfers its energy to the nearby acceptors (Scheme 6.1). The conjugated polymers thus actually act as the energy antennas, which enables the acceptors to collect the excitation energy harvested by the entire polymer chain. When the acceptor is indirectly excited by FRET, its fluorescence intensity could be much larger than that when the acceptor is directly excited at its absorption maximum. This exceptional property has been widely utilized to develop chemical and biological sensors with enhanced detection efficiency. So far many different sensors have been developed to detect DNA, RNA, metal ions and hazardous chemical species (21-23).

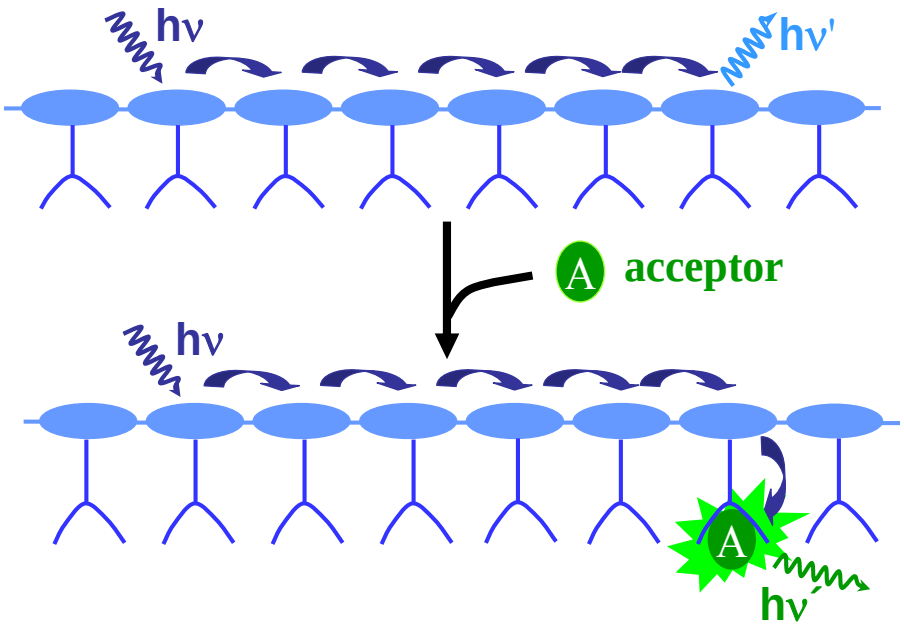

Scheme 1.1 Conjugated polymers as light harvesting complex for optical amplification by fluorescence resonance energy transfer

Conjugated polymers have been demonstrated to act as one-photon and two-photon light harvesting materials to achieve enhanced (one-photon excitation or two-photon excitation) fluorescence efficiency. We will take advantage of these

unique properties to explore their potential applications in biological and chemical sensing as well as phototherapy. We will also use various optical spectroscopy and imaging techniques to understand the working principles and dynamical processes in these applications.

1.3 Fluorescence and Energy Transfer

Fluorescence technology is widely used for a variety of investigations in many disciplines because of its high sensitivity, nondestructive nature, and multiplexing capabilities, such as biochemical, medical, and chemical research. Fluorescence is the emission of electromagnetic radiation light by a substance that has absorbed radiation of a different wavelength (Figure 1.2). The emission rates of fluorescence are typically 10^8 s^{-1}, so that a typical fluorescence lifetime is around 10 ns. And the lifetime (τ) of a fluorophore is the average time between its excitation state and its return to the ground state. It is reasonable to consider a 1 ns lifetime within the context of the light speed. Light travels 30 cm or about one foot in 1ns. Many fluorophores display subnanosecond lifetimes. Because fluorescence lifetime is very sensitive to the molecular structure and environments, measurement of the time-resolved fluorescence is widely practiced because of the increased information available from the data, as compared with stationary or steady-state measurements.

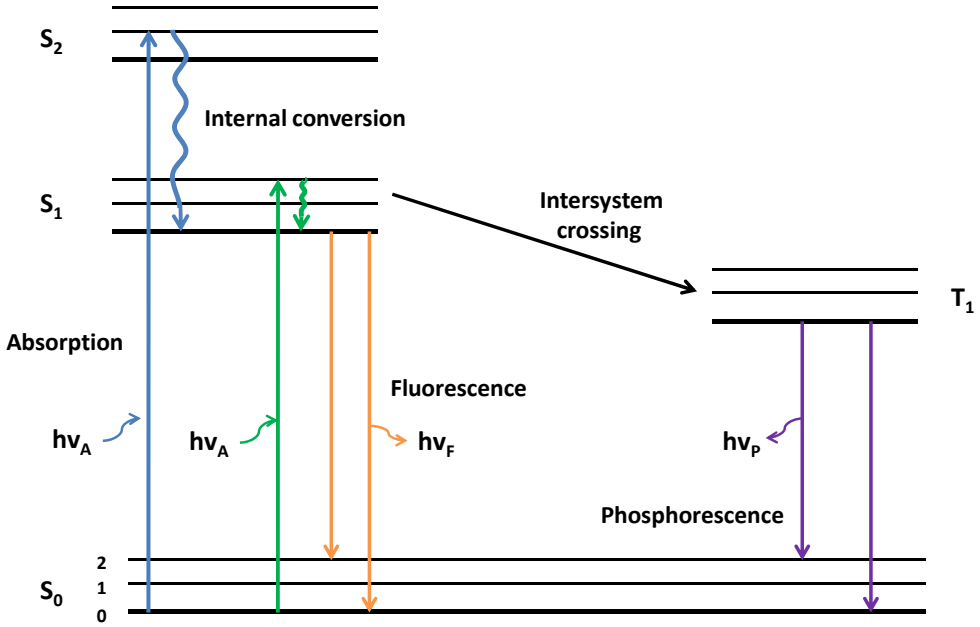

Figure 1.2 Jablonski energy diagram

In the presence of another molecule, the excitation energy of the fluorescent molecules could be transferred to another nearby molecules which will emit the light instead. This phenomenon is called energy transfer.

A typical energy transfer process is called Förster resonance energy transfer (FRET). FRET is a nonradiative process whereby an excited state donor D transfers energy to a proximal ground state acceptor A through long-range dipole–dipole

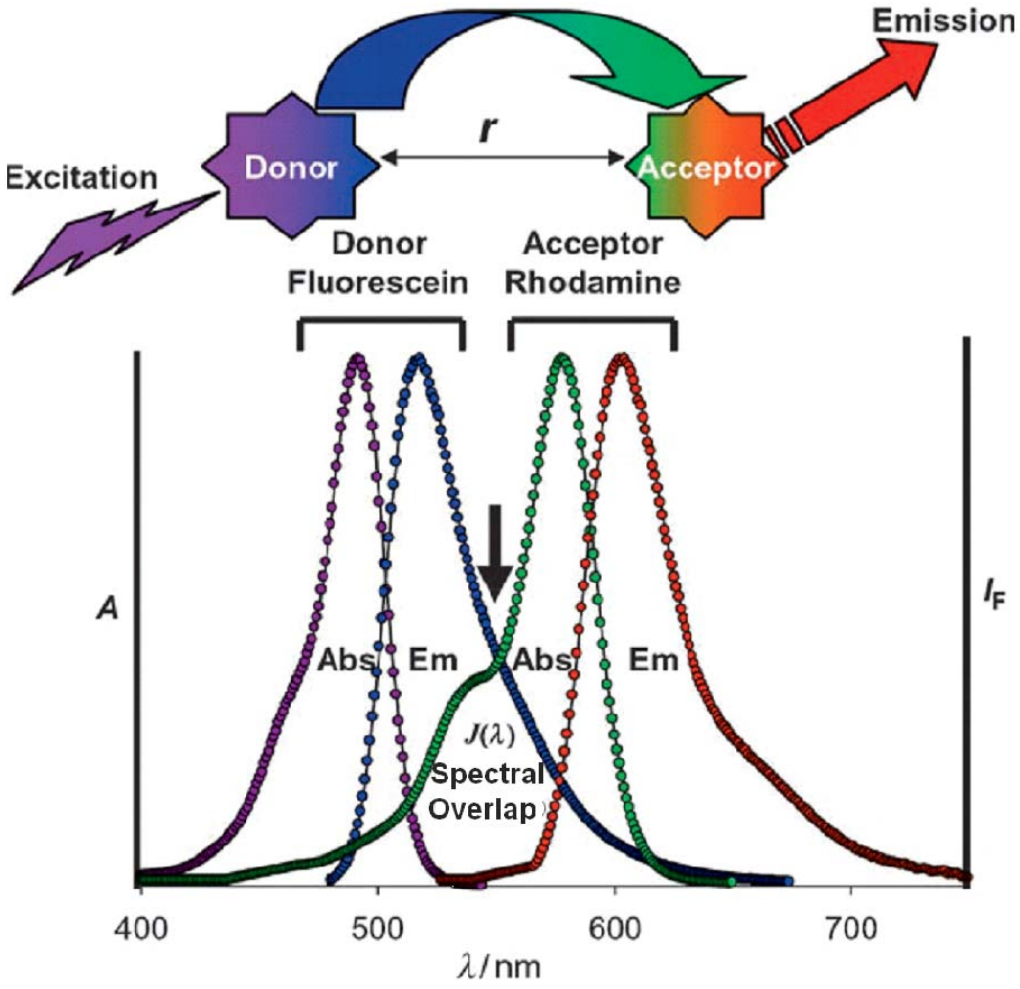

Figure 1.3 Förster Resonance Energy Transfer

interactions (Figure 1.3) (24). The rate of energy transfer is highly dependent on spectral overlap between the emission of donor and absorption of the acceptor, the relative orientation of the transition dipoles, and, most importantly, the distance between the donor and acceptor molecules (24). FRET usually occurs over distances of about 10 to 100 Å. The theoretical treatment of energy transfer between a single linked D/A pair separated by a fixed distance r was originally proposed by Förster (22, 24, 25). The energy transfer rate $k_T(r)$ between a single D/A pair is dependent on the distance r between D and A and can be expressed in terms of the Förster distance R_0.

R_0 is the distance between D and A at which 50% of the excited D molecules decay by energy transfer, while the other half decay through other radiative or nonradiative channels. R_0 can be calculated from the spectral properties of the D and A species (*eq 1.1*).

$$R_0 = 9.78 \times 10^3 [\kappa^2 n^{-4} Q_D J(\lambda)]^{1/6} \text{ (in Å)} \qquad \text{(eq 1.1)}$$

The factor κ^2 describes the D/A transition dipole orientation and can range in value from 0 (perpendicular) to 4 (collinear/parallel). The accumulated evidence has shown that the mobility and statistical dynamics of the dye linker lead to a κ^2 value of approximately 2/3 in almost all biological formats. This also sets an upper error limit of 35% on any calculated distance (21, 23, 24). The refractive index n of the medium is ascribed a value of 1.4 for biomolecules in aqueous solution. Q_D is the quantum yield (QY) of the donor in the absence of the acceptor and $J(\lambda)$ is the overlap integral, which represents the degree of spectral overlap between the donor emission and the acceptor absorption. The values for $J(\lambda)$ and R_0 increase with higher acceptor extinction coefficients and greater overlap between the donor emission spectrum and the acceptor absorption spectrum. Whether FRET will be effective at a particular distance r can be estimated by the "rule of thumb" $R_0 \pm 50\% R_0$ for the upper and lower limits of the Förster distance (21). The efficiency of the energy transfer can be determined from either steady-state (*eq 1.2*) or time-resolved (*eq 1.3*) measurements.

$$E = 1 - F_{DA}/F_D \qquad \text{(eq 1.2)}$$

$$E = 1 - \tau_{DA}/\tau_{D} \quad \text{(eq 1.3)}$$

F is the relative donor fluorescence intensity in the absence (F_D) and presence (F_{DA}) of the acceptor, and t is the fluorescent lifetime of the donor in the absence (τ_D) and presence (τ_{DA}) of the acceptor. FRET is very useful for bioanalysis because of its intrinsic sensitivity to nanoscale changes in D/A separation distance (proportional to r^6). This property has been used in FRET techniques ranging from the assay of interactions of an antigen with an antibody *in vitro* to the real-time imaging of protein folding *in vivo* (26, 27). The myriad FRET configurations and techniques currently in use are covered in many reviews (28, 29).

FRET has been employed to develop CPs based biosensors with enhanced detection efficiency (17-20, 30-41). Conjugated polymers are composed of many repetitive units. The excitation energy can migrate along the polymer chain before it is quenched via electron transfer to a nearby quencher (31, 42-44) or before the excitation energy is transferred to a nearby acceptor (17, 45-47). They can function as light harvesting materials and exhibit enhanced quenching efficiency by electron transfer or optical amplification via FRET (15, 17, 22, 48). These exceptional properties make conjugated polymers very useful in developing various sensory schemes to detect biological and chemical molecules with high sensitivity (15, 17, 48, 49).

1.4 Two-Photon Absorption

Two-photon absorption (TPA) is the simultaneous absorption of two photons by an

atom or molecule in the same quantum event. The energy of a photon is inversely proportional to its wavelength as $E = hc/\lambda$. The energy of a photon at a particular wavelength would then be equal to the sum of the energy of 2 photons at twice of that wavelength. For example, a molecule absorbing a photon whose wavelength is 400 nm can be excited by absorbing 2 photons of wavelength 800nm simultaneously.

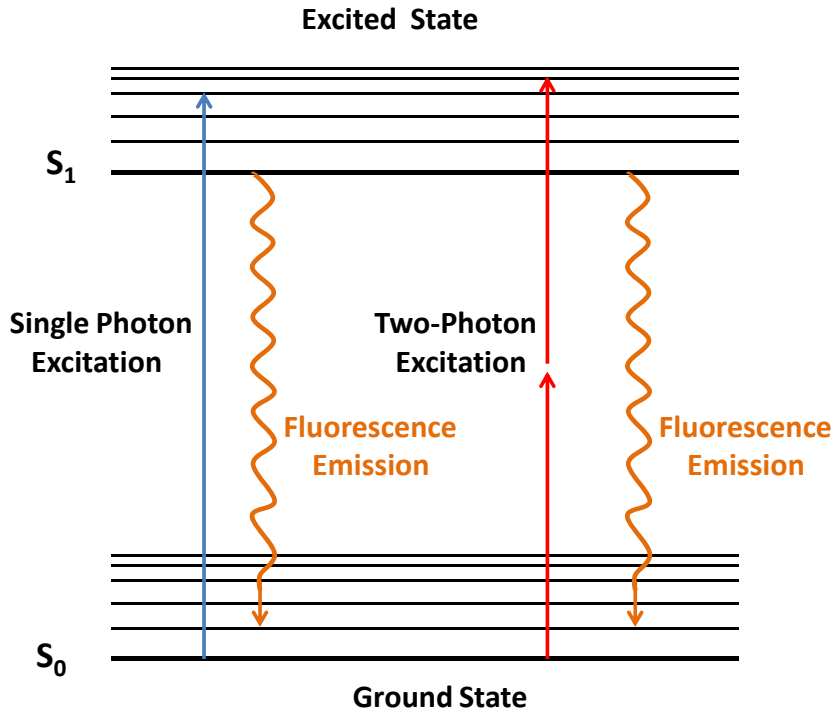

Figure 1.4 Jablonski Energy Diagram for Two Photon Absorption

This theoretical concept of exciting a molecule or atom by the simultaneous absorption of two photons in the same quantum event was first predicted by Maria Goppert-Mayer in 1931. For two-photon absorption to occur, an atom or molecule must first be excited by a photon to an intermediate virtual state of higher energy as shown in Figure 1.4.

Two-photon absorption usually requires the light with very high intensity, something that was a mere fantasy until the invention of lasers in the 1960s. In 1961, two-photon absorption was experimentally verified by Kaiser and Garret with the two-photon excitation of $CaF_2:Eu^{2+}$ crystal using pulsed lasers with very high intensity (50). Two-photon absorption spectroscopy was then used to study the electronic structure of molecular excited states due to the difference in selection rules with those of one-photon absorption (51).

Besides selection rules, another difference between two-photon and one-photon absorption is that in one-photon absorption, the rate of the absorption is directly proportional to the light intensity. In contrast, two-photon absorption is proportional to the square of the light intensity, which is otherwise known as the power-squared dependence of two-photon excitation, thus two-photon absorption happens only when the light density is very high. This quadratic dependence of the transition probability on the laser light intensity allows us to achieve three-dimensional (3D) spatial resolution for two-photon induced chemical or physical processes in materials. For a tightly focused laser beam, the intensity is maximal at the focus and it decreases quadratically with the distance (z) from the focal plane (the plane that is perpendicular to the axis of a lens and passes through the focal point) in the beam direction, for distances larger than the Rayleigh length. Therefore, the probability of which two-photon materials are excited therefore decreases very rapidly with the distance (as z^{-4}) from the focal plane. This, together with the exponential distribution of the intensity within the focal plane, confines

two-photon excitation in a small volume around the focus. In addition, the one-photon absorption of a material is typically weak in the wavelength range where two-photon absorption occurs, which allows exciting the material at a greater depth than that is possible with one-photon excitation. Furthermore, because the wavelength used for two-photon excitation is roughly twice that for one-photon excitation, the loss of the light intensity due to scattering is reduced by about a factor of 16. Since Rayleigh Scattering cross section α is proportional to $(1/\lambda)^4$ (52), using near-IR light at higher λ in two-photon excitation would result in much less scattering, thus resulting in a high-resolution 3D imaging with increased penetration depth as compared to one-photon excitation using UV light. Two-photon absorption is thus particularly useful when used in biological specimens, since most biological tissues experience much lower absorption in the near-IR region than in the UV region.

Since conjugated polymers have large two-photon absorption cross-sections compared to the small molecule counterparts (42, 43, 46, 47), our group have reported enhanced two-photon excitation fluorescence by FRET from a cationic conjugated polymer to a DNA intercalater. The fluorescence intensity of the DNA intercalator by two-photon excitation FRET (TPE-FRET) was found to be enhanced by a factor of over 35, compared to that when the intercalator is directly excited by two-photon absorption (53). This observation is of particular interest to phototherapy. DNA is the molecular target for many of the drugs that are used in cancer therapeutics (45). Two-photon excitation phototherapy has advantages over the one-photon counterpart by offering the advantages: a) the ability to work with a smaller more confined

treatment area; and b) the ability to treat deeper into diseased tissues. However, conventional drugs in clinical use usually have very small two-photon cross sections and their efficiencies are limited. Conjugated polymers can be utilized to act as a two-photon excitation light harvesting complex and transfer the harvested energy to the drug molecules, which can significantly enhance the drug efficiency in two-photon excitation phototherapy.

1.5 Time-Resolved Fluorescence Spectroscopy

Time-resolved spectroscopy is a useful tool to study dynamical processes in chemical or materials systems. In principle, this technique can be applied to any process that leads to a change in optical properties of a material. With the help of pulsed laser, it is possible to study processes which occur on time scales as short as 10^{-14} seconds.

Time-resolved fluorescence spectroscopy is an extension of fluorescence spectroscopy. The fluorescence of a sample is monitored as a function of time after excitation by a flash of light. Time-resolved fluorescence provides more information about the molecular environment of the fluorophore than steady-state fluorescence measurements. Time-resolved measurements are very useful in studying fluorescence quenching, because one can readily distinguish static and dynamic quenching. Formation of static ground-state complexes does not decrease the decay time because only the unquenched fluorephores are observed in a fluorescence experiment. Dynamic quenching is a rate process acting on the entire excited-state population and thus decreases the mean decay time of the excited-state population. Since the

fluorescence lifetime of a molecule is very sensitive to its molecular environment, measurement of the fluorescence lifetime(s) reveals much about the state of the fluorophore. Many macromolecular events, such as rotational diffusion, resonance energy transfer, and dynamic quenching, occur on the same time scale as the fluorescence decay. Thus, time-resolved fluorescence spectroscopy can be used to investigate these processes and gain insight into the chemical surroundings of the fluorophore.

It is important to remember that the fluorescence lifetime is an average time for a molecule to remain in the excited state before emitting a photon (24). Each individual molecule emits randomly after excitation. Many excited molecules will fluoresce before the average lifetime, but some will also fluoresce long after the average lifetime. Fluorescence lifetimes are generally on the order of 1-10 ns, although they can range from hundreds of nanoseconds to the sub-nanosecond time scale.

1.6 Introduction to Biosensor

A biosensor can be described as "an analytical device that contains a biologically active component that mediates a quantifiable chemical reaction or interaction" (54). It consists of 3 parts: 1) the sensitive biological element (biological materials such as tissue, microorganisms, organelles, cell receptors, enzymes, antibodies, nucleic acids, etc), 2) the transducer or the detector element (works in a physicochemical way; optical, piezoelectric, electrochemical, etc.) that transforms the signal resulting from

the interaction of the analyte with the biological element into another signal (i.e., transducers) that can be more easily measured and quantified, 3) associated electronics or signal processors that are primarily responsible for the display of the results in a user-friendly way. The first biosensor was demonstrated by Clark and Lyons in 1962 (55). They reported an 'enzyme electrode' using glucose oxidase as a selective biorecognition molecular for glucose. The enzyme was held next to a platinum electrode in a membrane sandwich. The Pt electrode responses to hydrogen peroxide produced by the enzyme-catalyzed reaction (*eq 1.4*).

$$\text{Glucose} + O_2 \xrightarrow{\text{glucose oxidase}} \text{Gluconic acid} + H_2O_2 \qquad \text{(eq 1.4)}$$

1.7 Optical Biosensor based on Conjugated Polymers

Conjugated polymers are great alternatives to the conventional fluorescence dyes as signaling reporters in biosensor design. External agents are able to perturb important properties of conjugated materials, such as conductivity, emission quantum yield, and exciton migration (15, 16). Conjugated polymers are often more sensitive in this respect, compared to their small molecule counterparts. These properties make conjugated polymer a good candidate for the transducer.

Several sensing mechanisms based on conjugated polymers have been developed: quenching-recovery mechanism, conformation change mechanism and Förster resonance energy transfer mechanism. Conjugated polymers can provide signal amplification through efficient energy harvesting and energy transfer in all of

these detection modes. Therefore, the sensory system based on CPs is highly sensitive and can be used to detect a trace amount of analyte, including small biomolecules, nucleic acids and various proteins.

Quenching-recovery mechanism takes the advantage of the superquenching property of conjugated polymers by electron or energy accepting quenchers. Whitten and co-workers reported fluorescence quenching and recovery of poly(2-methoxy-5-propyloxy sulfonate phenylene vinylene) in conjugation of biotin-dimethyl viologen and avidin in water (56). In the absence of avidin, the small biotin group in B-MV would not hinder association of the viologen portion of B-MV with conjugated polymers, and thus the conjugated polymer would result in strong fluorescence quenching. But in the presence of avidin, the avidin can bind with the biotin group in B-MV and thus preventing close association of MV with conjugated polymer, therefore, the fluorescence was recovered (Scheme1.2) (56).

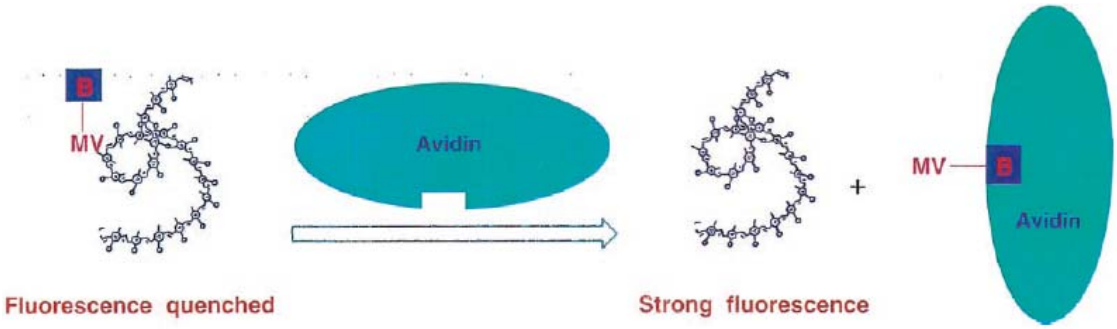

Scheme1.2 conjugated polymer -based biosensor developed by Whitten *et al*

Conformation change mechanism based on the conformational change of the polymers backbone, for example, the conjugation length change (41, 57, 58). These

mechanism based biosensors mainly use the water soluble polythiophene derivatives as the signal transduction. Leclerc and co-workers pioneered DNA detection with conjugated polymers based on the electrostatic attraction between a cationic polythiophene and DNA (57). In 2002, Leclerc found that the water soluble imidazolium-substituted poly(thiophene) was highly sensitive and selective to the presence of oligonucleotides (Scheme1.3) (57).

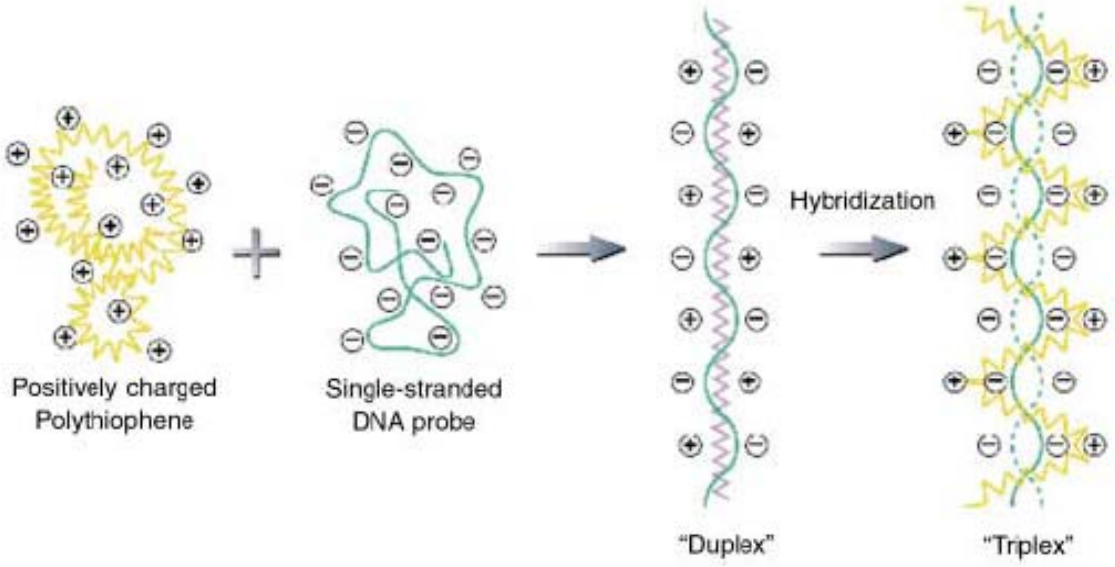

Scheme 1.3. Schematic description of the formation of polythiophene/single-stranded nucleic acid duplex and polythiophene/hybridized nucleic acid triplex forms.

Fluorescence resonance energy transfer mechanism was developed by Bazan, Heeger and co-workers (17-20). This method is relied on the amplified FRET from the CPs to a small chromophore. Conjugated polymers have high extinction coefficients stemming from their delocalized backbone. In addition, the generated excitons can migrate along the polymer chain from which FRET is efficient, resulting the optical amplification and increased sensitivity. Therefore, CPs have the potential to be excellent energy donors in FRET based sensing scheme. In 2002, Gaylord,

Bazan, and Heeger reported an example of DNA detection by FRET using CPs (17).

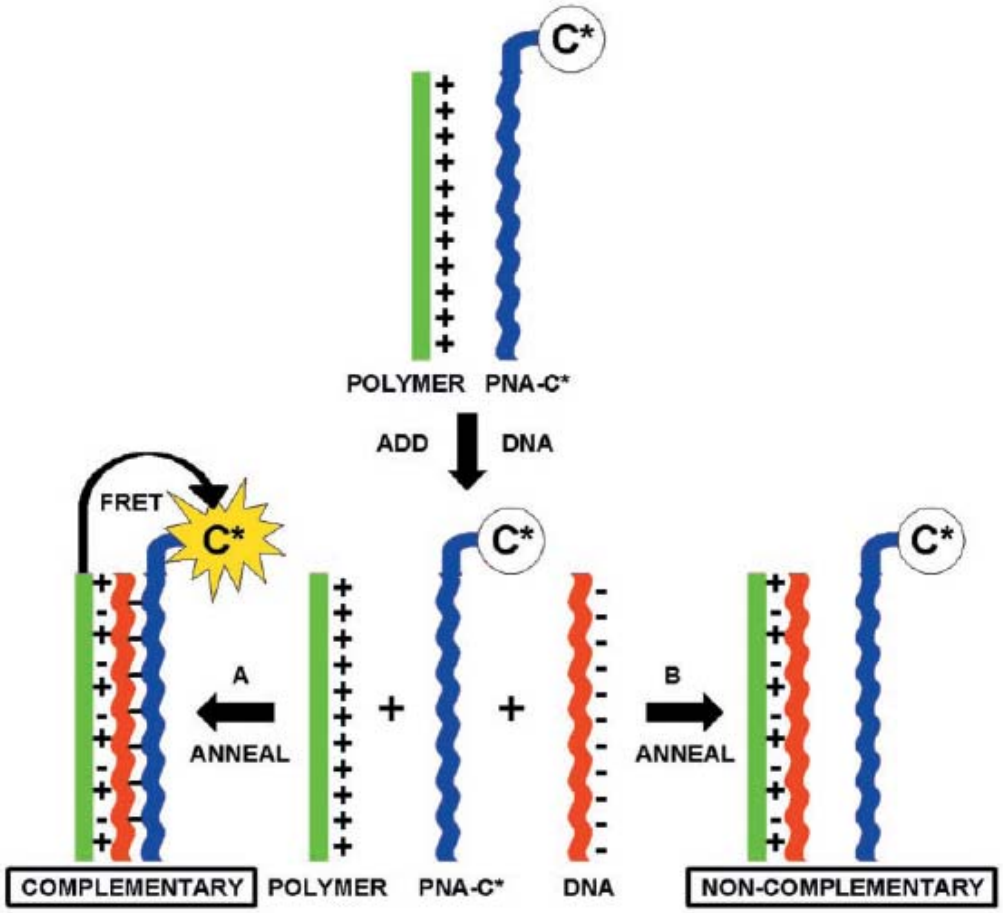

Scheme1.4. Schematic representation for the use of a water-soluble CP with a specific PNA-C* optical reporter probe to detect a complementary ssDNA sequence.

Their sensing system consists of three parts: the water soluble cationic conjugated polymer, a probe peptide nucleic acid (PNA) strand labeled with a choromophore dye at the 5' end, and the target DNA strand. In the initial solution no electrostatic interactions are present, resulting in an average CCP–C* distance too large for effective FRET (Scheme1.4) (17). Addition of a complementary Single-stranded target DNA (ssDNA), which hybridizes with the target PNA, endows the C*-bearing macromolecule with multiple negative charges. Electrostatic

interactions should cause the formation of a complex and a decrease in the average CP–C* distance, allowing FRET to occur. When the target ssDNA does not match the PNA sequence, hybridization does not take place. Therefore, the CCP-PNA-C* distance remains too large for FRET. PNA/ssDNA hybridization is therefore measured by FRET efficiency. The overall scheme serves as a probe for the presence of specific target ssDNA sequences in solution.

1.8 Outlines

In this thesis, we have used CPs as the optical platforms to develop highly sensitive chemical and biological sensors. Conjugated polymers have exceptional linear and nonlinear optical properties and can be utilized to act as a one- and two-photon excitation light harvesting complex to achieve enhanced sensitivity in the CPs based applications.

In Chapter 2, we have investigated enhanced two-photon fluorescence of dye molecule by two-photon excitation FRET using two different conjugated polymers, PFP and PFF. In Chapter 3, a simple scheme for label free DNA sequence detection was introduced by using CPs and a DNA intercalator with high sensitivity and further improved selectivity. The single nucleotide mismatch detection can be detected even at the room temperature. In Chapter 4, by using a combination of oligonucleotides, DNA intercalators and conjugated polymers, we demonstrated a practical scheme for detection of mercury with high sensitivity and selectivity. This scheme could also be used as a two-photon sensor with high sensitivity, which can detect mercury ions deep

into the biological environments. Chapter 5 describes a label free method to visualize the conformational switch of i-motif DNA driven by the environmental pH change using a water soluble polythiophene derivative, PMNT. In Chapter 6, a label-free method for the S1 nuclease cleavage of ssDNA based on CPs/DNA/DNA intercalator system based on FRET was presented.

1.9 References

1. Service, R. F. (2000) *Science* **290,** 425-427.

2. Shirakawa, H., Louis, E. J., Macdiarmid, A. G., Chiang, C. K. & Heeger, A. J. (1977) *Journal of the Chemical Society-Chemical Communications***,** 578-580.

3. Gustafsson, G., Cao, Y., Treacy, G. M., Klavetter, F., Colaneri, N. & Heeger, A. J. (1992) *Nature* **357,** 477-479.

4. Kraft, A., Grimsdale, A. C. & Holmes, A. B. (1998) *Angewandte Chemie-International Edition* **37,** 402-428.

5. Montali, A., Smith, P. & Weder, C. (1998) *Synthetic Metals* **97,** 123-126.

6. Armstrong, N. R., Wightman, R. M. & Gross, E. M. (2001) *Annual Review of Physical Chemistry* **52,** 391-422.

7. Cheng, C. H. W. & Lonergan, M. C. (2004) *Journal of the American Chemical Society* **126,** 10536-10537.

8. Pei, Q. B., Yang, Y., Yu, G., Zhang, C. & Heeger, A. J. (1996) *Journal of the American Chemical Society* **118,** 3922-3929.

9. Pei, Q. B., Yu, G., Zhang, C., Yang, Y. & Heeger, A. J. (1995) *Science* **269,** 1086-1088.

10. Stutzmann, N., Friend, R. H. & Sirringhaus, H. (2003) *Science* **299,** 1881-1884.

11. Novak, P., Muller, K., Santhanam, K. S. V. & Haas, O. (1997) *Chemical Reviews* **97,** 207-281.

12. Torsi, L., Dodabalapur, A., Rothberg, L. J., Fung, A. W. P. & Katz, H. E. (1996)

Science **272,** 1462-1464.

13. McGinnes.J, Corry, P. & Proctor, P. (1974) *Science* **183,** 853-855.

14. Vogel, A. & Venugopalan, V. (2003) *Chemical Reviews* **103,** 2079-2079.

15. McQuade, D. T., Pullen, A. E. & Swager, T. M. (2000) *Chemical Reviews* **100,** 2537-2574.

16. Thomas, S. W., Joly, G. D. & Swager, T. M. (2007) *Chemical Reviews* **107,** 1339-1386.

17. Gaylord, B. S., Heeger, A. J. & Bazan, G. C. (2002) *Proceedings of the National Academy of Sciences of the United States of America* **99,** 10954-10957.

18. Gaylord, B. S., Heeger, A. J. & Bazan, G. C. (2003) *Journal of the American Chemical Society* **125,** 896-900.

19. Gaylord, B. S., Massie, M. R., Feinstein, S. C. & Bazan, G. C. (2005) *Proceedings of the National Academy of Sciences of the United States of America* **102,** 34-39.

20. Wang, S., Gaylord, B. S. & Bazan, G. C. (2004) *Journal of the American Chemical Society* **126,** 5446-5451.

21. Dosremedios, C. G. & Moens, P. D. J. (1995) *Journal of Structural Biology* **115,** 175-185.

22. Forster, T. (1948) *Annalen Der Physik* **2,** 55-75.

23. Stryer, L. (1978) *Annual Review of Biochemistry* **47,** 819-846.

24. Lakowicz, J. R. (1999) *Principles of Fluorescence Spectroscopy* (Prenum

Publishers, New York).

25. Forster, T. (1949) *Zeitschrift Fur Naturforschung Section a-a Journal of Physical Sciences* **4,** 321-327.

26. Lillo, M. P., Szpikowska, B. K., Mas, M. T., Sutin, J. D. & Beechem, J. M. (1997) *Biochemistry* **36,** 11273-11281.

27. Schobel, U., Egelhaaf, H. J., Brecht, A., Oelkrug, D. & Gauglitz, G. (1999) *Bioconjugate Chemistry* **10,** 1107-1114.

28. Jares-Erijman, E. A. & Jovin, T. M. (2003) *Nature Biotechnology* **21,** 1387-1395.

29. Miyawaki, A., Sawano, A. & Kogure, T. (2003) *Nature Reviews Molecular Cell Biology***,** S1-S7.

30. Achyuthan, K. E., Bergstedt, T. S., Chen, L., Jones, R. M., Kumaraswamy, S., Kushon, S. A., Ley, K. D., Lu, L., McBranch, D., Mukundan, H., Rininsland, F., Shi, X., Xia, W. & Whitten, D. G. (2005) *Journal of Materials Chemistry* **15,** 2648-2656.

31. Fan, C. H., Plaxco, K. W. & Heeger, A. J. (2002) *Journal of the American Chemical Society* **124,** 5642-5643.

32. He, F., Tang, Y. L., Yu, M. H., Wang, S., Li, Y. L. & Zhu, D. B. (2006) *Advanced Functional Materials* **16,** 91-94.

33. Ho, H. A., Bera-Aberem, M. & Leclerc, M. (2005) *Chemistry-a European Journal* **11,** 1718-1724.

34. Ho, H. A., Dore, K., Boissinot, M., Bergeron, M. G., Tanguay, R. M.,

Boudreau, D. & Leclerc, M. (2005) *Journal of the American Chemical Society* **127,** 12673-12676.

35. Kim, I. B., Erdogan, B., Wilson, J. N. & Bunz, U. H. F. (2004) *Chemistry-a European Journal* **10,** 6247-6254.

36. Kim, I. B., Wilson, J. N. & Bunz, U. H. F. (2005) *Chemical Communications***,** 1273-1275.

37. Kumaraswamy, S., Bergstedt, T., Shi, X. B., Rininsland, F., Kushon, S., Xia, W. S., Ley, K., Achyuthan, K., McBranch, D. & Whitten, D. (2004) *Proceedings of the National Academy of Sciences of the United States of America* **101,** 7511-7515.

38. Liu, B. & Bazan, G. C. (2004) *Chemistry of Materials* **16,** 4467-4476.

39. Pinto, M. R. & Schanze, K. S. (2004) *Proceedings of the National Academy of Sciences of the United States of America* **101,** 7505-7510.

40. Tang, Y. L., He, F., Yu, M. H., Feng, F. D., An, L. L., Sun, H., Wang, S., Li, Y. L. & Zhu, D. B. (2006) *Macromolecular Rapid Communications* **27,** 389-392.

41. Ho, H. A. & Leclerc, M. (2004) *Journal of the American Chemical Society* **126,** 1384-1387.

42. Najechalski, P., Morel, Y., Stephan, O. & Baldeck, P. L. (2001) *Chemical Physics Letters* **343,** 44-48.

43. Schroeder, R., Ullrich, B., Graupner, W. & Scherf, U. (2001) *Journal of Physics-Condensed Matter* **13,** L313-L320.

44. Sun, H. B., Kawakami, T., Xu, Y., Ye, J. Y., Matuso, S., Misawa, H., Miwa, M.

& Kaneko, R. (2000) *Optics Letters* **25,** 1110-1112.

45. Hurley, L. H. (2002) *Nature Reviews Cancer* **2,** 188-200.

46. Strehmel, B., Sarker, A. M. & Detert, H. (2003) *Chemphyschem* **4,** 249-259.

47. Woo, H. Y., Liu, B., Kohler, B., Korystov, D., Mikhailovsky, A. & Bazan, G. C. (2005) *Journal of the American Chemical Society* **127,** 14721-14729.

48. Wang, S. & Bazan, G. C. (2003) *Advanced Materials* **15,** 1425-1428.

49. Zhou, Q. & Swager, T. M. (1995) *Journal of the American Chemical Society* **117,** 12593-12602.

50. Kaiser, W. & Garrett, C. G. B. (1961) *Physical Review Letters* **7,** 229-231.

51. Birge, R. R. (1986) *Accounts of Chemical Research* **19,** 138-146.

52. Bhawalkar, J. D., He, G. S. & Prasad, P. N. (1996) *Reports on Progress in Physics* **59,** 1041-1070.

53. Tian, N. & Xu, Q. H. (2007) *Advanced Materials* **19,** 1988-1991.

54. Mathewson, P. R. F., J. W. (1992) *Biosensor Design and Application* (American Chemical Society, Washington. DC.).

55. Clark, L. C. & Lyons, C. (1962) *Annals of the New York Academy of Sciences* **102,** 29-45.

56. Chen, L. H., McBranch, D. W., Wang, H. L., Helgeson, R., Wudl, F. & Whitten, D. G. (1999) *Proceedings of the National Academy of Sciences of the United States of America* **96,** 12287-12292.

57. Ho, H. A., Boissinot, M., Bergeron, M. G., Corbeil, G., Dore, K., Boudreau, D. & Leclerc, M. (2002) *Angewandte Chemie-International Edition* **41,**

1548-1551.

58. Tang, Y. L., Feng, F. D., He, F., Wang, S., Li, Y. L. & Zhu, D. B. (2006) *Journal of the American Chemical Society* **128,** 14972-14976.

Chapter 2

Conjugated Polymers as Two-Photon Light Harvesting Materials for Two-Photon Excitation Energy Transfer

2.1 Introduction

Conjugated polymers can function as light harvesting materials and exhibit optical amplification through Förster resonance energy transfer (FRET) (1-4), which has been widely used in chemical and biological senescing (2, 4-22). Conjugated polymers are also known to have large two-photon absorption cross-sections compared to the small molecule counterpart (23-25). Materials with large two-photon cross sections have potential applications in data storage, phototherapy, 3-D imaging and microfabrication (26-29). Compared with one-photon, two-photon excitation based applications have unique advantage, such as deep penetration, 3-D imaging capability and less scattering. However, most conventional organic chromophores that have optimized for one-photon applications have limited two-photon absorption cross section.

Recently a lot of research efforts have been devoted in designing and synthesize materials with large TPA cross section. Two-photon excitation

fluorescence imaging requires materials has large two-photon absorption cross section and high emission efficiency, which sometimes cannot be achieved at the time. Two-photon excitation phototherapy and imaging have advantages over the one-photon counterparts by offering the advantages: a) the ability to work with a smaller more confined treatment area; and b) the ability to treat deeper into diseased tissues. As an alternative approach, large two-photon excitation fluorescence (or drug efficiency) could be achieved by two-photon excitation fluorescence resonance energy transfer from molecules with large TPA cross sections. Materials with large TPA cross sections could be used in combination with existing chromophores that have been optimized for one-photon imaging and phototherapy. The materials with large TPA cross sections act as two-photon light harvesting complex and energy donor to transfer the harvested energy to the chromophores (photosensitizer). Thus the photosensitizer molecule is indirectly excited through two-photon excitation fluorescence resonance energy transfer (FRET), the efficiency of the existing chromophores could be significantly enhanced through fluorescence resonance energy transfer. Based on this principle, different TPE-FRET schemes have been developed, including chemically assembling the TPA donors into dendrimer arms with a photosensitizer as the central core (30), assembly or covalently linking molecules with larger TPA cross sections (such as semiconducting nanoparticles (31) and other small molecules (32) with large TPA cross sections) with photosensitizer molecules.

Taking advantage of large two-photon absorption cross section of conjugated polymers, in a recent communication, our group reported that conjugated polymers

could be used as TPA light harvesting complex to transfer the excitation energy to a DNA intercalator by FRET (33). The fluorescence intensity of the DNA intercalator by two-photon excitation FRET (TPE-FRET) was found to be enhanced by a factor of over 35, compared to that when the intercalator was directly excited by two-photon absorption.

2.2 Experimental

2.2.1 Materials

The cationic conjugated polymers, poly[(9,9-di(3,3'-N,N'-trimethyl- ammonium) propylfluorenyl-2,7- diyl)-alt-co-(1,4-phenylene)] diiodide salt (PFP) and poly[(9,9-di(3,3'-N,N'-trimethyl-ammonium) propylfluorenyl-2,7- diyl)-alt-co-(9,9-dioctylfluorenyl-2,7-diyl)] diiodide salt (PFF), were obtained from American Dye Source. The molecular weight is 10000 – 15000. dsDNA was obtained from Sigma and YOYO-1 was from Invitrogen.The molecular structures of chemicals were shown in Table 2.1.

Table 2.1 Molecular Structures of of PFP, PFF, YOYO-1 and sequences of dsDNA.

PFP	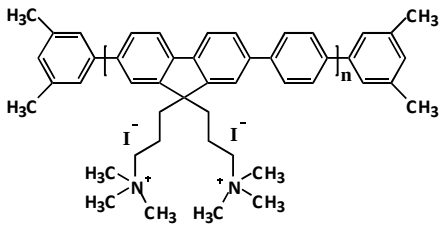
PFF	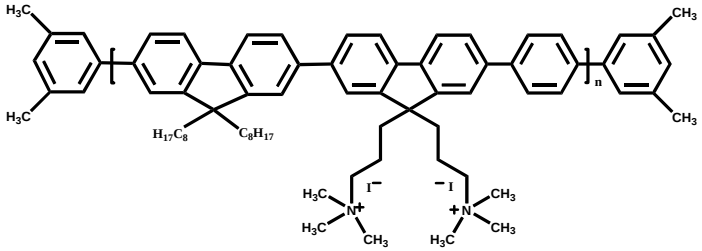
YOYO-1	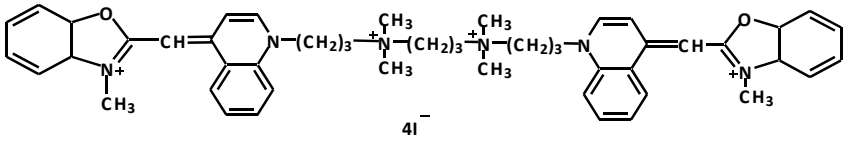
dsDNA	5’ — TCTTGACTATGTGGGTGCTAACTC—3’ 3’—AGAACTGATACACCCACGATTGAG—5’

Measurements were performed in phosphate buffer (50 mM, PH = 7.0) at room temperature.

2.2.2 Methods: One-photon and two-photon excitation fluorescence measurements

UV-Vis absorption spectra were measured with a SHIMADZU UV-2450 spectrophotometer and fluorescence measurements were performed using a Perkin-Elmer fluoremeter LS55.

The experimental setup for two-photon excitation (TPE) fluorescence was

shown in Scheme 2.1. The excitation source for two-photon excitation fluorescence is a femtosecond Ti:sapphire oscillator from Spectra Physics (Tsunami). The output laser pulses have pulse duration of 40 fs with a repetition rate of 76 MHz and center wavelength at 800 nm. The total output energy is 300 mW. The samples are excited by directing a tightly collimated, high intensity laser beam onto the sample. The emission from the sample was collected at a 90 angle by a pair of high numerical aperture lens and optical fibres and directed to the spectrometer, which is a monochromator (Acton, Spectra Pro 2300i) coupled CCD (Princeton Instruments, Pixis 100B) system. To avoid internal filter effects, the excited volume was located near the cell wall on the collection optics side. This configuration minimizes the fluorescence path inside the sample cell and thus reduces self-absorption. A short pass filter with cut-off wavelength at 750 nm (SPF 750) was placed before the spectrometer to minimize the intensity of pumping light scattering.

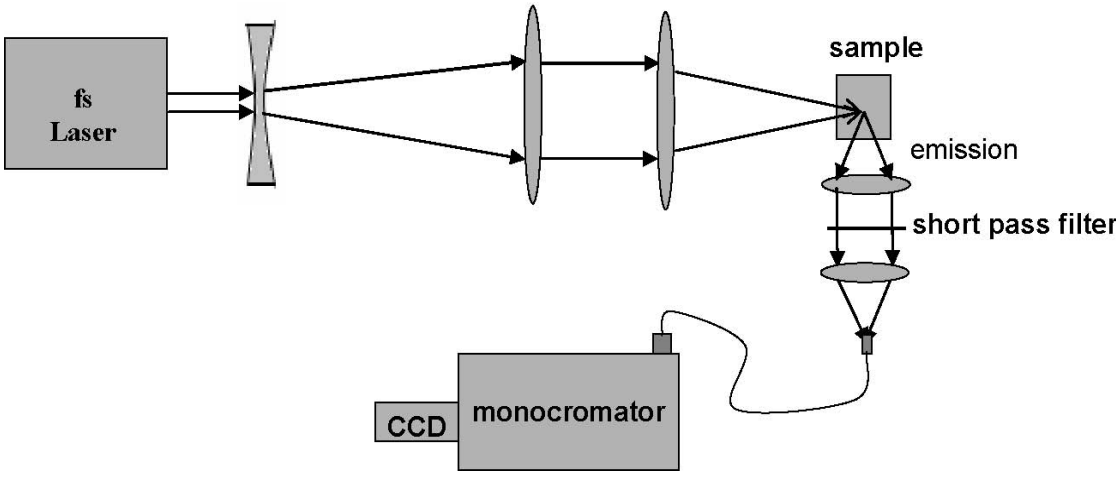

Scheme 2.1 Experimental setup for two-photon excitation fluorescence measurements

2.3 Results and Discussion

In this work, we reported further improved scheme using two different conjugated polymers, PFP and PFF. With proper choice of DNA/drug ratio, addition of PFP and PFF can enhance the two-photon excitation fluorescence of YOYO-1 by 53 and 99 times, respectively. The TPE-FRET system, as shown in Scheme 2.2 consists of a cationic conjugated polymer, dsDNA and a DNA intercalator. The origins of such large enhancement have been investigated.

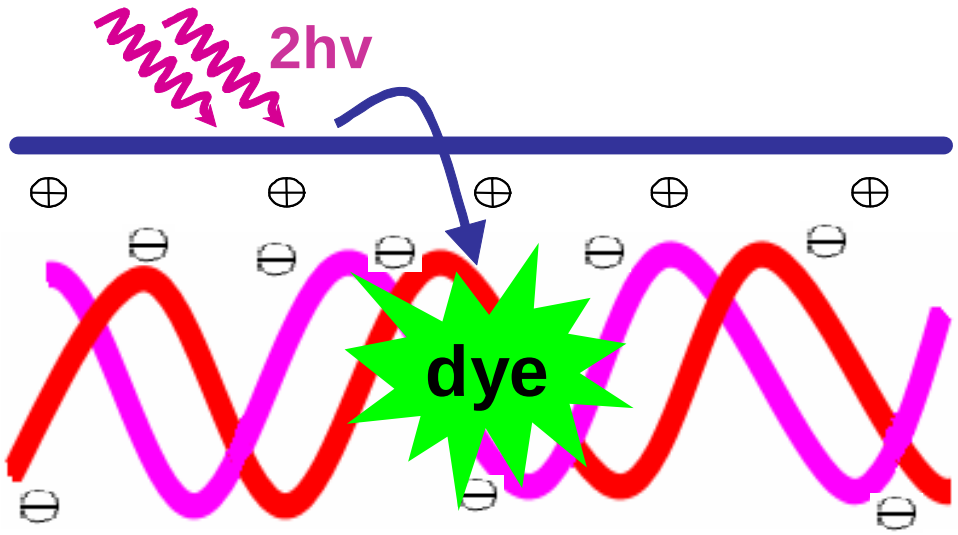

Scheme 2.2 Two-photon excitation fluorescence resonance energy transfer

Two different cationic conjugated polymers, PFP and PFF, were used as two-photon excitation light harvesting complexes and energy donor. YOYO-1 was chosen as energy acceptor because its absorption spectrum overlaps well with the emission spectrum of PFP and PFF to ensure FRET. The absorption and emission spectra of PFP, PFF and YOYO-1 are shown in Figure 2.1. YOYO-1 has relatively high affinity with DNA. Its fluorescence intensity increases many times upon

intercalation into dsDNA (34). YOYO-1 is a potential drug molecule and has been reported able to cause photo-cleavage of DNA (35). It has also been widely used as a staining agent for DNA imaging applications. The electrostatic interactions between the cationic conjugated polymers and dsDNA can bring the donor and acceptor into proximity for efficient energy transfer to occur.

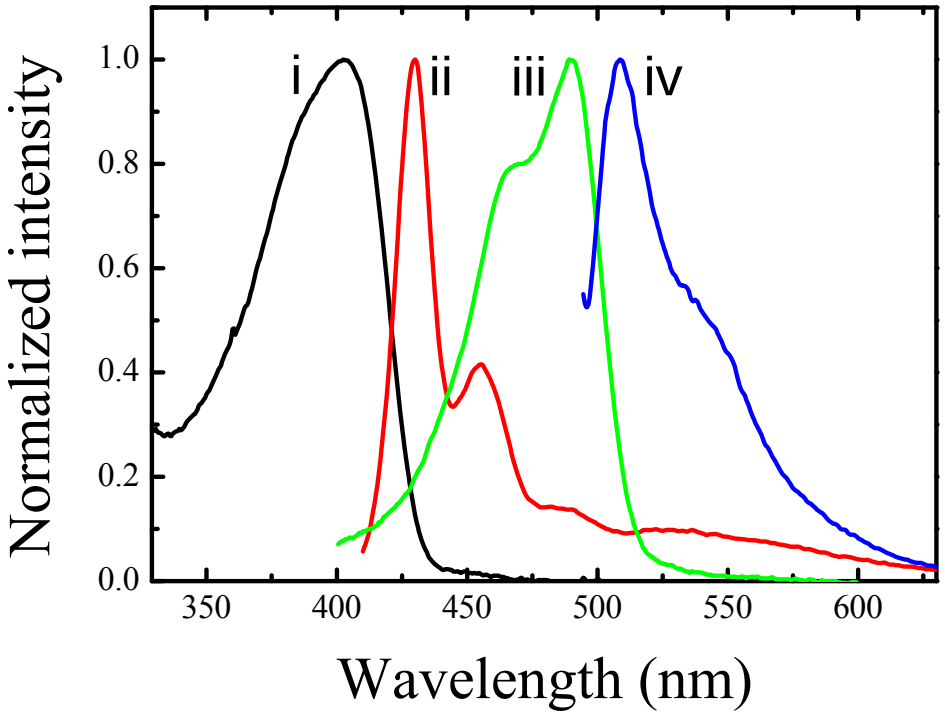

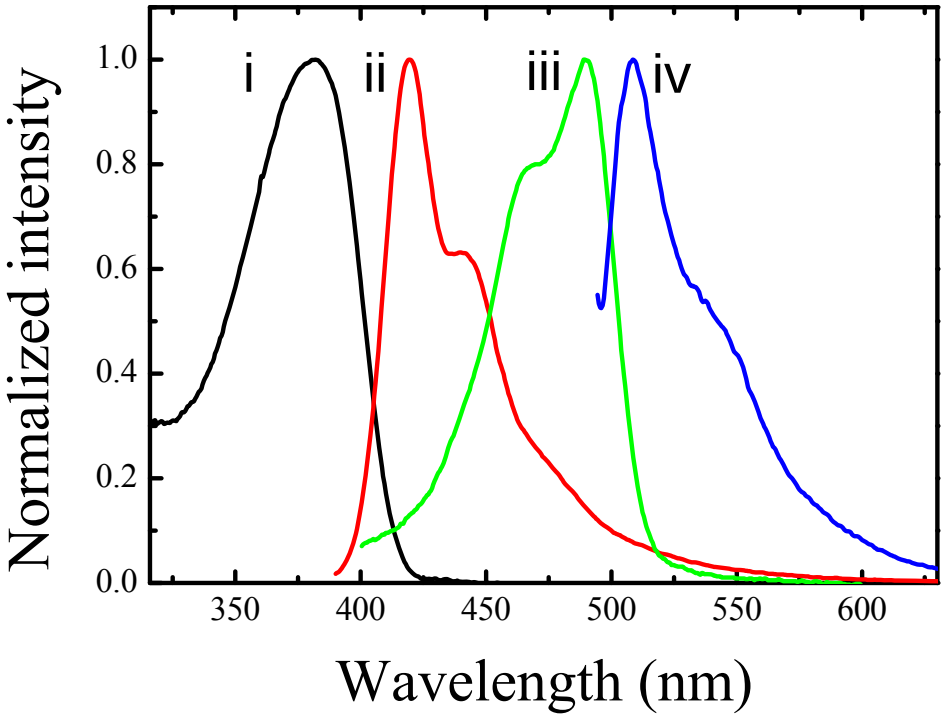

Figure 2.1. Absorption and emission spectra of donor and acceptor pairs. a) Absorption (i for PFP, iii for YOYO-1) and emission (ii for PFP, iv for YOYO-1) spectra of PFP and YOYO-1, respectively. b) Absorption (i for PFF, iii for YOYO-1) and emission (ii for PFF, iv for YOYO-1) spectra of PFF and YOYO-1, respectively.

Figure 2.2 shows the emission spectra of PFP/dsDNA/YOYO-1 systems upon one-photon excitation of the energy donor, PFP, at 380 nm. The emission intensity of YOYO-1 gradually increases upon addition of PFP until saturation. The emission intensity in PFP/dsDNA/YOYO-1 via FRET could be enhanced up to 8.7 times compared to that when YOYO-1 was directly excited at its absorption maximum, 490 nm, in dsDNA/YOYO-1 (with residue emission contribution from PFP subtracted). When PFF was used to substitute PFP, an enhancement factor of 7.0 times was obtained. Such optical amplification effects of conjugated polymers have been previously utilized in development of conjugated polymer based biological and chemical biosensors with enhanced detection efficiency. The energy transfer from PFP to intercalated YOYO-1 is better than that from PFF to YOYO-1, likely due to a larger fluorescence yield of PFP (21% for PFP versus 6% for PFF).

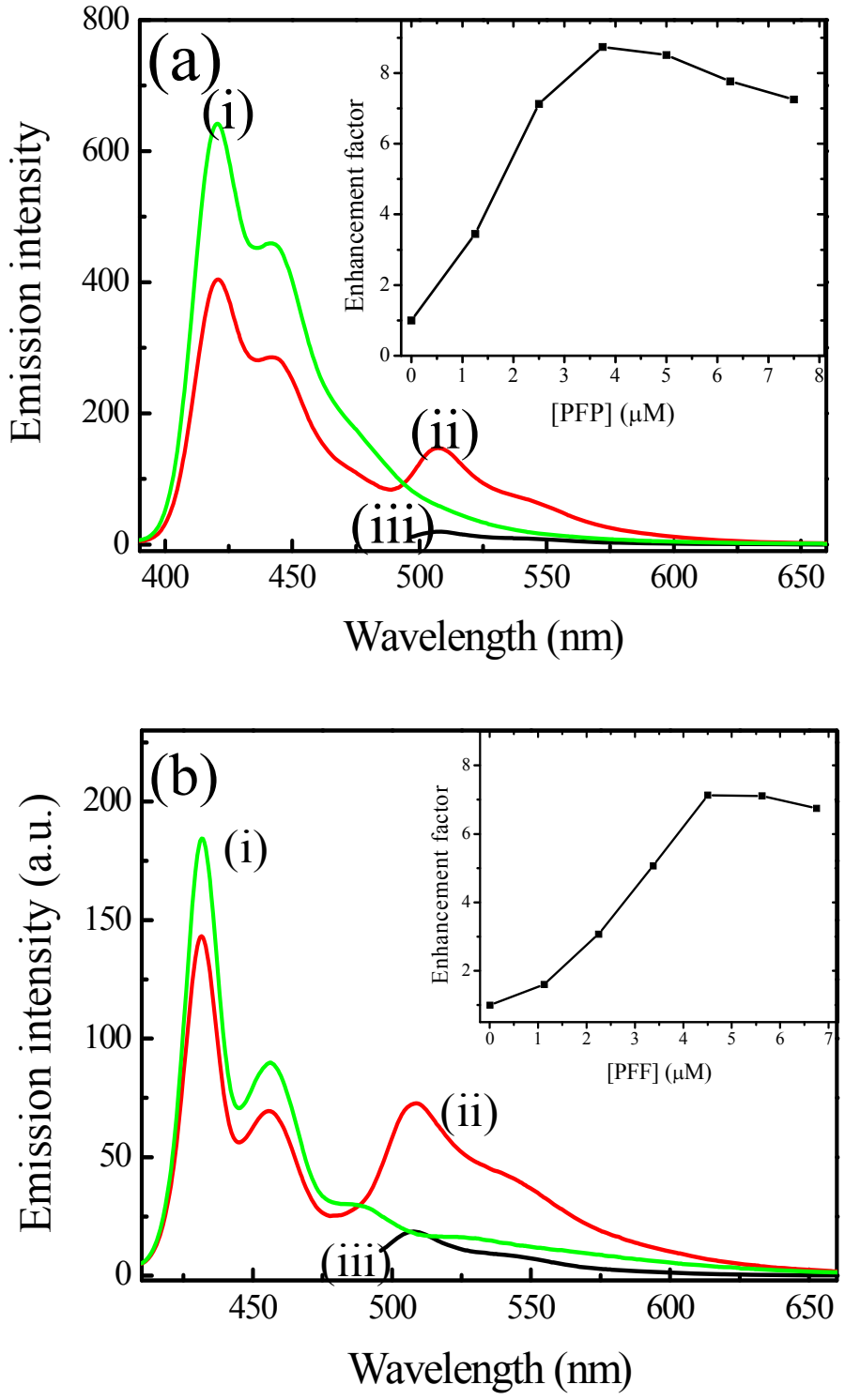

Figure 2.2. (a) One photon excitation emission spectra of PFP (i, λ_{ex}=380nm), PFP/dsDNA/YOYO-1 (ii, λ_{ex}= 380nm) and YOYO-1 alone (iii, λ_{ex}= 490nm). [dsDNA]=1.0*10^{-7}M; [YOYO-1] =1.6*10^{-7}M; [PFP]=1.42*10^{-5}M in repeat units. (b) One photon excitation emission spectra of PFF (i, λex=380nm), PFF/dsDNA/YOYO-1 (ii, λex= 400nm) and YOYO-1 alone (iii, λex= 490nm). [dsDNA]=1.0*10^{-7}M; [YOYO-1] =1.6*10^{-7}M; [PFF] =1.07*10^{-5}M in repeat units

The two-photon excitation (TPE) emission spectra of PFP/dsDNA/YOYO-1 system are shown in Figure 2.3. The samples are excited with femtosecond laser pulses with central wavelength at 800 nm and pulse duration of 40 fs. Both conjugated polymers and YOYO-1 could be excited by 800 nm laser pulse via two-photon absorption processes. Very weak two-photon induced emission was observed in dsDNA/YOYO-1 due to the small two-photon absorption cross section of YOYO-1 at 800 nm. Upon gradual addition of conjugated polymer into dsDNA/YOYO-1 buffered solution, the two-photon induced emission of YOYO-1 was found to be significantly enhanced, which gradually increases with further addition of conjugated polymers until saturation An enhancement factor of up to 53 was obtained when PFP was used as the two-photon excitation donor and an enhancement factor of 99 when PFF was used as the two-photon excitation donor.

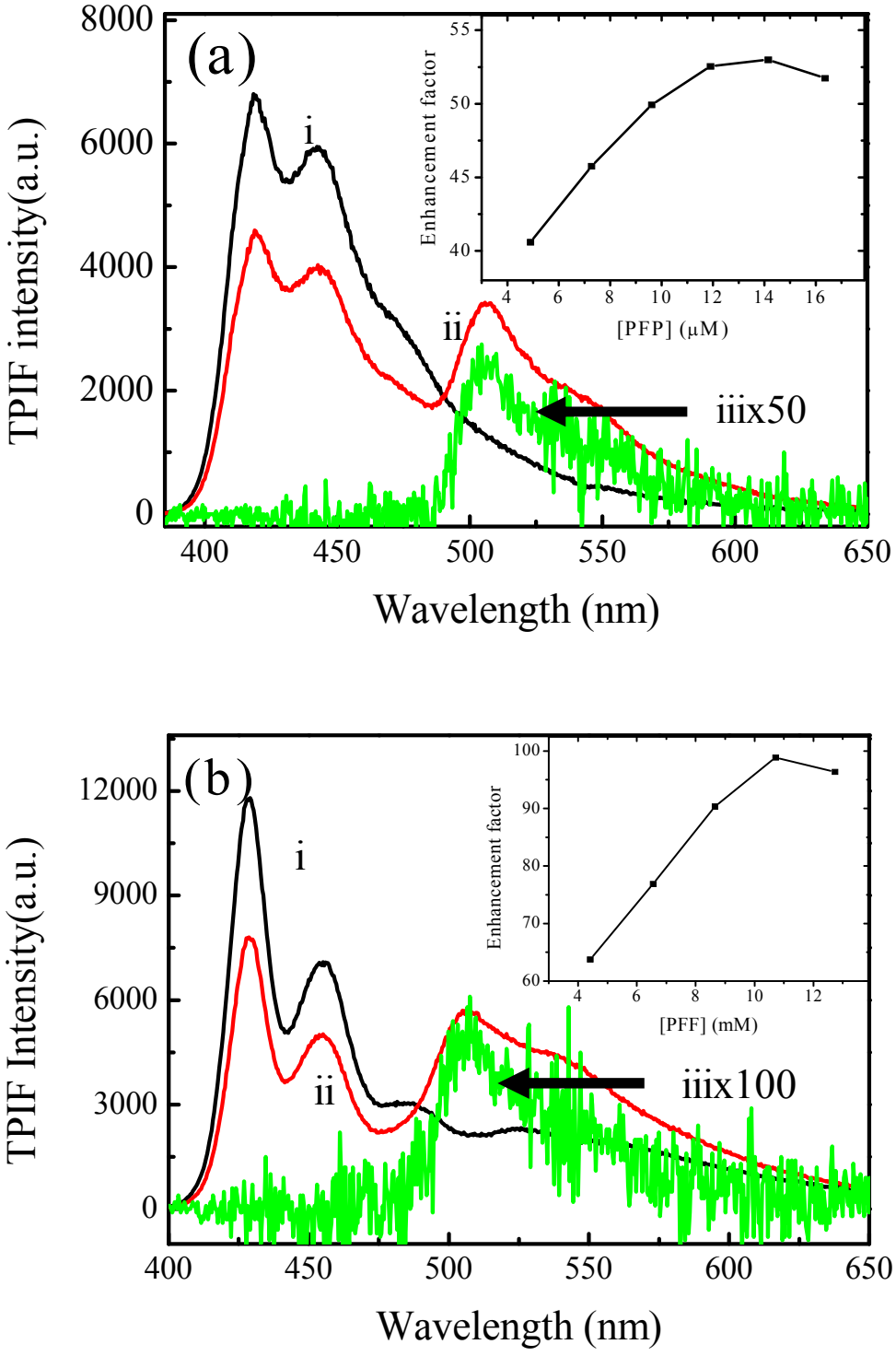

Figure 2.3. Two-photon excitation resonance energy transfer (a) Two photon excitation emission spectra of PFP (i), PFP/dsDNA/YOYO-1 (ii) and YOYO-1 alone (iii). λex=800nm; [dsDNA]=1.0*10^{-7}M; [YOYO-1] =1.6*10^{-7}M; [PFP] =1.42*10^{-5}M in repeat units. (b) Two photon excitation emission spectra of PFF (i), PFF/dsDNA/YOYO-1 (ii) and YOYO-1 alone (iii). λex=800nm; [dsDNA]=1.0*10^{-7}M; [YOYO-1] =1.6*10^{-7}M; [PFF] =1.07*10^{-5}M in repeat units.

Two factors are responsible for the observed large enhancement factor via TPE-FRET. The first one is owing to a larger two-photon absorption cross section of conjugated polymers due to its large conjugation length, compared to that of YOYO-1. The excitation energy harvested by the conjugated polymers can be further transferred to the intercalated YOYO-1 molecules via FRET. The second reason is that conjugated polymers are made of many segments. Excitation energy harvested by any segment can migrate along the polymer chain until the energy is transferred to the acceptor via FRET. So the intercalator YOYO-1 collects the energy harvested by many segments of the conjugated polymers by two-photon absorption.

Here we only show the results of TPE emission excited at 800 nm because results at 800 nm are most important for practical applications. Two-photon excitation is a weak process and usually requires high intensity lasers such as femtoseond lasers. Applications of two-photon excitation fluorescence microscopy and two-photon photodynamic therapy usually uses Ti: sapphire oscillator, the most readily available femtosecond excitation source, which has a central wavelength of around 800 nm. Excitation at other wavelengths will yield a different enhancement factors. We also tried to measure the two-photon absorption cross section of two conjugated polymers conjugated polymers using two-photon induced fluorescence. The results are shown in Figure 2.4. The value of two-photon absorption cross section was calculated using rhodamine B as a reference. The results indicated that PFF has larger two photon cross sections than that of PFP in the wavelength range of 780-840 nm. At 800 nm,

the TPA cross section of PFF is about 3.6 times larger than that of PFP, which explains the fact that use of PFF results in a larger fluorescence enhancement by TPE-FRET.

The two-photon cross section of both PFP and PFF increase as the wavelength was shifted from 800 nm to 770 nm. This result is consistent with the previously reported TPE excitation spectrum of polyfluorence (36), which has a two-photon absorption peak at 650 nm and one photon absorption peak at 384 nm. One-photon absorption and two-photon absorption have different parity selection rules. Two-photon excitation usually occurs with total energy higher than that of one-photon excitation energy. For molecules possessing a center of symmetry, two-photon excitation usually excites the molecules to S_2 or higher states, which subsequently decays to S_1 state to fluoresce. Direct excitation of the molecules to one-photon allowed S_1 state by two-photon absorption is not efficient unless perturbations such as vibrational coupling lower this symmetry (37).

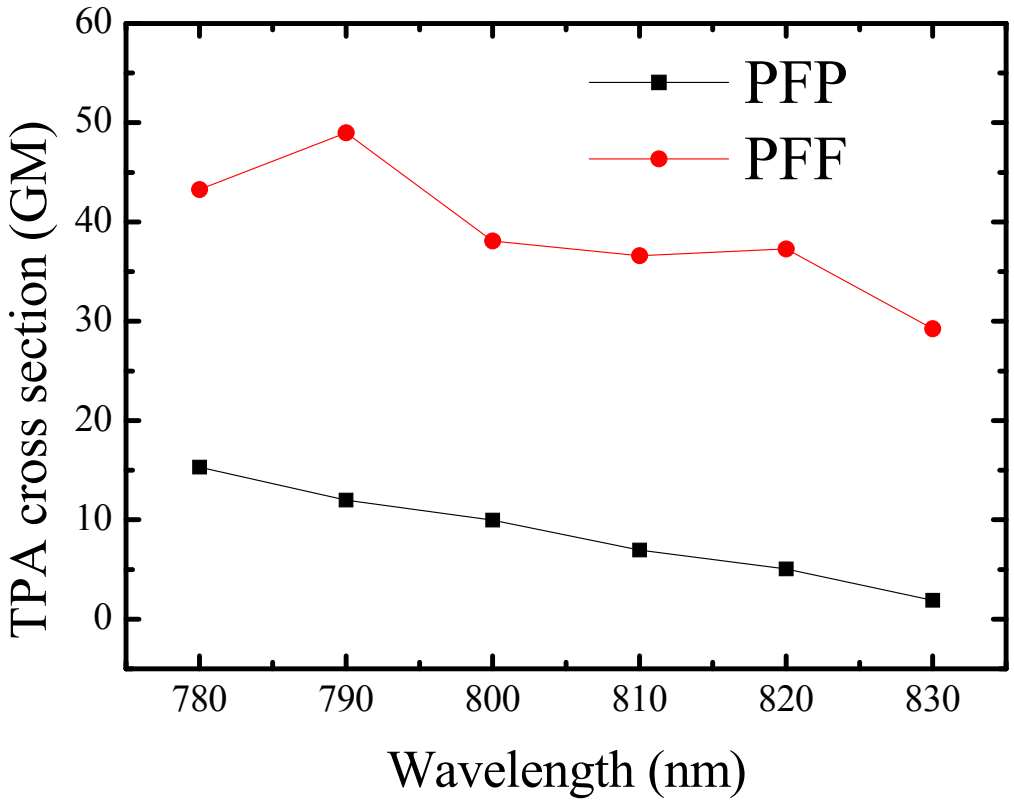

Figure 2.4. Two-photon absorption cross section (per repeat unit) of PFP and PFF.

The two-photon excitation fluorescence of YOYO-1 was also measured (results not shown). YOYO-1 has one-photon absorption maxima at 490 nm. Our measurements showed its two-photon absorption cross section of YOYO-1 increase with increasing wavelength in the range of 780-840 nm and peak at wavelength longer than 840 nm, beyond our laser window. The variation is less than 35% when the excitation wavelength was tuned from 780 to 840 nm.

Based on these results, an even larger enhancement factor would be expected if a shorter excitation wavelength is used. We are particularly interested in the enhancement effects at 800 nm just because of its importance in practical applications.

When excited at 800 nm, an enhancement factor of nearly 100 in TPE emission of YOYO-1 was observed due to the application of conjugated polymers through fluorescence resonance energy transfer. Here we used two commercially available cationic polyfluorene derivatives, PFP and PFF, to demonstrate the enhanced two-photon excitation fluorescence by FRET. The results suggested that an even larger enhancement factor would be resulted with shorter excitation wavelength. Since the primary interested working wavelength range would be around 800 nm, using other conjugated polymers with optimum excitation wavelength and larger TPA cross sections around 800 nm as two-photon excitation light harvesting complex can achieve much larger enhancement effects. The two-photon excitation emission efficiency of the intercalators can also be further enhanced by using DNA binding molecules with favorable transition dipole moment orientation along with the conjugated polymer molecules to give more efficient energy transfer.

2.4 Conclusion

In summary, this work shows that two-photon induced emission of the DNA intercalators can be significantly enhanced by using cationic conjugated polymers. An enhancement factor of nearly 100 times could be resulted due to fluorescence resonance energy transfer. It has important implications in two-photon excitation phototherapy and multi-photon imaging. For applications in two-photon excitation photo-therapy, existing drugs that are used in conventional one-photon excitation

phototherapy could be used, and their drug efficiency could be significantly enhanced by simple addition of conjugated polymers.

2.5 References

1. Gaylord, B. S., Heeger, A. J. & Bazan, G. C. (2002) *Proceedings of the National Academy of Sciences of the United States of America* **99,** 10954-10957.
2. He, F., Tang, Y. L., Wang, S., Li, Y. L. & Zhu, D. B. (2005) *Journal of the American Chemical Society* **127,** 12343-12346.
3. Wang, S., Gaylord, B. S. & Bazan, G. C. (2004) *Journal of the American Chemical Society* **126,** 5446-5451.
4. Xu, Q. H., Wang, S., Korystov, D., Mikhailovsky, A., Bazan, G. C., Moses, D. & Heeger, A. J. (2005) *Proceedings of the National Academy of Sciences of the United States of America* **102,** 530-535.
5. Achyuthan, K. E., Bergstedt, T. S., Chen, L., Jones, R. M., Kumaraswamy, S., Kushon, S. A., Ley, K. D., Lu, L., McBranch, D., Mukundan, H., Rininsland, F., Shi, X., Xia, W. & Whitten, D. G. (2005) *Journal of Materials Chemistry* **15,** 2648-2656.
6. Bunz, U. H. F. (2000) *Chemical Reviews* **100,** 1605-1644.
7. Ho, H. A., Bera-Aberem, M. & Leclerc, M. (2005) *Chemistry-a European Journal* **11,** 1718-1724.
8. Ho, H. A., Boissinot, M., Bergeron, M. G., Corbeil, G., Dore, K., Boudreau, D. & Leclerc, M. (2002) *Angewandte Chemie-International Edition* **41,** 1548-1551.
9. Ho, H. A., Dore, K., Boissinot, M., Bergeron, M. G., Tanguay, R. M.,

Boudreau, D. & Leclerc, M. (2005) *Journal of the American Chemical Society* **127,** 12673-12676.

10. Ho, H. A. & Leclerc, M. (2004) *Journal of the American Chemical Society* **126,** 1384-1387.

11. Kim, I. B., Wilson, J. N. & Bunz, U. H. F. (2005) *Chemical Communications***,** 1273-1275.

12. Kumaraswamy, S., Bergstedt, T., Shi, X. B., Rininsland, F., Kushon, S., Xia, W. S., Ley, K., Achyuthan, K., McBranch, D. & Whitten, D. (2004) *Proceedings of the National Academy of Sciences of the United States of America* **101,** 7511-7515.

13. McQuade, D. T., Hegedus, A. H. & Swager, T. M. (2000) *Journal of the American Chemical Society* **122,** 12389-12390.

14. McQuade, D. T., Pullen, A. E. & Swager, T. M. (2000) *Chemical Reviews* **100,** 2537-2574.

15. Nilsson, K. P. R. & Inganas, O. (2003) *Nature Materials* **2,** 419-U10.

16. Nilsson, K. P. R., Rydberg, J., Baltzer, L. & Inganas, O. (2003) *Proceedings of the National Academy of Sciences of the United States of America* **100,** 10170-10174.

17. Pinto, M. R. & Schanze, K. S. (2004) *Proceedings of the National Academy of Sciences of the United States of America* **101,** 7505-7510.

18. Wosnick, J. H., Mello, C. M. & Swager, T. M. (2005) *Journal of the American Chemical Society* **127,** 3400-3405.

19. Xu, H., Wu, H. P., Huang, F., Song, S. P., Li, W. X., Cao, Y. & Fan, C. H. (2005) *Nucleic Acids Research* **33,** e83.

20. Yang, C. Y. J., Pinto, M., Schanze, K. & Tan, W. H. (2005) *Angewandte Chemie-International Edition* **44,** 2572-2576.

21. Kim, I. B., Erdogan, B., Wilson, J. N. & Bunz, U. H. F. (2004) *Chemistry-a European Journal* **10,** 6247-6254.

22. Thomas, S. W., Joly, G. D. & Swager, T. M. (2007) *Chemical Reviews* **107,** 1339-1386.

23. Schroeder, R., Ullrich, B., Graupner, W. & Scherf, U. (2001) *Journal of Physics-Condensed Matter* **13,** L313-L320.

24. Strehmel, B., Sarker, A. M. & Detert, H. (2003) *Chemphyschem* **4,** 249-259.

25. Woo, H. Y., Liu, B., Kohler, B., Korystov, D., Mikhailovsky, A. & Bazan, G. C. (2005) *Journal of the American Chemical Society* **127,** 14721-14729.

26. Cumpston, B. H., Ananthavel, S. P., Barlow, S., Dyer, D. L., Ehrlich, J. E., Erskine, L. L., Heikal, A. A., Kuebler, S. M., Lee, I. Y. S., McCord-Maughon, D., Qin, J. Q., Rockel, H., Rumi, M., Wu, X. L., Marder, S. R. & Perry, J. W. (1999) *Nature* **398,** 51-54.

27. Denk, W., Strickler, J. H. & Webb, W. W. (1990) *Science* **248,** 73-76.

28. Olson, C. E., Previte, M. J. R. & Fourkas, J. T. (2002) *Nature Materials* **1,** 225-228.

29. So, P. T. C., Dong, C. Y., Masters, B. R. & Berland, K. M. (2000) *Annual Review of Biomedical Engineering* **2,** 399-429.

30. Oar, M. A., Serin, J. A., Dichtel, W. R. & Frechet, J. M. J. (2005) *Chemistry of Materials* **17,** 2267-2275.

31. Clapp, A. R., Pons, T., Medintz, I. L., Delehanty, J. B., Melinger, J. S., Tiefenbrunn, T., Dawson, P. E., Fisher, B. R., O'Rourke, B. & Mattoussi, H. (2007) *Advanced Materials* **19,** 1921-1926.

32. Chen, C. Y., Tian, Y. Q., Cheng, Y. J., Young, A. C., Ka, J. W. & Jen, A. K. Y. (2007) *Journal of the American Chemical Society* **129,** 7220-7221.

33. Tian, N. & Xu, Q. H. (2007) *Advanced Materials* **19,** 1988-1991.

34. Netzel, T. L., Nafisi, K., Zhao, M., Lenhard, J. R. & Johnson, I. (1995) *Journal of Physical Chemistry* **99,** 17936-17947.

35. Akerman, B. & Tuite, E. (1996) *Nucleic Acids Research* **24,** 1080-1090.

36. Najechalski, P., Morel, Y., Stephan, O. & Baldeck, P. L. (2001) *Chemical Physics Letters* **343,** 44-48.

37. Wakebe, T. & Van Keuren, E. (1999) *Japanese Journal of Applied Physics Part 1-Regular Papers Short Notes & Review Papers* **38,** 3556-3561.

Chapter 3

Label Free DNA Sequence Detection with Enhanced Sensitivity and Selectivity using Cationic Conjugated Polymers and PicoGreen

3.1. Introduction and theories

DNA sequence detection is important for applications in many areas, such as medical diagnosis, gene expression analysis and biomedical studies (1-3). Various optical and electrochemical methods have been developed (3-10). A major challenge in DNA sequence detection is to achieve highly sensitive detection methods with high selectivity, in particular, the capability of detecting single nucleotide mismatch (9-14).

Conjugated polymers are known to provide an advantage of collective optical response (7, 8, 12, 15-22). The electronic structure of the conjugated polymers coordinates the action of a large number of absorbing units. The excitation energy can migrate along the polymer backbone before transferring to the chromophore reporter, which will result in amplification of fluorescent signals (7, 8, 15, 17, 18, 20). Conjugated polymers thus can function as light-harvesting materials and exhibit optical amplification via Förster resonance energy transfer (FRET). Because of these exceptional properties, conjugated polymers have been used as the

optical platforms for highly sensitive chemical and biological sensors (7-9, 15, 17,18,20). In the application of DNA sequence detection, water soluble, positively charged (cationic) conjugated polymers were usuallay used (7, 8, 12, 15-20). When the negatively charged DNA are labeled with fluorescent molecules, electrostatic interactions bring the fluorescent labels sufficiently close to the conjugated polymers to enable efficient FRET.

The long-range excitation energy transfer from donor to acceptor via the dipole–dipole interactions was initially described by Förster (23). The rate of energy transfer through a Förster mechanism is given by (24,25)

$$k_{FRET} \propto \frac{\kappa^2}{r^6} \int_0^\infty F_D(\lambda)\varepsilon_A(\lambda)\lambda^4 d\lambda \qquad \text{(eq.3.1)}$$

which shows that the energy transfer rate is dependent on the donor and acceptor separation distance (r), the orientation factor (κ^2), the spectral overlap between fluorescence spectrum of the donor ($F_D(\lambda)$) and absorption spectrum of the acceptor ($\varepsilon_A(\lambda)$) as denoted by the integral.

Fluorescent detection methods usually require labeling probes with chromophores. Such labeling processes usually add cost and increase protocol complexity. Label free detection (26,27) is of great interest due to the simplicity and reduced cost. So far most conjugated polymer based DNA sensors require the use of fluorescent labeling probe (7, 8, 15, 17). DNA intercalating dyes, such as ethidium

bromide, increase their emission intensities significantly upon binding to double stranded DNA (dsDNA). This phenomenon could be potentially utilized to develop label free protocols for DNA sequence detection as shown in Scheme 3.1, in which conjugated polymers can be used in combination with the DNA intercalators to achieve enhanced detection efficiency. This scheme was originally proposed by Wang et. al. (8) In their initial approach, ethidium bromide (EB) was used as the intercalator. However, the energy transfer from conjugated polymers to the intercalated EB was not efficient due to unfavorable orientation of their transition dipole moments. To overcome this problem, they introduced a fluorescein probe tethered to the end of the DNA strand (probe) to act as a FRET gate to relay the excitation energy and obtained efficient energy transfer for fluorescence enhancement. However, the advantage of label free detection was lost due to the introduction of fluorescein label in their modified approach.

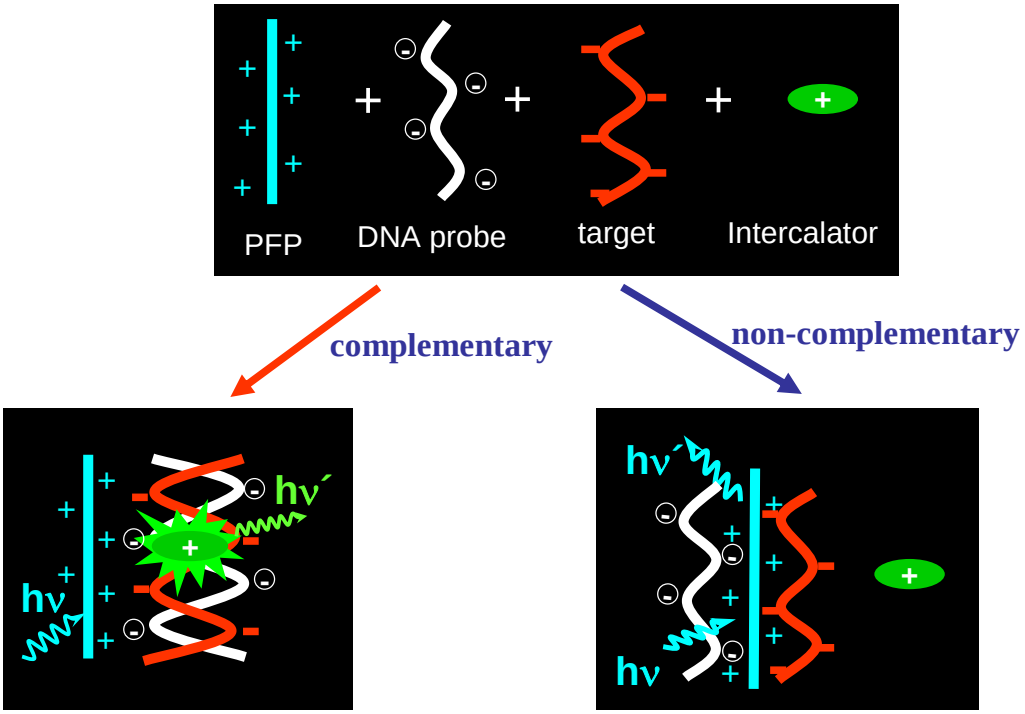

Scheme 3.1 DNA sequence detection based on a FRET gate mechanism

Here we propose an alternative solution to improve the energy transfer efficiency. According to Eq.1, in addition to the orientation factor, another factor, the small absorption coefficient of the EB molecule, is also responsible for inefficient direct energy transfer from conjugated polymers to the intercalated EB. So, alternatively, the energy transfer efficiency could be improved by utilizing DNA intercalators with large absorption coefficients. The intercalated dyes actually have some degrees of freedom of motion at the intercalation site (28), which somewhat relax this unfavorable orientational restrictions. Efficient energy transfer from conjugated polymers to the intercalated dyes could be obtained by using DNA intercalators with large absorption coefficients. In this report, we demonstrated the use of a combination of PicoGreen (PG) and conjugated polymers to develop a label

free DNA sequence detection method with enhanced sensitivity and further improved selectivity. PicoGreeen has a large absorption coefficient (ε=7.0x10^{4}cm^{-1}M^{-1}) (29), about 12.3 times that of ethidium bromide (EB) at its absorption maxima; thus the energy transfer efficiency can be significantly improved. The conjugated polymers were used for two purposes. First, the optical amplification effect of the conjugated polymers through FRET will enhance the detection efficiency. Secondly, because DNA intercalators have stronger binding interactions with dsDNA compared to ssDNA, cationic conjugated polymers could act as competitive DNA binding agents to repel some DNA intercalators away selectively for dsDNA and ssDNA, thus improve the selectivity between complementary (in forms of dsDNA) and non-complementary (in forms of ssDNA) DNA strands. Our results show that not only the sensitivity could be enhanced by up to 19-fold, the selectivity was also significantly improved by using cationic conjugated polymers. The improved selectivity allowed us able to detect single nucleotide mismatch even at the room tempertaure.

We used a waters-soluble conjugated polymer, poly[(9,9-di(3,3'-N,N'-trimethyl-ammonium)propylfluorenyl-2,7-diyl)-alt-co-(1,4-phenylene)] diiodide salt (PFP), as the energy donor, and PicoGreen (PG), as the DNA intercalator and energy acceptor. The absorption spectrum of PicoGreen has good overlap with the emission spectrum of PFP (Figure 3.1), ensuring efficient energy transfer from PFP to PicoGreen. The chemical structures of PFP, PicoGreen and the DNA sequences are shown in Table 3.1. Hybridization reactions of DNA and all the measurements

were performed in 0.05M phosphate buffer solutions (pH=7.4).

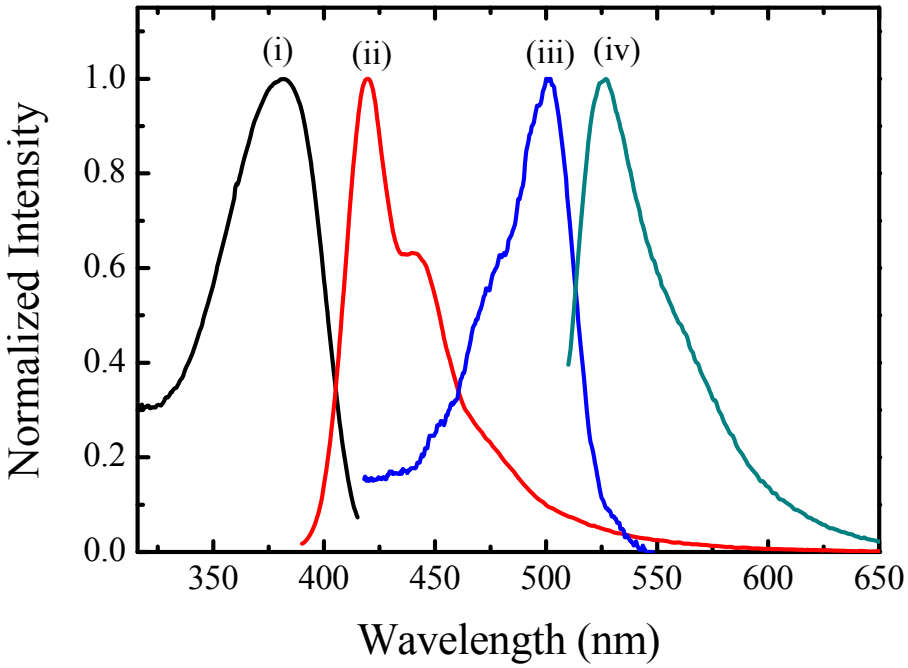

Figure 3.1. Absorption (i for PFP, iii for PG) and emission (ii for PFP, iv for PG) spectra of PFP and PicoGreen.

3.2 Experimental

3.2.1 Materials and Sample Preparation.

poly[(9,9-di(3,3'-N,N'-trimethyl-ammonium)propylfluorenyl-2,7-diyl)-alt-co-(1,4-phenylene)] diiodide salt (PFP) was purchased from American Dye Source Inc. The molecular weight is 10000 – 15000. PicoGreen (PG) was obtained from Invitrogen and the DNA strands were obtained from Sigma. The molecular structure of PFP, PG and the sequence of the ssDNA are shown in Table 3.1.

Table 3.1 Molecular structure of PFP, EB, 6-FAM and sequences of ssDNA(ssFAM-DNA. Complementary, NC1, NC3, NC5, NC8)

PFP	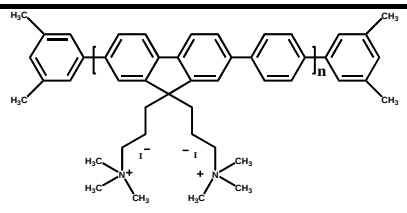
PicoGreen	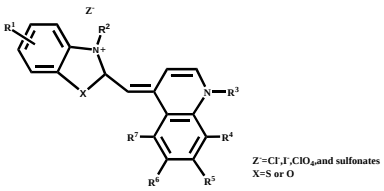
$ssDNA_P$	5'---TCTTGACTATGTGGGTGCTAACTC---3'
$ssDNA_C$	3'---AGAACTGATACACCCACGATTGAG---5'
$ssDNA_{1NC}$	3'---AGAACTGATACGCCCACGATTGAG---5'
$ssDNA_{3NC}$	3'---AGAACGGATACGCCCACGGTTGAG---5'
$ssDNA_{NC}$	3'---CATATCGCTCATCAACTGCGGGTT---5'

3.2.2 FRET Experiment.

UV-Vis absorption spectra were measured with a SHIMADZU UV-2450 spectrophotometer, and fluorescence measurements were done on a Perkin-Elmer fluoremeter with temperature control system. The concentration of DNA was determined by measuring its absorbance at 260 nm in a 200 μL quartz cuvette. The function for ssDNA concentration calculation is [ssDNA] = 33 x 10^{-2} x A/MW, where A refers to UV absorption at 260nm of ssDNA in 1 mm cuvette. MW refers to molecular weight of ssDNA. The hybridization reactions of DNA were performed in a 50 mM sodium citrate buffer (pH 7.4).

3.3 Results and Discussion

Figure 3.2 shows the changes in the emission intensity of PicoGreen upon addition of complementary (ssDNAp+ $ssDNA_C$) and non-complementary (ssDNAp+$ssDNA_{NC}$) DNA. The fluorescence intensities of PicoGreen solutions increased in the presence of both the complementary (ssDNAp+ $ssDNA_C$) and noncomplementary (ssDNAp+$ssDNA_{NC}$) DNA. However, the fluorescence intensities of PG/(ssDNAp+ $ssDNA_C$) were larger than those of PG/(ssDNAp+$ssDNA_{NC}$), with their fluorescence intensity ratio ranging from 2.6 to 4.0, depending on the base pair/dye ratio. The results showed a fairly good selectivity between complementary and non-complementary DNA when PicoGreen was used as the intercalator.

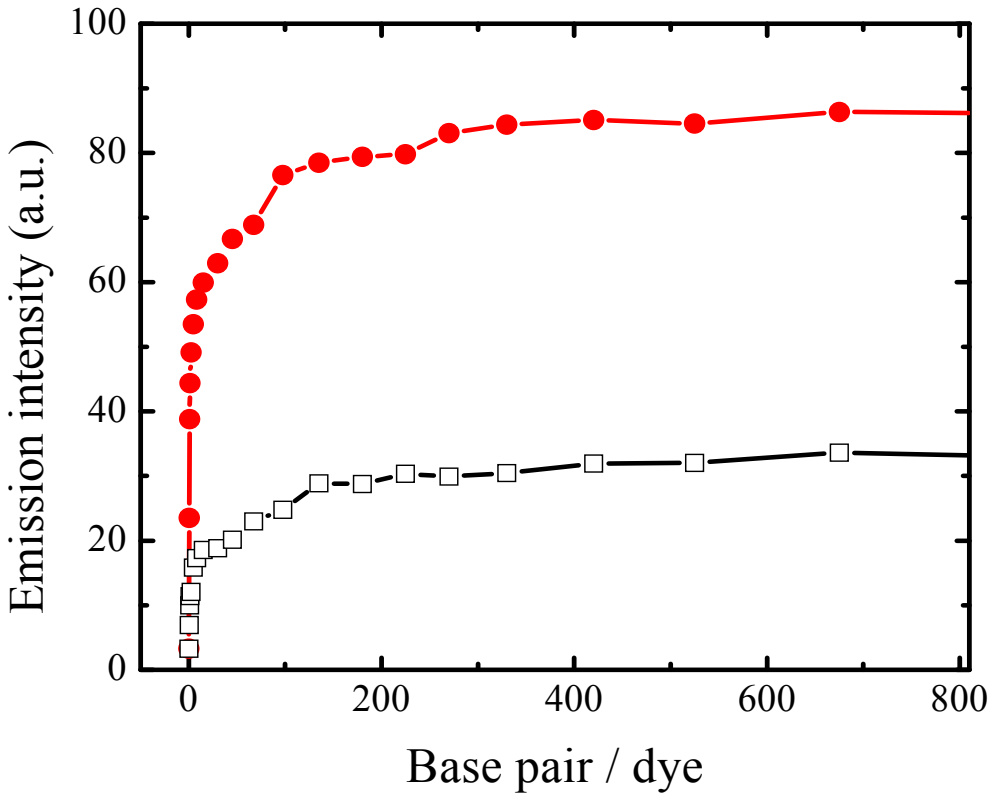

Figure 3.2. Fluorescence intensity titration measurements of PicoGreen with complementary ($ssDNA_p$+$ssDNA_C$, solid circles) and non-complementary ($ssDNA_p$+$ssDNA_{NC}$, open squares) DNA strands.

PFP was further added to enhance the detection sensitivity (Figure 3.3). The emission intensity of PG/($ssDNA_p$+$ssDNA_C$) could be enhanced by up to 19-fold through FRET (when PicoGreen was indirectly excited by FRET under excitation of PFP at 380 nm), compared to that when PG/($ssDNA_p$+$ssDNA_C$) was directly excited at the absorption maxima of PicoGreen at 500 nm in the absence of PFP. This additional fluorescence enhancement implies further improved sensitivity for DNA sequence detection by using conjugated polymers. Detection limit of less than 100pM could be easily achieved using a normal fluorescence spectrometer.

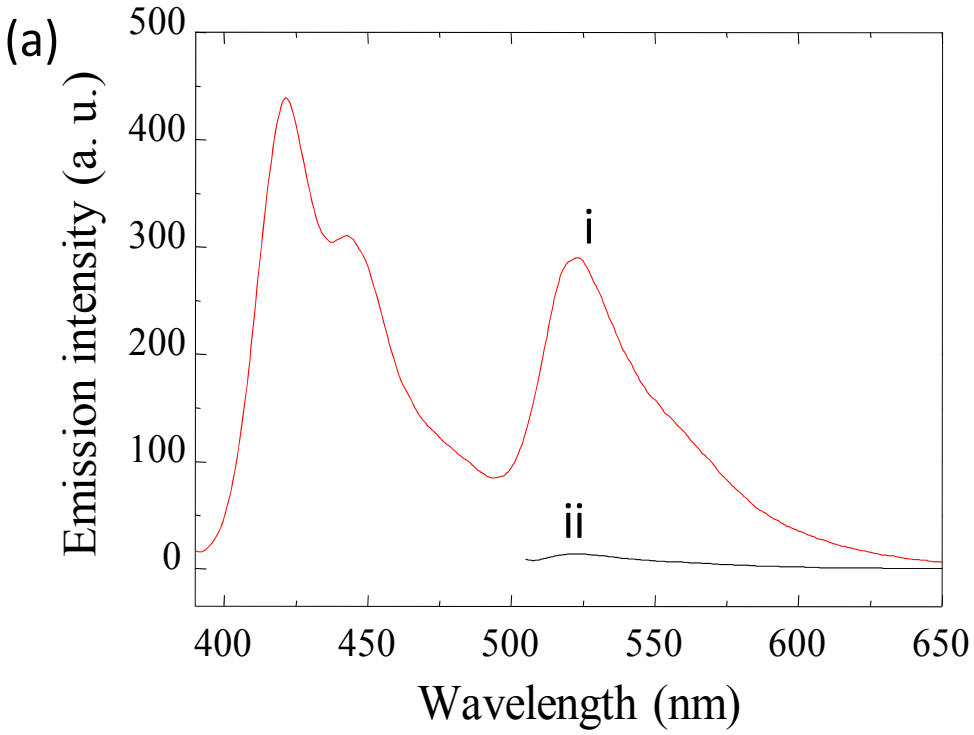
(a)
Emission intensity (a. u.)
500
400
300
200
100
0
i
ii
400
450
500
550
600
650
Wavelength (nm)

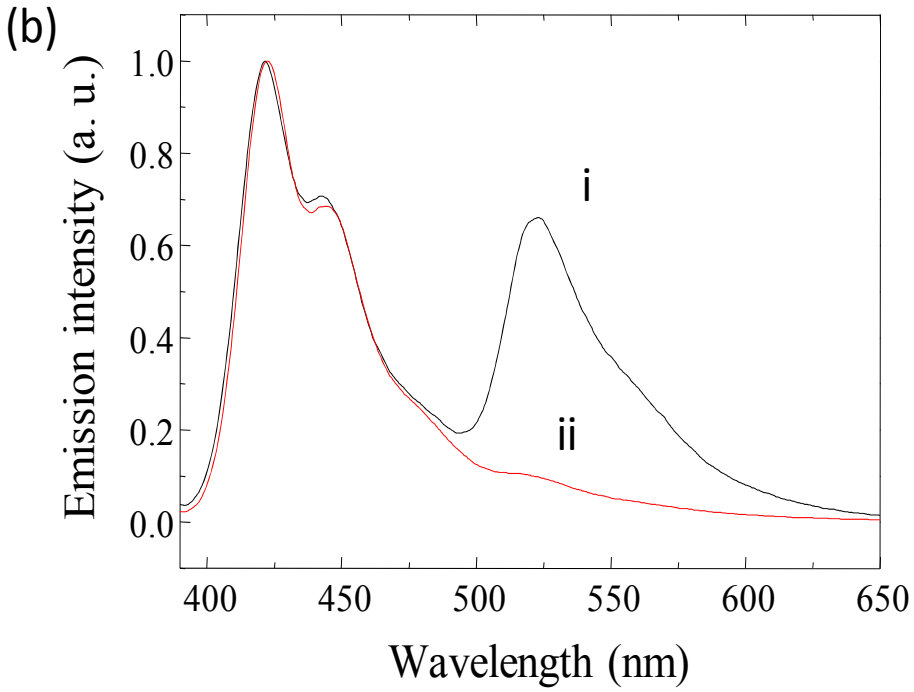
(b)
Emission intensity (a. u.)
1.0
0.8
0.6
0.4
0.2
0.0
i
ii
400
450
500
550
600
650
Wavelength (nm)

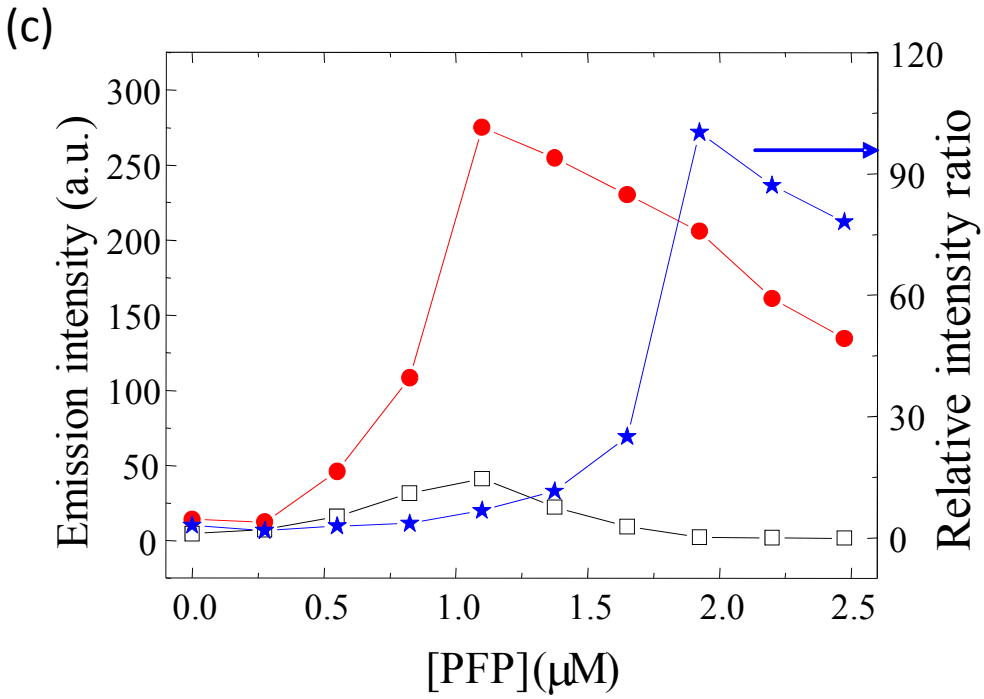

Figure 3.3. (a) Emission spectra of PFP/PG/($ssDNA_p$+$ssDNA_C$) (i, λ_{ex}: 380 nm) and PG/($ssDNA_p$+$ssDNA_C$) (ii, λ_{ex}: 500 nm); (b) Normalized emission spectra of PFP/PG/($ssDNA_p$+ $ssDNA_C$) (i) and PFP/PG/ ($ssDNA_p$ + $ssDNA_{NC}$) (ii), λ_{ex}: 380 nm. [ssDNAp] = [$ssDNA_C$] = [$ssDNA_{NC}$] = $2*10^{-8}$M; [PG] = $4*10^{-8}$ M; [PFP] = $1.38*10^{-6}$ M in repeat units; (c) The emission intensities of PicoGreen at 525 nm in PFP/PG/ ($ssDNA_p$+$ssDNA_C$) (solid circles) and PFP/PG/($ssDNA_p$+ $ssDNA_{NC}$) (open squares) by FRET (λ_{ex}= 380 nm) as well as their relative intensity ratios upon gradual addition of PFP.

In addition to the improved sensitivity, it is very interesting to note that the selectivity between the complementary and non-complementary DNA has also been significantly improved. Figure 3.3b & 3.3c show different emission intensities of PFP/PG/($ssDNA_p$+$ssDNA_C$) and PFP/PG/($ssDNA_p$ + $ssDNA_{NC}$) by FRET under excitation of PFP at 380 nm. In the presence of 1.37 μM of PFP, the PFP/PG/($ssDNA_p$+$ssDNA_C$) (for the complementary DNA strands) samples showed efficienct energy transfer from PFP to PicoGreen. However, in PFP/PG/($ssDNA_p$+$ssDNA_{NC}$) (for the non-complementary DNA strands), nearly no

PicoGreen emisison was observed. The energy transfer efficiency in PG/($ssDNA_p$+$ssDNA_C$) was much higher than that in PG /($ssDNA_p$+$ssDNA_{NC}$). The selectivity has been significantly improved in the presence of PFP. For the given amount of PicoGreen and DNA used, the emission intenisty of PG/($ssDNA_p$+$ssDNA_C$) was only ~3.1 time of that of PG/($ssDNA_p$+$ssDNA_{NC}$). However, when PFP was added, difference in the emission intensity of PicoGreen via FRET for between the complementray and noncomplementary cases became much larger. For example, the emission intensity ratio of PicoGreen in PFP/PG/($ssDNA_p$+$ssDNA_C$) to that in PFP/PG/($ssDNA_p$+ $ssDNA_{NC}$) was 33 by FRET upon addition of 1.65 μM of PFP, and increased even up to ~100 upon addition of 1.9 μM of PFP. Figure 3.3c shows the emission intensities of PicoGreen at 525 nm in the presence of complementary and non-complementary DNA by FRET upon addition of different amounts of PFP (with residue contributions from PFP subtracted). It can be seen that the PicoGreen emission intensities initially increased upon gradual addition of PFP, then decreased upon further addition of PFP, for both complementary and non-complementary cases. The PicoGreen emission in the complementary case was much stronger than that in the non-complementary case. The decrease of PicoGreen emission intensity is likely due to the dissociation of the PicoGreen molecules from DNA when PFP is added. In the presence of the positively charged PFP, PFP will compete with PicoGreen in binding to DNA. Some PicoGreen molecules will be repelled away from DNA and become non-fluorescent. For complementary DNA strands, double stranded DNA (dsDNA) is formed;

PicoGreen molecules mainly bind with dsDNA through the intercalation interactions. While for non-complementary DNA strands, DNA strands remain as distinct single stranded DNA (ssDNA); PicoGreen molecules bind to ssDNA mainly through electrostatic interactions. Electrostatic interaction is a weaker interaction compared to intercalation. PicoGreen molecules are thus more easily repelled away from the single stranded DNA upon the addition of PFP. This effect is further confirmed by inspection of PicoGreen emission intensity under direct excitation of PicoGreen at 500 nm upon gradual addition of PFP (Figure 3.4). When PFP was added, the emission intensities of PG/($ssDNA_p$+ $ssDNA_C$) and PG/($ssDNA_p$+$ssDNA_{NC}$) both decreased. However, the emission of PG/($ssDNA_p$+$ssDNA_{NC}$) decreased faster than PG/($ssDNA_p$+$ssDNA_{NC}$). These results suggest that the binding interaction between PicoGreen and ($ssDNA_p$ +$ssDNA_C$) is stronger than that between PicoGreen and ($ssDNA_p$+$ssDNA_{NC}$). The difference in their binding strength is responsible for the further improved selectivity between the complementary and noncomplementary DNA when PFP is used.

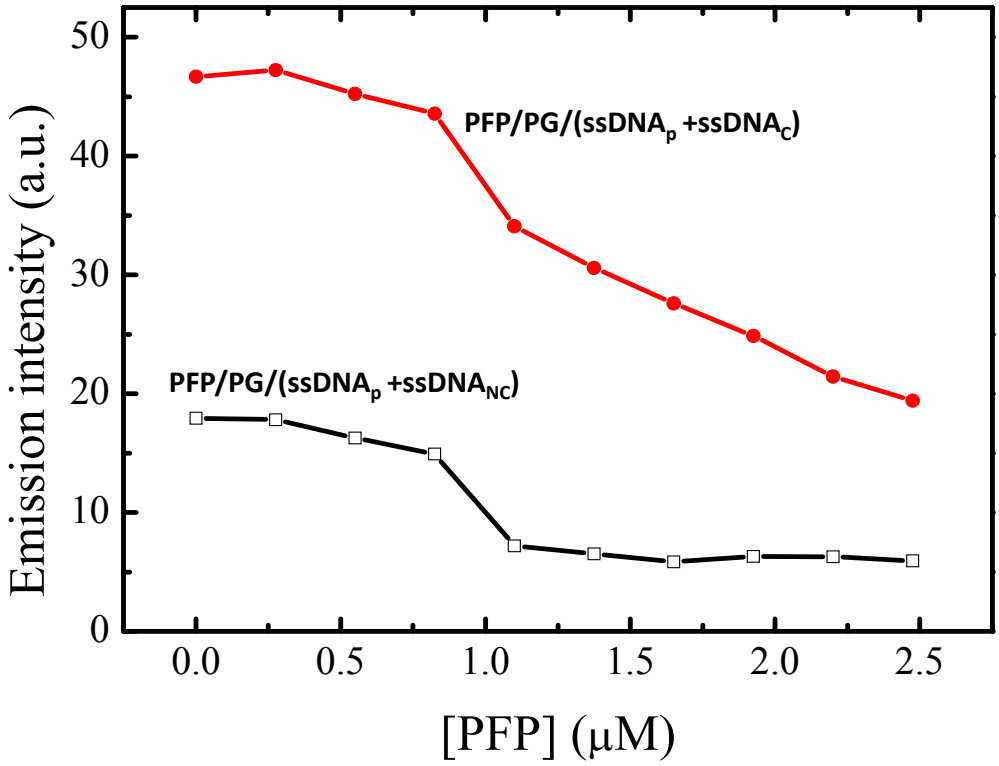

Figure 3.4. Effects of PFP on fluorescence intensity of PFP/PG/(ssDNA$_p$ + ssDNA$_C$) and PFP/PG/(ssDNA$_p$ + ssDNA$_{NC}$) under direct excitation of PicoGreen at 500 nm: [ssDNAp] = [ssDNA$_C$] = [ssDNA$_{NC}$] = 2*10^{-8}M; [PG] = 4*10^{-8} M.

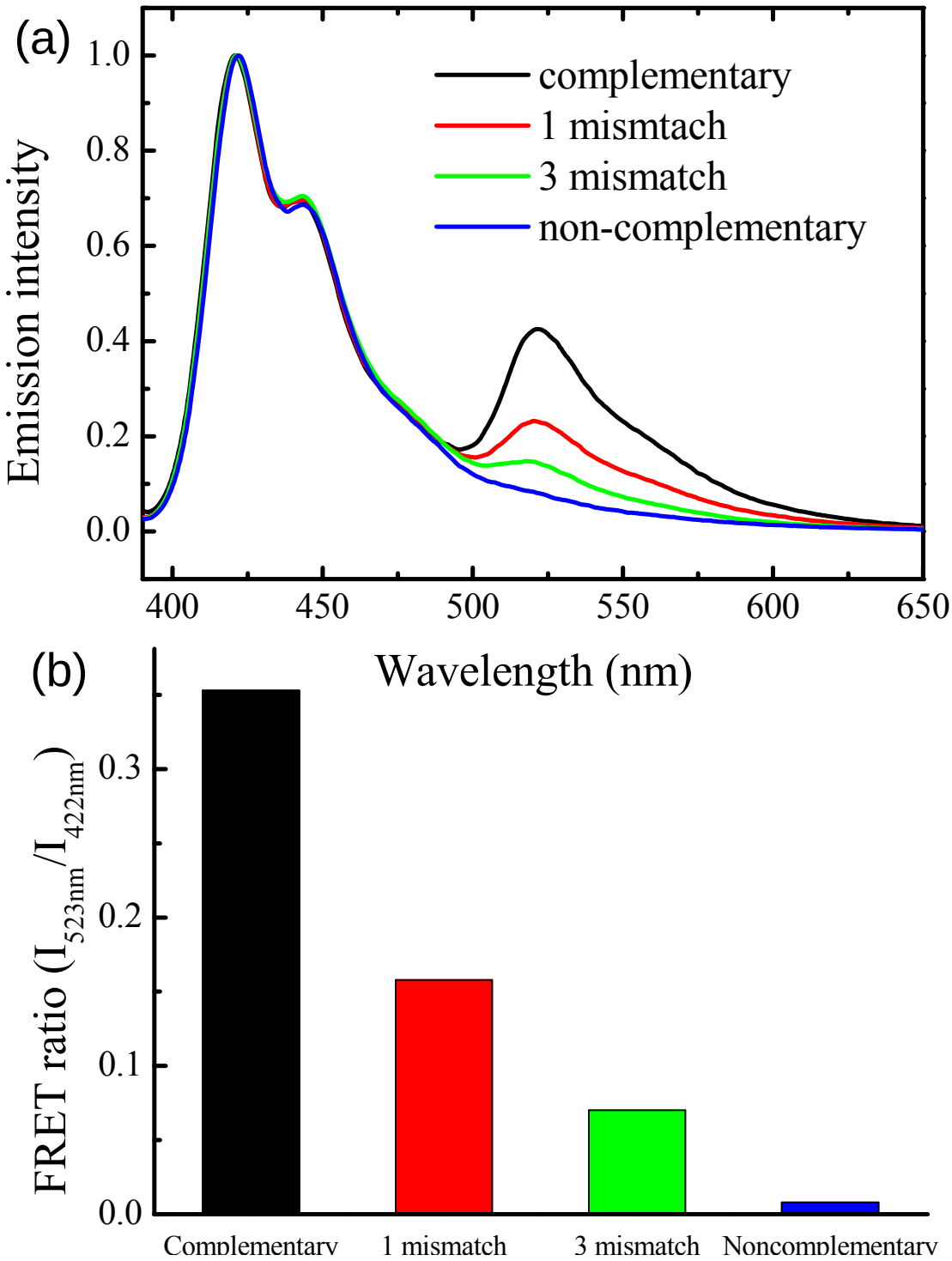

Figure 3.5. Normalized emission spectra (a) and FRET ratio (I_{523nm}/I_{422nm}) (b) of PFP/PG/DNA with increasing number of mismatched base pairs: [ssDNAp] = [$ssDNA_C$] = [$ssDNA_{1NC}$] = [$ssDNA_{3NC}$] = [$ssDNA_{NC}$] = $2*10^{-8}$M; [PG] = $4*10^{-8}$ M; [PFP] = $1.9*10^{-6}$ M in repeat units; λ_{ex}: 380 nm.

The fact that PFP can help to further improve the selectivity can be taken

advantaged to achieve single nucleotide mismatch detection. Figure 3.5 shows the emission spectra of PFP/PG/DNA with increasing number of mismatched base pairs at room temperature (24°C). The energy transfer efficiency became reduced with the increasing number of mismatched base pairs in DNA strands. The emission spectrum of the complexes with one base pair mismatch is distinctively different from that of the fully complementary case. The single base pair mismatch could be easily detected even at the room temperature. This difference could be further improved by raising the temperature (Figure 3.6). At an elevated temperature, 57°C, only the samples with fully complementary DNA strands showed efficient energy transfer (Figure 3.7).

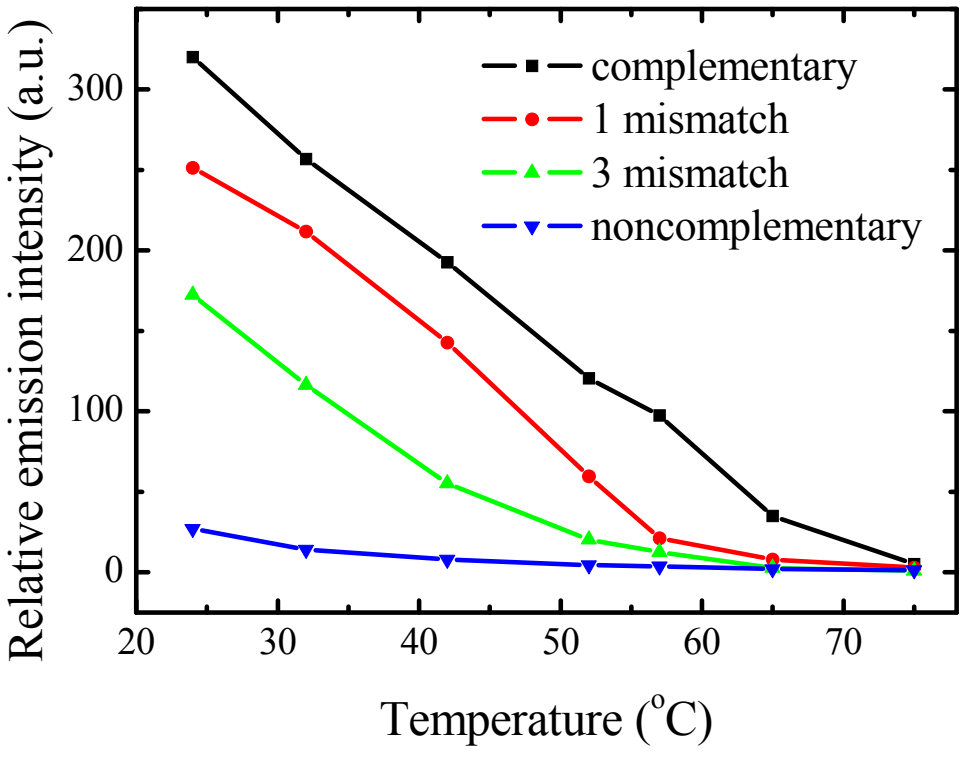

Figure 3.6. The temperature effects on fluorescence intensities of the PFP/PG/DNA via FRET for DNA with different numbers of mismatched base pair. [ssDNAp] = [$ssDNA_C$] = [$ssDNA_{1NC}$] = [$ssDNA_{3NC}$] = [$ssDNA_{NC}$] = $2*10^{-8}$M; [PG] = $4*10^{-8}$ M; [PFP] = $1.1*10^{-6}$ M in repeat units; λ_{ex}: 380 nm.

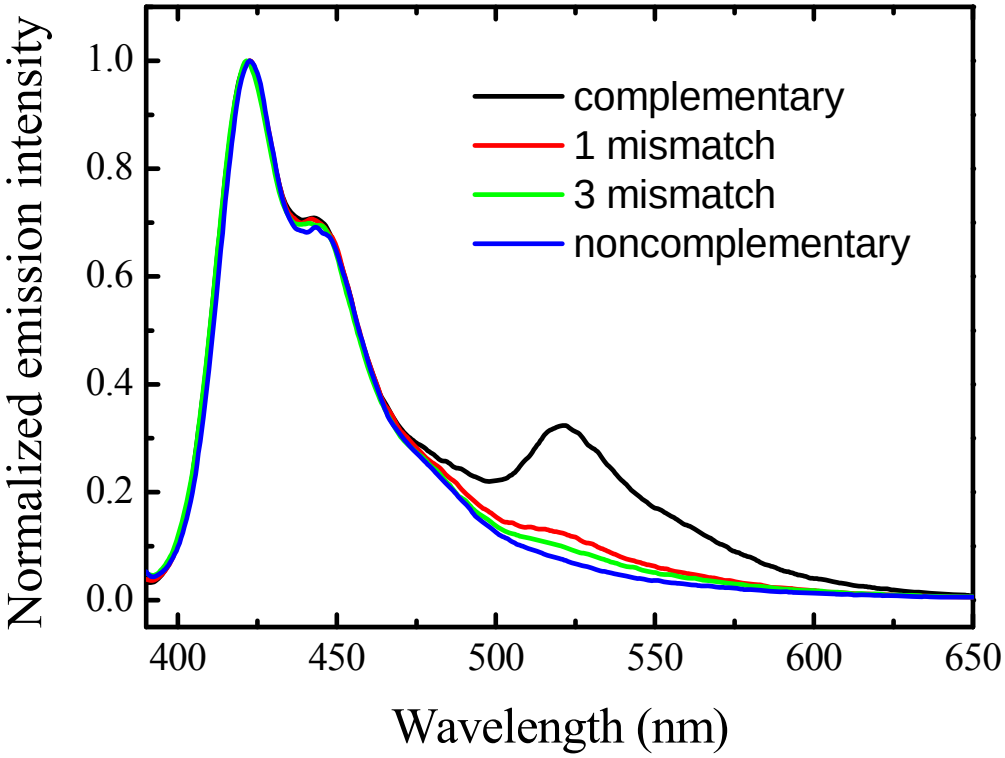

Figure 3.7. Normalized emission spectra of PFP/PG/DNA with different numbers of mismatched base pairs at 57°C: [ssDNAp] = [$ssDNA_C$] = [$ssDNA_{1NC}$] = [$ssDNA_{3NC}$] = [$ssDNA_{NC}$] = $2*10^{-8}$M; [PG] = $4*10^{-8}$ M; [PFP] = $1.1*10^{-6}$ M in repeat units; λ_{ex}: 380 nm.

However, nearly no energy transfer occurred for the complexes with any base pair mismatch. Different combinations of conjugated polymers and DNA interclators were previously used to develop label-free DNA detection (8, 30, 31). It was originally proposed by Wang et. al.(8) They used a combination of PFP and ethidium bromide as the energy donor/acceptor pair in their initial experiments. However, the energy transfer efficiency was not high due to unfavorable orientation between the energy donor and acceptor. To overcome the problem, different approaches have been used, such as introduction of fluorescein label as FRET gate (8) or synthesis of new conjugated materials with specific shape and spatial registry (31), which either lose

the advantage of label free detection or increase the protocol complexity and the cost. Liu et. al. (30) also used a combination of PFP and thiazole orange and demonstrated that energy transfer was more efficient for G-rich single stranded DNA, which could be used for detection of DNA involving G-rich sequences. Their approach was limited to G-rich DNA only and the universality was lost. Even though a few previously reported methods can also achieve high selectivity to distinguish single-nucleotide mistatch (9-14), these methods either need sophosticated processes, or expensive PNA, DNAzymes, fluorescent labeling, or lack of universality. In this report, we report a universal and genuine label-free DNA detection method with high sesnitivity and exceptional selectivity. The materials used are all commercially available. It is low cost, simple to use, and works in a "mix-and-detect" manner. The cationic conjugated polymer was used to improve both the sensitivity and selectivity. The single base pair mismatch could be easily detected even at the room temperature.

3.4 Conclusion

In summary, we have demonstrated that PicoGreen can be used in combination with cationic conjugated polymers to develop label free DNA sensors with enhanced detection efficiency and further improved selectivity. The detection sensitivity could be improved by up to 19-fold through FRET using PFP as a light harvesting complex, to take advantage of its collective optical response and optical amplification effects. The selectivity has also been significantly improved due to the addition of cationic conjugated polymers. The single nucleotide mismatch detection

has been demonstrated even at the room temperature. The improved selectivity is ascribed to the stronger binding interaction between PicoGreen with dsDNA compared to that between PicoGreen and ssDNA, which results in selective repelling of PicoGreen away from the DNA strands.

3.5 References

1. Stork, M., Gaylord, B. S., Heeger, A. J. & Bazan, G. C. (2002) *Advanced Materials* **14**, 361-366.

2. Balakin, K. V., Korshun, V. A., Mikhalev, II, Maleev, G. V., Malakhov, A. D., Prokhorenko, I. A. & Berlin, Y. A. (1998) *Biosensors & Bioelectronics* **13**, 771-778.

3. Taton, T. A., Mirkin, C. A. & Letsinger, R. L. (2000) *Science* **289**, 1757-1760.

4. Kushon, S. A., Ley, K. D., Bradford, K., Jones, R. M., McBranch, D. & Whitten, D. (2002) *Langmuir* **18**, 7245-7249.

5. Ho, H. A., Boissinot, M., Bergeron, M. G., Corbeil, G., Dore, K., Boudreau, D. & Leclerc, M. (2002) *Angewandte Chemie-International Edition* **41**, 1548-1551.

6. Fan, C. H., Plaxco, K. W. & Heeger, A. J. (2003) *Proceedings of the National Academy of Sciences of the United States of America* **100**, 9134-9137.

7. Gaylord, B. S., Heeger, A. J. & Bazan, G. C. (2002) *Proceedings of the National Academy of Sciences of the United States of America* **99**, 10954-10957.

8. Wang, S., Gaylord, B. S. & Bazan, G. C. (2004) *Journal of the American Chemical Society* **126**, 5446-5451.

9. Xu, H., Wu, H. P., Huang, F., Song, S. P., Li, W. X., Cao, Y. & Fan, C. H. (2005) *Nucleic Acids Research* **33**, e83.

10. Gaylord, B. S., Massie, M. R., Feinstein, S. C. & Bazan, G. C. (2005)

Proceedings of the National Academy of Sciences of the United States of America **102**, 34-39.

11. He, F., Tang, Y. L., Yu, M. H., Feng, F., An, L. L., Sun, H., Wang, S., Li, Y. L., Zhu, D. B. & Bazan, G. C. (2006) *Journal of the American Chemical Society* **128**, 6764-6765.

12. Tian, N., Tang, Y. L., Xu, Q. H. & Wang, S. (2007) *Macromolecular Rapid Communications* **28**, 729-732.

13. Feng, X. L., Duan, X. R., Liu, L. B., An, L. L., Feng, F. D. & Wang, S. (2008) *Langmuir* **24**,12138-12141

14. He, F., Feng, F., Duan, X. R., Wang, S., Li, Y. L. & Zhu, D. B. (2008) *Analytical Chemistry* **80**, 2239-2243.

15. Thomas, S. W., Joly, G. D. & Swager, T. M. (2007) *Chemical Reviews* **107**, 1339-1386.

16. Fan, C. H., Plaxco, K. W. & Heeger, A. J. (2002) *Journal of the American Chemical Society* **124**, 5642-5643.

17. He, F., Tang, Y. L., Wang, S., Li, Y. L. & Zhu, D. B. (2005) *Journal of the American Chemical Society* **127**, 12343-12346.

18. Tian, N. & Xu, Q. H. (2007) *Advanced Materials* **19**, 1988-1991.

19. Ho, H. A. & Leclerc, M. (2004) *Journal of the American Chemical Society* **126**, 1384-1387.

20. Liu, B., Wang, S., Bazan, G. C. & Mikhailovsky, A. (2003) *Journal of the American Chemical Society* **125**, 13306-13307.

21. Chen, L. H., McBranch, D. W., Wang, H. L., Helgeson, R., Wudl, F. & Whitten, D. G. (1999) *Proceedings of the National Academy of Sciences of the United States of America* **96**, 12287-12292.

22. Dwight, S. J., Gaylord, B. S., Hong, J. W. & Bazan, G. C. (2004) *Journal of the American Chemical Society* **126**, 16850-16859.

23. Forster, T. (1948) *Annals of Physics* **2**, 55.

24. Lakowicz, J. R., (2006) *Principles of fluorescence spectroscopy*. 3rd ed.; Springer: New York.

25. Scholes, G. D. (*2003) Annual Review of Physical Chemistry* **54**, 57-87.

26. Xiao, Y., Lubin, A. A., Heeger, A. J. & Plaxco, K. W. (2005) *Angewandte Chemie-International Edition* **44**, 5456-5459.

27. Xiao, Y., Qu, X. G., Plaxco, K. W. & Heeger, A. J. (2007) *Journal of the American Chemical Society* **129**, 11896-11897.

28. Neidle, S., (2002) *Nucleic acid structure and recognition*. Oxford University Press: Oxford; New York.

29. Singer, V. L., Jones, L. J., Yue, S. T. & Haugland, R. P. (1997) *Analytical Biochemistry* **249**, 228-238.

30. Liu, B. & Bazan, G. C. (2007) *Macromolecular Rapid Communications* **28**, 1804-1808.

31. Liu, B., Dan, T. T. T. & Bazan, G. C. (2007) *Advanced Functional Materials* **17**, 2432-2438.

Chapter4

Highly Sensitive and Selective Detection of Mercury Ions by Using Oligonucleotides, DNA Intercalators and Conjugated Polymers

4.1 Introduction

Development of highly sensitive and selective methods to detect mercury (Hg) contaminant in aqueous media is of great interest due to the serious threat of mercury pollution to human health and environment (1-3). A variety of optical methods have been developed for the detection of mercury ions using organic chromophores (4-9), oligonucleotides (10-14), conjugated polymers (10, 13, 15), metal nanoparticles (16, 17), semiconductor quantum dots (18) and DNAzymes (19). Many mercury detection methods work in a "turn-off" mode (4, 5, 9, 11-13, 15), since heavy metal ions such as Hg^{2+}, usually serve as a fluorescence quencher. The sensor schemes working in a "turn-off" mode usually have limited sensitivity. Most mercury detection methods have a detection limit of μM or above. Recently a lot of efforts have been directed toward development of "turn-on" sensor schemes with improved sensitivity by using small molecules (5, 14), conjugated polymers (10) and DNAzymes (19). Exceptional detection limits as low as 40 nM and even 3 nM have been achieved (10, 14, 19).

Conjugated polymers are known to provide an advantage of collective optical response. They can function as light harvesting materials and exhibit optical amplification via Föster resonance energy transfer (FRET) (20-24). Because of these exceptional properties, conjugated polymers offer potential use in detecting biological and chemical target molecules with high sensitivity (20-24). It has been reported that mercury ions can selectively link T-T pairs to form T-Hg^{2+}-T complexes (10-14). This phenomenon has been utilized to develop highly selective mercury sensors (10-14). Inspired by the previous work on use of conjugated polymers and DNA intercalators for DNA sequence detections (23), here we report a label free method to detect Hg^{2+} with high sensitivity and selectivity in aqueous mediums, by combining the advantages of specific binding interactions between Hg^{2+} and thymine, and optical amplification properties of conjugated polymers.

4.2 Experimental

4.2.1 Materials

The cationic conjugated polymer, Poly (9, 9–bis (6-*N*, *N*, *N*-triethylammonium) -hexyl-fluorene phenylene) (PFP) containing iodide counter anions was obtained from American Dye Source (Catalog No: ADS181BE). The molecular weight is 10000 – 15000. The PFP was dissolved in DMF to get a stock solution of which the concentration is $1*10^{-3}$ M, then dilute to concentration we need by water.

T_{24} DNA was obtained from Sigma-Aldrich. The concentration of DNA was determined by measuring its absorbance at 260 nm in a 200 μL quartz cuvette. The function for ssDNA concentration calculation is [ssDNA] =$33*10^{-2}$*A/MW

A refers to UV absorption at 260nm of ssDNA in 1mm cuvette. MW refers to molecular weight of ssDNA.

YOYO-1 and TOTO-1 was from Invitrogen. Other chemicals were all from Sigma. The molecular structures of chemicals and sequence of T24 DNA was shown in Table 4.1.

Table 4.1 Molecular Structures of PFP, YOYO-1, TOTO-1 and sequences of T24 DNA.

PFP	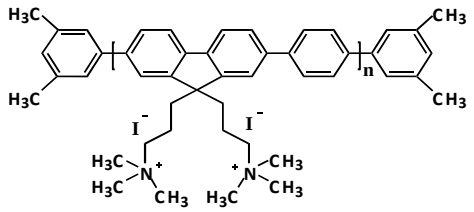
YOYO-1	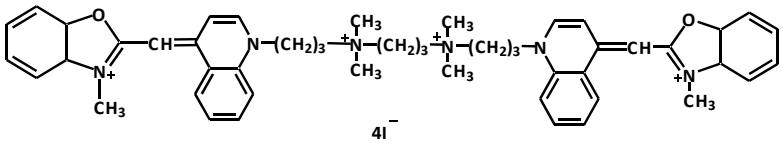
TOTO-1	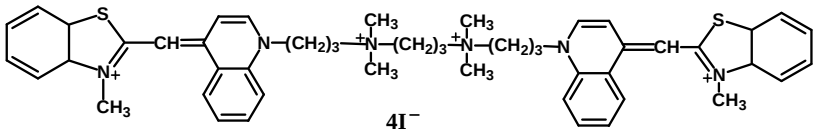
T24-DNA	5'---TTTTTTTTTTTTTTTTTTTTTTTT---3'

Measurements were performed in phosphate buffer (50 mM, PH = 7.0) at room temperature.

4.2.2 Methods: One-photon and two-photon excitation fluorescence measurements

UV-Vis absorption spectra were measured with a SHIMADZU UV-2450 spectrophotometer and fluorescence measurements were performed using a Perkin-Elmer fluoremeter.

The experimental setup for two-photon excitation (TPE) fluorescence was shown in Scheme 4.1. The excitation source for two-photon excitation fluorescence is a femtosecond Ti:sapphire oscillator from Spectra Physics (Tsunami). The output laser pulses have pulse duration of 40 fs with a repetition rate of 76 MHz and center wavelength at 800 nm. The total output energy is 300 mW.

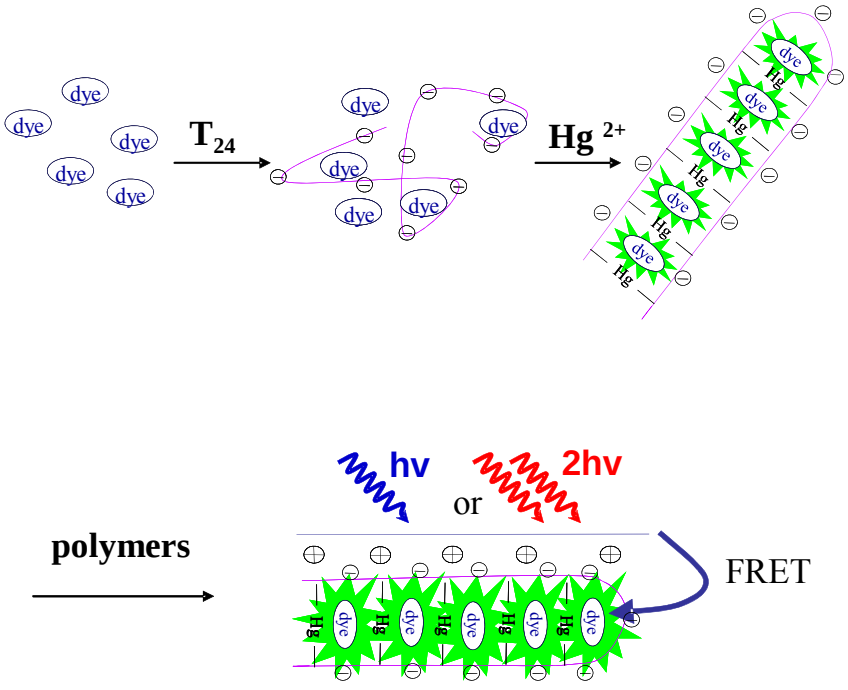

Scheme 4.1 Schematic representation of our Hg^{2+} sensor

The system uses a combination of oligonucleotides, DNA intercalators and conjugated polymers (shown in Scheme 4.1). This method is simple and rapid,

working in a fluorescence "turn-on" manner. In the absence of Hg^{2+}, poly-T exists in a random-coil structure in aqueous solutions. Because the interactions between the randomly coiled poly-T and DNA intercalator are weak and fluorescence quantum yield of the complex is usually low, the fluorescence of such a mixture is weak. In the presence of Hg^{2+}, T-Hg^{2+}-T complex formation induces poly-T changing its random-coil conformation to that of a folded "dsDNA-like" structure. Because some DNA intercalators have a high affinity for dsDNA over random coiled ssDNA and the fluorescence quantum yield significantly increases upon binding to dsDNA (25), the fluorescence intensity of the DNA intercalator significantly increases in the presence of Hg^{2+}. DNA intercalators, such as TOTO-3, were recently used to detect Hg^{2+} with high sensitivity. During the reviewing process of this work, Wang et. al.(26) reported a similar approach by using sybr Green I and mercury specific DNA and achieved a sensitivity of 1.3 nM. In this work, we used a cationic conjugated polymer to further improve the sensitivity through optical amplification effects. YOYO-1 and TOTO-1 were used as DNA intercalator instead, because their absorption spectrum overlaps well with the emission spectra of the conjugated polymer used, to ensure efficient energy transfer between conjugated polymers and DNA intercalator. The electrostatic interactions between the positively charged polymers and negatively charged oligonucleotides will bring the conjugated polymers and intercalators into close proximity and efficient energy transfer from conjugated polymers to the intercalators will occur. The energy transfer process will result in amplification of fluorescence

signals due to large overall absorption cross sections and collective optical response of the conjugated polymers.

4.3 Results and Discussion

Figure 4.1 shows the fluorescence spectra of YOYO-1/T_{24} in the absence and presence of Hg^{2+}. The fluorescence of YOYO-1 (75 nM) in 50 mM PBS buffer (pH=7.4) in the presence of T_{24} (50 nM) is very weak when excited at its absorption maxima of YOYO-1 at 490 nm. Upon gradual addition of Hg^{2+} into the mixture of YOYO-1 and T_{24}, the fluorescence intensity of YOYO-1 gradually increases. The enhancement factor increases up to 6.6 times when [Hg^{2+}] increases to 2.0 μM. The limit of detection (LOD) was estimated to be 3.2 nM at a signal-to-noise ratio of 3.

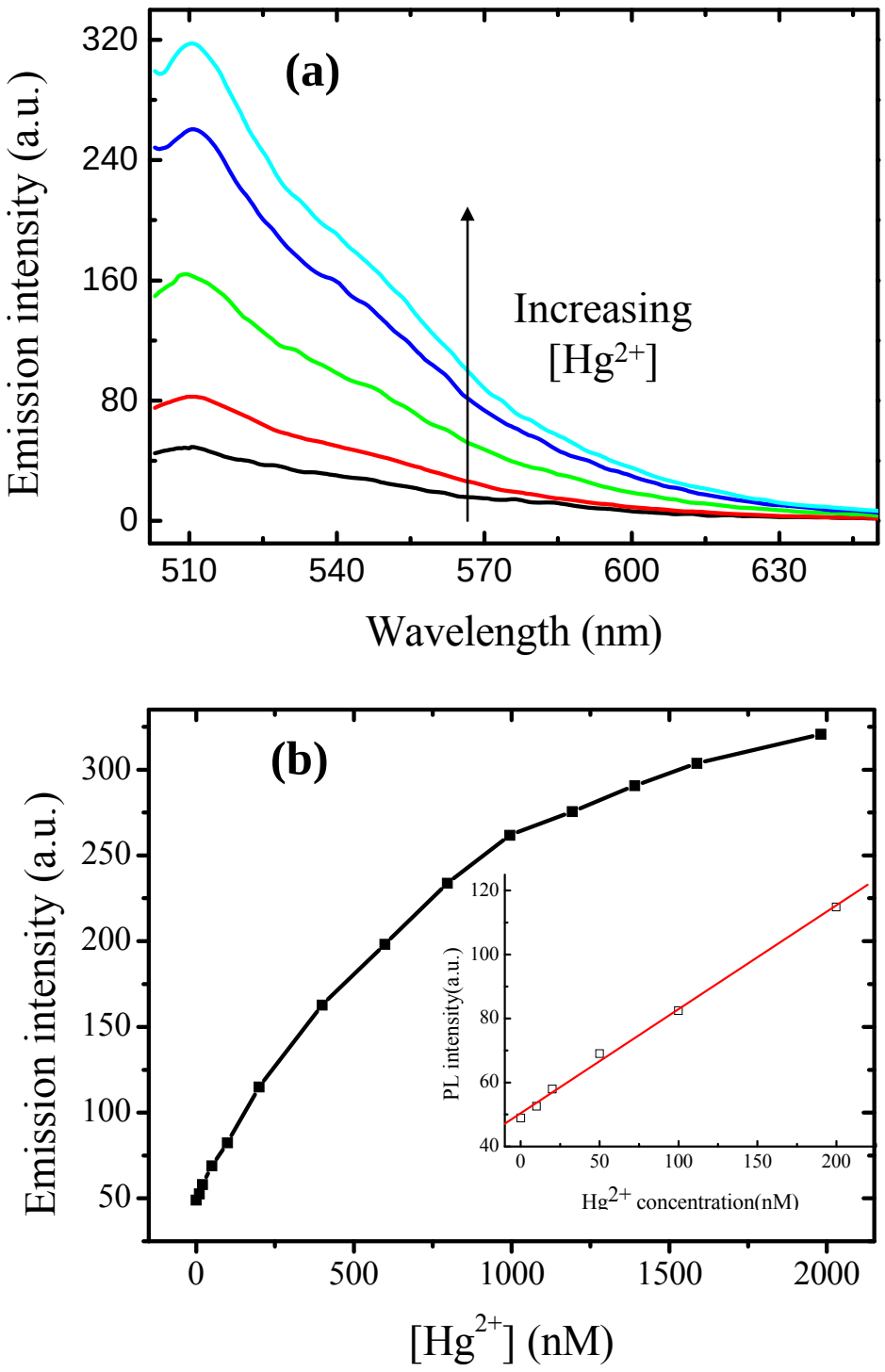

Figure 4.1 (a) Emission spectra of YOYO-1/T_{24} after addition of different amounts of Hg^{2+} (0, 100, 400, 1000 and 2000 nM): [YOYO-1] = 75 nM; [T_{24}]=50 nM; λ_{ex}=490 nm; (b) Emission intensities of YOYO-1/T_{24} at 510 nm with titration of Hg^{2+}.

The specificity of this method was demonstrated by performing similar experiments using other metal ions such as Na^{+}, K^{+}, Mg^{2+}, Fe^{3+}, Cu^{2+}, Zn^{2+}, Pb^{2+},

Cd^{2+}, Ag^{+}, Au^{3+} and Ca^{2+} under the same experimental conditions as that of Hg^{2+}. In contrast to significant fluorescence enhancement as observed for Hg^{2+}, little change or even quenching in the fluorescence intensity of YOYO-1/T_{24} was observed upon addition of these metal ions (Figure 4.2). This result indicates that YOYO-1/T_{24} probe is highly selective for Hg^{2+} over other metal ions. The specific detection of Hg^{2+} is attributed to the formation of a stable T-Hg^{2+}-T complex and consequently a folded "dsDNA-like" hairpin structure. The formation of T-Hg^{2+}-T complex has been previously demonstrated with NMR spectra by Miyake et al.(11) YOYO-1 binds strongly to this folded DNA hairpin structure and thus exhibits a large increase in its fluorescence quantum yield.

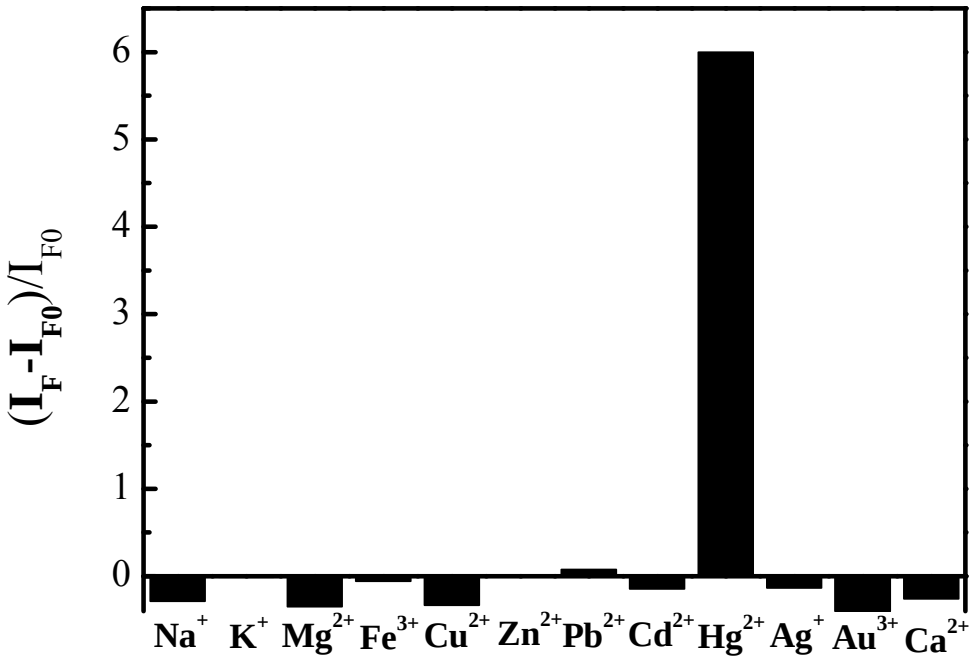

Figure 4.2 Relative fluorescence intensity increases [(I_F-I_{F0})/ I_{F0}] at 510 nm of T_{24}/YOYO-1/metal ions in 50mM (pH=7.4) PBS buffer solution: [T_{24}]=50 nM; [YOYO-1]=75 nM; [metal ions]= 2.0 μM; λ_{ex}=490 nm. I_{F0} and I_F are fluorescence intensities of T_{24}/YOYO-1complex at 510 nm in the absence and presence of metal ions, respectively.

Next, we used a cationic conjugated polymer, PFP, to further improve its sensitivity by utilizing optical amplification properties of conjugated polymers through FRET. In a solution containing YOYO-1(75 nM), T_{24} (50 nM) and Hg^{2+} (2.0 μM), PFP solution is gradually added and the emission spectra were measured with an excitation wavelength of 380 nm, near the absorption maxima of PFP. The emission of YOYO-1 was further enhanced upon gradual addition of PFP (Figure 4.3a). Additional enhancement of 12-fold in its emission intensity was obtained when 1.24 μM of PFP was added. Based on this further enhancement, the LOD could be improved up to 0.27 nM. This is an exceptionally low LOD for mercury detection using optical methods, much lower than maximum level of mercury permitted by USA EPA in the drinking water: sub-10 nM.

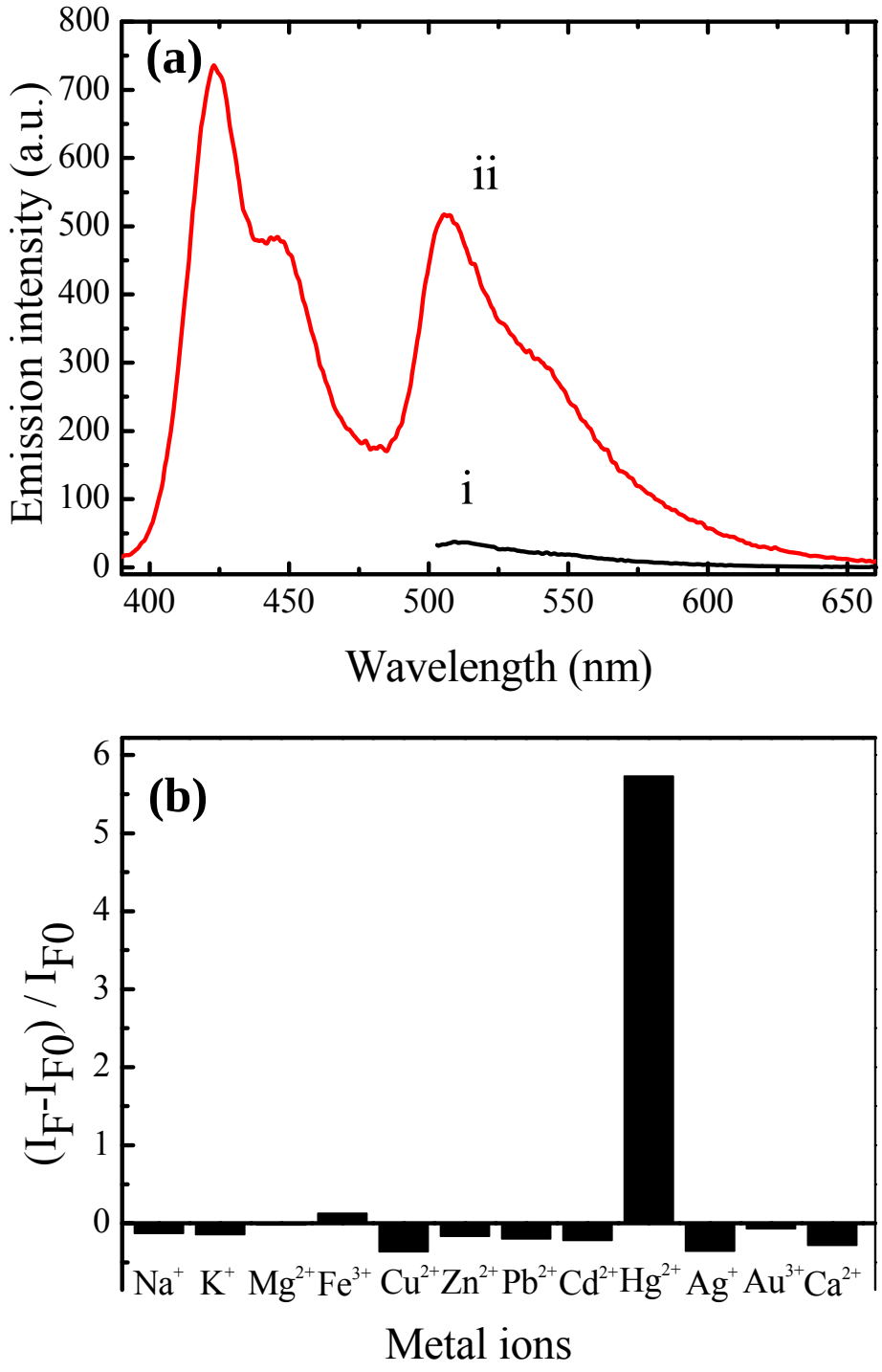

Figure 4.3. (a) Emission spectra of T_{24}/YOYO-1/ Hg^{2+} in the absence (i) and presence (ii) of PFP in 50 mM (pH = 7.4) PBS buffer solution; (b) Relative fluorescence intensity increases $[(I_F-I_{F0})/ I_{F0}]$ at 510 nm of PFP/T_{24}/YOYO-1/metal ions: [PFP] = 1.24 μM; [T_{24}]=50 nM; [YOYO-1] = 75 nM; [metal ions]= 2.0 μM; λ_{ex}=380 nm. I_{F0} and I_F are fluorescence intensities of PFP/T_{24}/YOYO-1 complex in the absence and presence of metal ions, respectively.

The specificity of this method in the presence of conjugated polymers was also demonstrated by performing similar experiments for different metal ions (PFP/YOYO-1/T_{24}/Metal ions) under the same experimental conditions. The results (Figure 4.3b) show high selectivity for Hg^{2+} over other metal ions, similar to that in the absence of conjugated polymers (Figure 4.2). Little change or even quenching in the fluorescence intensity of YOYO-1/T_{24} was observed upon addition of these metal ions, in contrast to significant fluorescence enhancement as observed for Hg^{2+}.

Conjugated polymers are also known to have large two-photon absorption cross sections and can display significantly enhanced two-photon excitation (TPE) fluorescence by FRET (27). The TPE fluorescence of T_{24}/YOYO-1 in the absence and presence of PFP have also been measured using femtosecond laser pulses at 800 nm (Figure 4.4). Addition of conjugated polymers can enhance the TPE emission of YOYO-1 by a factor of up to 37 times compared to that in the absence of PFP. Two-photon excitation has unique advantages such as deep penetration and 3D capability. One-photon excitation is known to have limited penetration depth in biological environments. Two-photon sensing can overcome the limitation of conventional one-photon sensing to enable detections deep into biological environments such as cells and tissues. This result suggests that the proposed scheme could also be used as a two-photon sensor to detect mercury ions deep into cells or tissues, with significant improved sensitivity. A detection limit of as low as ~6 nM could be achieved under two-photon excitation.

We have also performed the experiments using another DNA intercalator, TOTO-1, to substitute YOYO-1. Similar results have been obtained as that for YOYO-1.

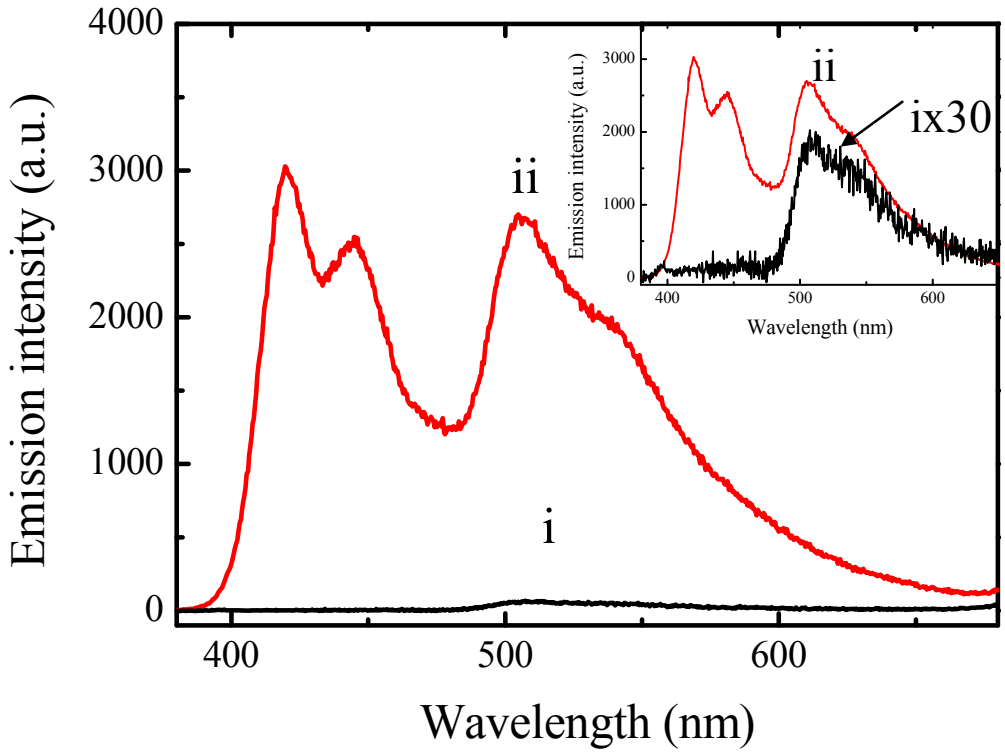

Figure 4.4. Two-photon excitation (λ_{ex}=800 nm) emission spectra of T_{24}/YOYO-1/ Hg^{2+} in the absence (i) and presence (ii) of PFP: [T_{24}] =50 nM, [YOYO-1] = 75 nM; [Hg^{2+}] =2.0 μM; [PFP] = 1.24 μM; The inset shows the comparison of two-photon emission spectra of (i) amplified by 30 times and (ii).

We have also performed the same experiments using another DNA intercalator, TOTO-1 to substitute YOYO-1. TOTO-1/T_{24} is less fluorescent than YOYO-1/T_{24}. The maxima absorption wavelength of TOTO-1 is located at ~510 nm, red shifted compared to that of YOYO-1 (~490 nm). The overlap between the emission spectrum of PFP and the absorption spectrum of TOTO-1 is smaller than that of PFP/YOYO-1

pair. The energy transfer from the conjugated polymer, PFP, to TOTO-1 is thus not as efficient as that between PFP and YOYO-1, as indicated by our experimental results.

Addition of Hg^{2+} into TOTO-1/T_{24} resulted in a fluorescence enhancement of 9.6 times (Figure 4.5). The use of TOTO-1 also showed exceptional selectivity for Hg^{2+} over other metal ions (Figure 4.6). Further addition of PFP results in additional enhancement factor of 7.9 (Figure 4.7). The overall limit of detection was estimated to be about 0.38 nM.

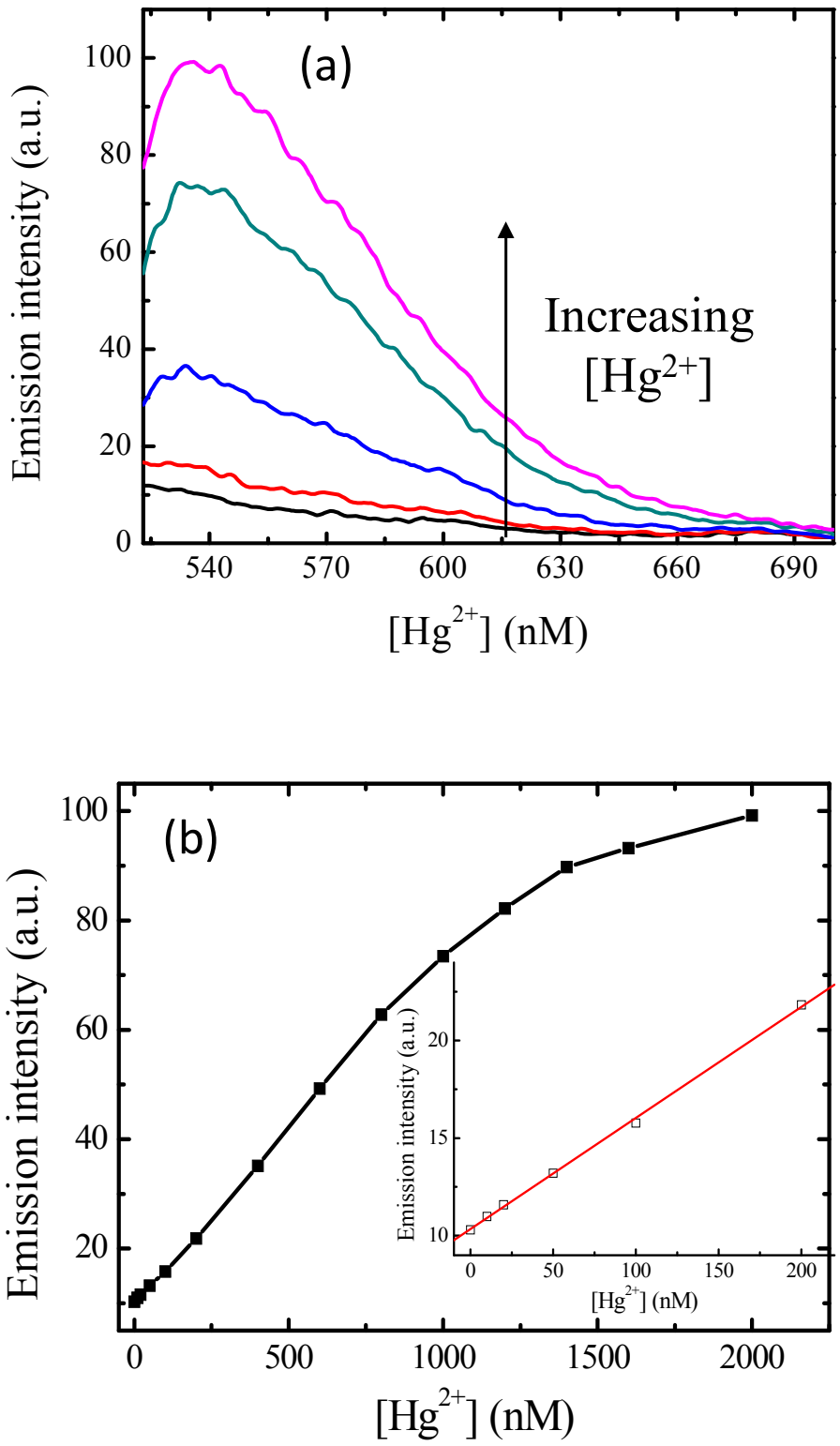

Figure 4.5. (a) Emission spectra of TOTO-1/T_{24} after addition of different amounts of Hg^{2+} (0, 100, 400, 1000 and 2000 nM): [TOTO-1] = 75 nM; [T_{24}] = 50 nM; λ_{ex}=510 nm; (b) Emission intensities of TOTO-1/T_{24} at 535 nm with titration of Hg^{2+}.

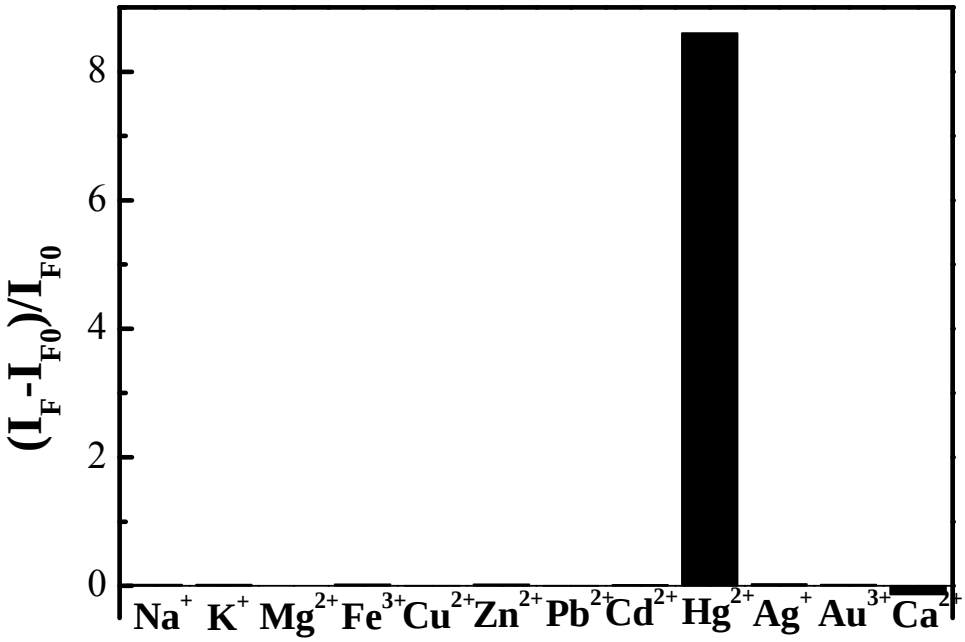

Figure 4.6. Relative fluorescence increases [(I_F-I_{F0})/ I_{F0}] at 535 nm of T24/TOTO-1/metal ions in 50 mM (pH=7.4) PBS buffer solution: [T24] = 50 nM; [TOTO-1] = 75 nM; [metal ions] = 2.0 μM; λex = 510 nm. I_{F0} and I_F are fluorescence intensities of T24/TOTO-1 complex at 535 nm in the absence and presence of metal ions respectively.

Comparison of the data in Figure 4.3 and Figure 4.7 shows that the acceptor/donor intensity ratios are quite different when TOTO-1 or YOYO-1 was used as the intercalator, even though the enhancement factors for TOTO-1 (7.9) and YOYO-1 (12) are only slightly different after conjugated polymers was used to improve the detection sensitivity. The large difference in their acceptor /donor intensity ratios is mainly due to different fluorescence efficiencies of the two acceptors. Upon intercalation, the fluorescence yield of YOYO-1 is about four times higher than that of TOTO-1, which will result in a larger difference in their acceptor/donor intensity ratios in their fluorescence spectra.

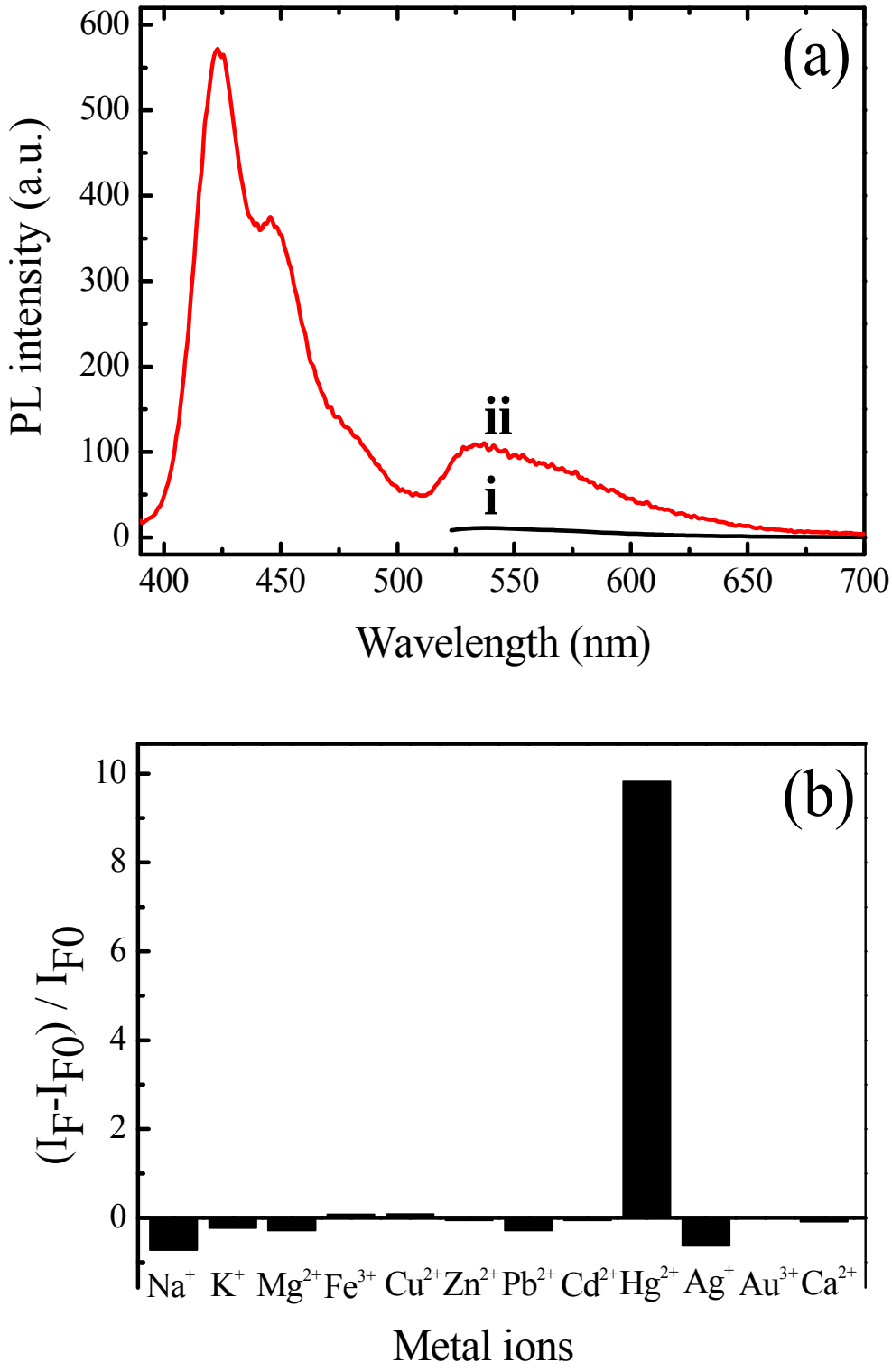

Figure 4.7. (a) Emission spectra of T_{24}/TOTO-1/ Hg^{2+} in the absence (i) and presence (ii) of PFP; (b) Relative fluorescence intensity increases $[(I_F-I_{F0})/ I_{F0}]$ at 535 nm of PFP/T_{24}/TOTO-1/metal ions: [PFP] = 1.24 μM; [T_{24}]=50 nM; [TOTO-1]=75 nM; [metal ions]= 2.0 μM; λ_{ex}=380 nm. I_{F0} and I_F are fluorescence intensities of PFP/T_{24}/TOTO-1 complex in the absence and presence of metal ions, respectively.

Our results also suggest that Hg^{2+} will significantly affect the interactions between the intercalator and DNA. The interactions between Hg^{2+} and thymine will result in formation of a stable T-Hg^{2+}-T complex that leads to a "dsDNA-like" or partially folded structure. The DNA intercalators (YOYO-1 and TOTO-1) will bind strongly to the "dsDNA-like" hairpin structure, and consequently, intercalators will exhibit a large increase in their fluorescence quantum yields. It has been widely known that the fluorescence intensities of these DNA intercalators increase significantly upon binding to dsDNA. But, on the other hand, the existence of Hg^{2+} will also introduce steric and electrostatic hindrance for the intercalators binding to DNA. Because of this, the fluorescence intensity of YOYO-1 only increased about 17 times in total (2.6-fold increase due to addition of T_{24} and another 6.6-fold increase when mercury ions were added), which is much lower than the previously reported up to 460-fold fluorescence enhancement when YOYO-1 was intercalated into the normal dsDNA. These results suggested that the interaction between YOYO-1 and T_{24}/Hg is much weaker than that between YOYO-1 and the normal dsDNA.

The two-photon excitation (TPE) fluorescence of T_{24}/YOYO-1 in the absence and presence of PFP have also been measured using femtosecond laser pulses at 800 nm (Figure 4.8). Addition of conjugated polymers (PFP) can enhance the TPE emission of YOYO-1 by a factor of up to 37 times compared to that in the absence of PFP. A detection limit of as low as ~6 nM could be achieved under two-photon excitation.

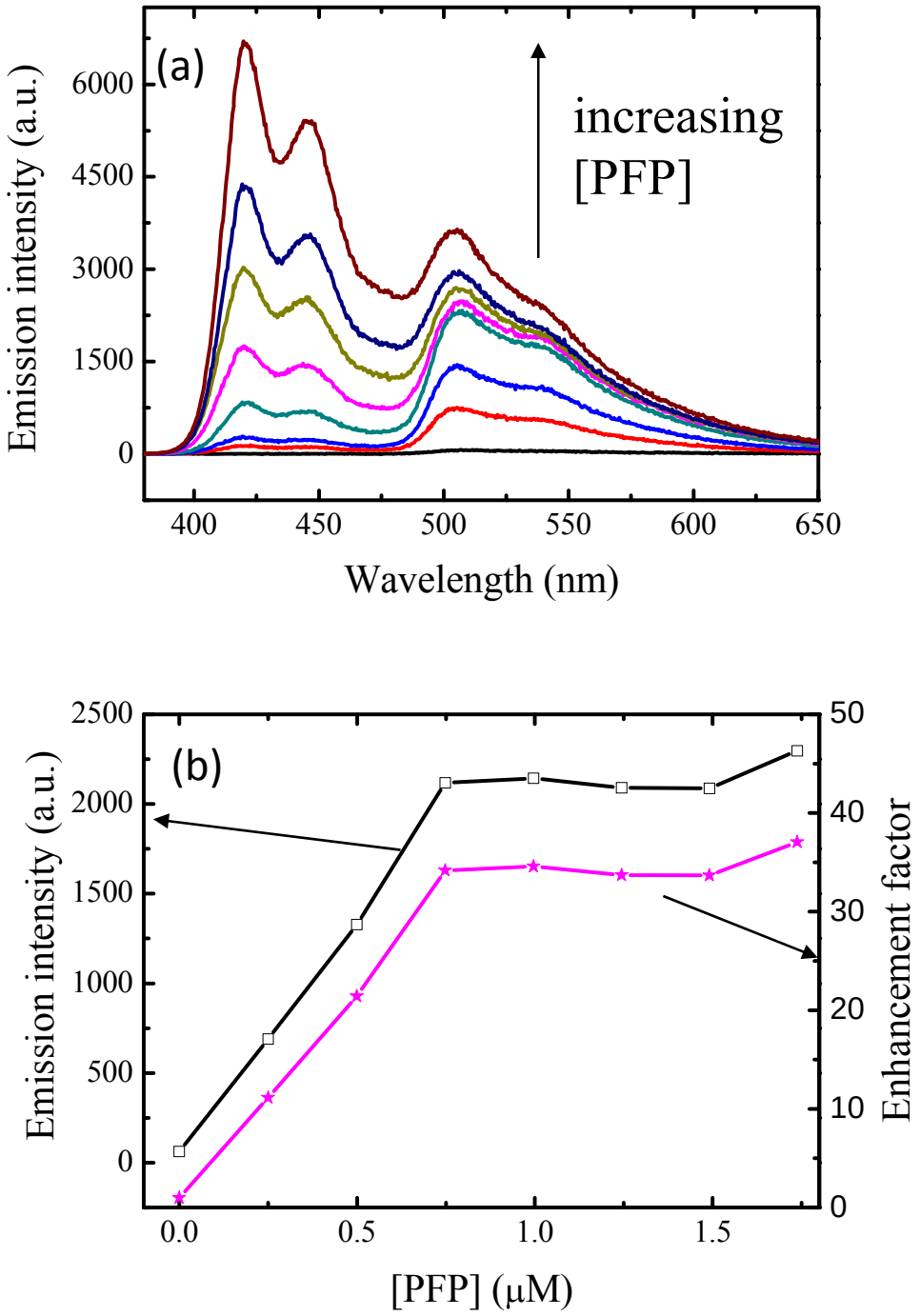

Figure 4.8. (a) Two-photon excitation emission spectra of YOYO-1/T_{24}/Hg^{2+} after addition of different amounts of PFP: [YOYO-1] = 75 nM; [T_{24}]=50 nM; [Hg^{2+}]=2.0 μM; λ_{ex}=800 nm; (b) Two photon excitation emission intensities (with contributions from PFP residue emission subtracted) of YOYO-1 at 510 nm in YOYO-1/T_{24}/Hg^{2+}/PFP and the corresponding enhancement factors.

The two-photon excitation (TPE) fluorescence of T_{24}/TOTO-1 in the absence and presence of PFP are shown in Figure 4.9. Addition of conjugated polymers (PFP)

can enhance the TPE emission of TOTO-1 by a factor of up to 23 times compared to that in the absence of PFP.

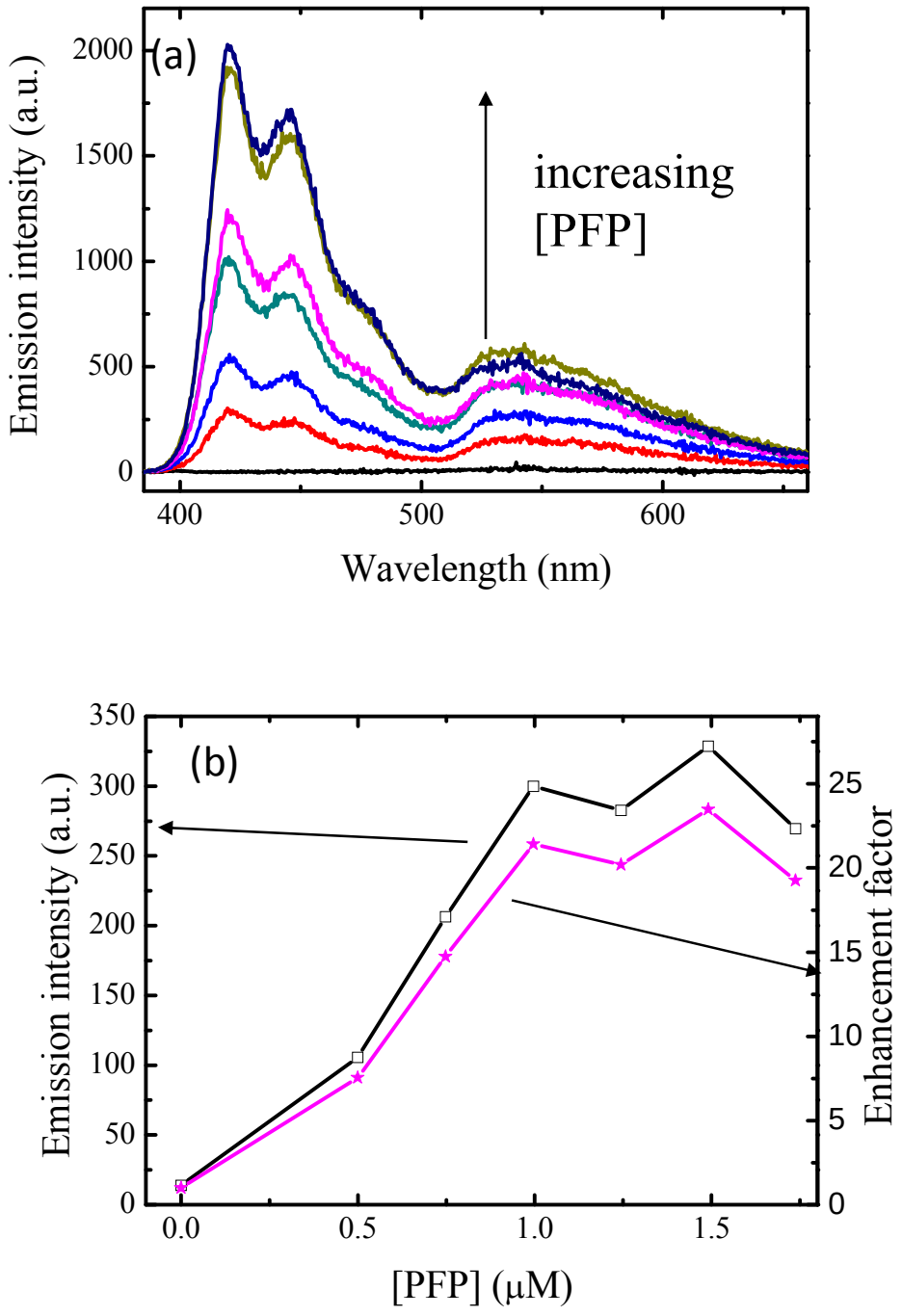

Figure 4.9. (a) Two-photon excitation emission spectra of TOTO-1/T_{24}/Hg^{2+} after addition of different amounts of PFP: [TOTO-1] = 75 nM; [T_{24}] = 50 nM; [Hg^{2+}]=2.0 μM; λ_{ex}=800 nm; (b) Two photon excitation emission intensities (with contributions from PFP residue emission subtracted) of TOTO-1 at 535 nm in TOTO-1/T_{24}/Hg^{2+}/PFP and the corresponding enhancement factors.

4.4 Conclusion

In summary, we have demonstrated a practical scheme for detection of mercury at room temperatures with high sensitivity and selectivity by using a combination of oligonucleotides, DNA intercalators and conjugated polymers. It combines the advantages of specific binding interactions between Hg^{2+} and thymine, and optical amplification properties of conjugated polymers. The detection limit of sub-nM can be easily reached using this method. This method is label free, low cost and simple to use. It works in a "mix-and-detect" manner and takes only a few minutes to complete the detection. All the materials used are commercially available. This scheme could also be used as a two-photon sensor for detection of mercury ions deep into the biological environments with high sensitivity. This method could be widely applicable and rationalized for use to detect other metal ions by replacing natural DNA bases with metal-dependent synthetic artificial bases.

4.5 References

1. Hylander, L. D. & Goodsite, M. E. (2006) *Science of the Total Environment* **368,** 352-370.
2. Zahir, F., Rizwi, S. J., Haq, S. K. & Khan, R. H. (2005) *Environmental Toxicology and Pharmacology* **20,** 351-360.
3. Zheng, N., Wang, Q. C., Zhang, X. W., Zheng, D. M., Zhang, Z. S. & Zhang, S. Q. (2007) *Science of the Total Environment* **387,** 96-104.
4. Che, Y., Yang, X. M. & Zang, L. (2008) *Chemical Communications***,** 1413-1415.
5. Descalzo, A. B., Martinez-Manez, R., Radeglia, R., Rurack, K. & Soto, J. (2003) *Journal of the American Chemical Society* **125,** 3418-3419.
6. Nolan, E. M. & Lippard, S. J. (2003) *Journal of the American Chemical Society* **125,** 14270-14271.
7. Nolan, E. M. & Lippard, S. J. (2007) *Journal of the American Chemical Society* **129,** 5910-5918.
8. Tatay, S., Gavina, P., Coronado, E. & Palomares, E. (2006) *Organic Letters* **8,** 3857-3860.
9. Zhu, X. J., Fu, S. T., Wong, W. K., Guo, H. P. & Wong, W. Y. (2006) *Angewandte Chemie-International Edition* **45,** 3150-3154.
10. Liu, X. F., Tang, Y. L., Wang, L. H., Zhang, J., Song, S. P., Fan, C. H. & Wang, S. (2007) *Advanced Materials* **19,** 1662-1662.
11. Miyake, Y., Togashi, H., Tashiro, M., Yamaguchi, H., Oda, S., Kudo, M.,

Tanaka, Y., Kondo, Y., Sawa, R., Fujimoto, T., Machinami, T. & Ono, A. (2006) *Journal of the American Chemical Society* **128,** 2172-2173.

12. Ono, A. & Togashi, H. (2004) *Angewandte Chemie-International Edition* **43,** 4300-4302.

13. Tang, Y. L., He, F., Yu, M. H., Feng, F. D., An, L. L., Sun, H., Wang, S., Li, Y. L. & Zhu, D. B. (2006) *Macromolecular Rapid Communications* **27,** 389-392.

14. Chiang, C. K., Huang, C. C., Liu, C. W. & Chang, H. T. (2008) *Analytical Chemistry* **80,** 3716-3721.

15. Kim, I. B. & Bunz, U. H. F. (2006) *Journal Of The American Chemical Society* **128,** 2818-2819.

16. Lee, J. S., Han, M. S. & Mirkin, C. A. (2007) *Angewandte Chemie-International Edition* **46,** 4093-4096.

17. Xue, X. J., Wang, F. & Liu, X. G. (2008) *Journal of the American Chemical Society* **130,** 3244-3245.

18. Li, H. B., Zhang, Y., Wang, X. Q., Xiong, D. J. & Bai, Y. Q. (2007) *Materials Letters* **61,** 1474-1477.

19. Liu, J. & Lu, Y. (2007) *Angewandte Chemie-International Edition* **46,** 7587-7590.

20. Gaylord, B. S., Heeger, A. J. & Bazan, G. C. (2002) *Proceedings of the National Academy of Sciences of the United States of America* **99,** 10954-10957.

21. He, F., Tang, Y. L., Wang, S., Li, Y. L. & Zhu, D. B. (2005) *Journal of the*

American Chemical Society **127,** 12343-12346.

22. Liu, B., Wang, S., Bazan, G. C. & Mikhailovsky, A. (2003) *Journal of the American Chemical Society* **125,** 13306-13307.

23. Wang, S., Gaylord, B. S. & Bazan, G. C. (2004) *Journal of the American Chemical Society* **126,** 5446-5451.

24. Xu, Q. H., Gaylord, B. S., Wang, S., Bazan, G. C., Moses, D. & Heeger, A. J. (2004) *Proceedings of the National Academy of Sciences of the United States of America* **101,** 11634-11639.

25. Netzel, T. L., Nafisi, K., Zhao, M., Lenhard, J. R. & Johnson, I. (1995) *Journal of Physical Chemistry* **99,** 17936-17947.

26. Wang, J. & Liu, B. (2008) *Chemical Communications***,** 4759-4761.

27. Tian, N. & Xu, Q. H. (2007) *Advanced Materials* **19,** 1988-1991.

Chapter 5

Direct Visualization of Conformational Switch of i-Motif DNA with a Cationic Conjugated Polymer

5.1 Introduction

DNA can form various defined nanoscale structures by self-assembly due to the unique specific interactions between their base pairs (1-3). The properties of their structural polymorphism and conformational flexibility have been taken advantage to develop various DNA-based nanodevices (4-12). Many DNA devices involve inter-conversion between different conformations of DNA, such as from single or double stranded DNA to i-motif structure (13-17).The i-motif structure, discovered in 1993, is a cytosine-rich oligomer that forms a DNA quadruplex in which two parallel duplexes associate in a head-to-tail orientation with their C:C+ pairs face-to-face intercalated with each other to form a compact structure (18). The i-motif structure can be formed at acidic pH condition and becomes unfolded at basic and very acid pH conditions. Based on the unique structure and pH dependence of i-motif DNA, many DNA based nono-devices have been reported (8, 9, 15, 16). In most DNA based nanodevices, the associated conformational switch could be driven by DNA/RNA strands, acids/bases, enzymes and light (8, 12, 19-21). The visualization of the DNA conformational change is usually based on fluorescence signal change, in

which the oligonucleotide needs to be labeled with fluorescent molecules (8, 9, 12, 16).

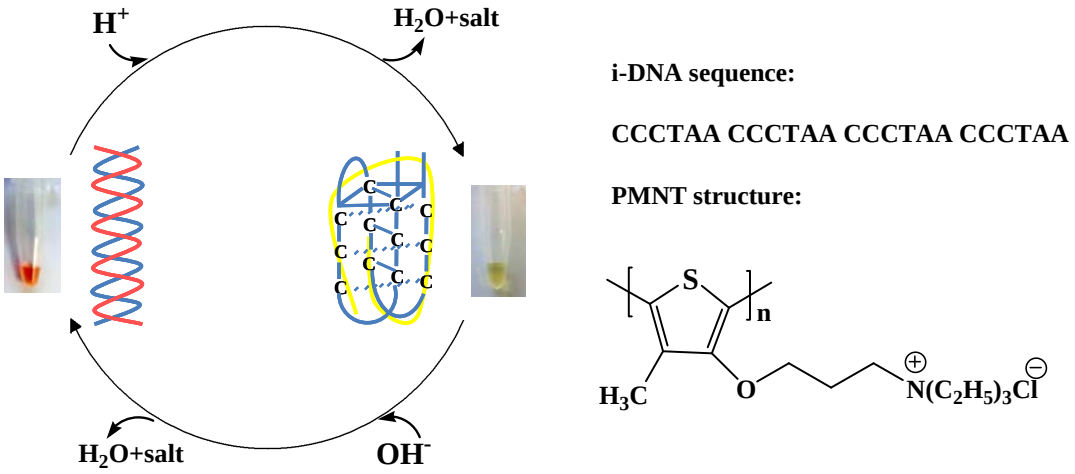

Scheme 5.1. Schematic illustration of reversible pH driven conformational switch of DNA, the sequence of i-DNA sequence, and molecular structure of PMNT. The interconversion of the closed and open states of the "i-DNA" was mediated by alternating addition of H^+ and OH^-.

We present a label free method using a water soluble polythiophene derivative to visualize the conformational switch of i-motif DNA driven by the environmental pH change. The conformational switch of i-motif DNA was companied by a solution color change, which can be directly visualized by naked eyes without the need of any sophisticated instrumentation. The conformational change was also accompanied by dramatic change in fluorescence intensity. The detection sensitivity could thus be further improved by using the fluorescence method. The pH dependent conformational change and accompanied changes in color and fluorescence signal can undergo reversibly for many cycles. This i-DNA/PMNT complex could act as an environmentally friendly optical switch with a fast response.

5.2 Experimental

5.2.1 Materials.

Materials: Cationic water-soluble poly [3-(3¢-*N*,*N*,*N*-triethylamino-1¢-propyloxy) -4-methyl-2,5-thiophene hydrochloride] (PMNT) was prepared according to the procedure in the literature.(22) i-DNA strands were purchased from Sigma.The molecular structure of PMNT and the sequence of i-motif DNA are shown in scheme 5.1.

5.2.2 Instrumentation and experiment procedure.

UV-Visible absorption and emission spectra were measured by using a SHIMADZU UV-2450 spectrophotometer and a Perkin-Elmer LS55 luminescence spectrometer respectively. Circular Dichroism (CD) measurements were conducted on a JASCO J-810 spectropolarimeter.

In a typical procedure, stock solution of i-DNA(100μM) and PMNT solution(1mM) were mixed and diluted with potassium phosphate buffer to give a final concentration of $2*10^{-6}$ M i-DNA (strand) and $7.8*10^{-5}$M PMNT (repeat unit) for UV and CD measurement. For fluorescence measurement, the final concentration of i-DNA and PMNT are $5.1*10^{-8}$M and $2.0*10^{-6}$M respectively. The pH value of this solution was changed from 4.5 to 8. The cycles of switching were accomplished by alternately adding HCl and NaOH. The solution temperature for all the measurement was 25°C.

Fluorescence lifetimes were measured by a time-correlated single-photon counting (TCSPC) technique (PicoQuant, PicoHarp 300). The frequency-doubled output of a mode-locked Ti:sapphire laser (Tsunami, Spectra-Physics) was used for excitation of the sample at 400 nm. The output pulses from Ti:sapphire centered at 800 nm had a duration of 40 femtosecond (fs) with a repetition rate of 80 MHz. The Ti:sapphire laser was pumped by 5 W output of a frequency doubled diode pumped Nd:YVO_4 laser (Millennia Pro, Spectra-Physics). For lifetime measurements the fluorescence was collected by an optical fiber which is directed to the detector. An avalanche photodiode (APD) was used as detector. Outputs of the APD (start pulse) and a fast photodiode (stop pulse) were processed by the PicoHarp 300 module. The width of the instrument response function was ～200 ps. The decay profiles were fit by deconvolution with the instrumental response function. The samples were exactly the same samples used for fluorescence spectroscopy.

5.3 Results and Discussion

As illustrated in Scheme 5.1, our system consists of an i-motif DNA and a polythiophene derivative, poly (3-alkoxy-4-methyl-thiophene) (PMNT). The i-motif DNA is a 24-mer single stranded oligonucleotide containing four stretches of CCC. This DNA sequence has been known to undergo conformational change when exposed to different environmental pH(8, 16, 17). At low pH, the cytosine residues are partially protonated and form a $C:C^+$ base pair, which result in formation of a compact i-motif structure. When the pH is raised to basic, the C^+ residues are

deprotonated and it unfolds to a random single stranded chain. This sequence has been previously successfully applied to construct several functional DNA nanodevices (8, 16, 17).

The pH driven conformational switch of i-motif DNA could be visualized by using a polythiophene derivative, PMNT. The chemical structure of PMNT is shown in Scheme 5.1. Water-soluble polythiophene derivatives have been known to exhibit interesting chromic properties (color change) due to conformational changes of their flexible conjugated backbones (23). They were believed to adopt different conformations upon forming complexes with DNA of different conformations such as single and double stranded DNA and G-quadruplex (24). The conformational change of the polythiophene derivatives results in changes of absorption and emission properties, which can be conveniently monitored. In particular, the change of the absorption property of the polythiophene leads to a color change of the polymer solution, which could even be directly visualized by naked eyes. Taking advantage of these interesting properties, various schemes have been developed using polythiophene derivatives as optical probes to detect DNA, protein, enzyme activity and metal ions (22, 24-26).

The interactions between the polythiophene derivative and i-motif DNA have not been studied so far. Similar to G-quadruplex, i-motif has a compact structure. PMNT is expected to have interesting interactions with the compact i-motif-DNA. Here we extend the application of PMNT to directly visualize the conformational

switch of i-DNA. In a solution containing PMNT and i-DNA, the conformation of PMNT that formed a complex with DNA was found to change in response to the conformational change of i-DNA, displaying a different appearance color. In an acidic solution (pH = 4.5 or below), i-DNA folded into a closed i-motif structure. In this closed state, the PMNT would wrap around the compact i-motif structure, resulting in a twisting structure. PMNT in this twisting structure is expected to have a relatively short conjugation length, as evidenced by a blue-shifted absorption spectrum with absorption maximum at 390 nm (Figure 5.1). The color of the solution appeared yellow. When the pH value was raised to 6.0 or above, i-DNA unfolded and adopted an open state. A DNA/PMNT complex would form due to electrostatic attractions. In this DNA/PMNT complex, the PMNT will take a more planar structure and have a larger conjugation length. The absorption spectra of the PMNT will thus become red shifted. Data in Figure 5.1 confirms that the absorption spectra of the complex became broadened and red-shifted when the pH was raised to 6 or above. The appearance color of the solution changed to red. It can be also seen from Figure 5.1 that the absorption spectra at different pH showed an isobestic point at ~450 nm, indicating a transition between two states. The plot of the absorption maxima ratio A500nm/A390nm shows a transition point at pH 5. The absorption spectra of PMNT alone at pH 2-9 have also been measured (Figure 5.2) and only subtle changes were observed, confirming that the absorption change in i-DNA/PMNT complex was indeed induced by the conformational change of i-DNA.

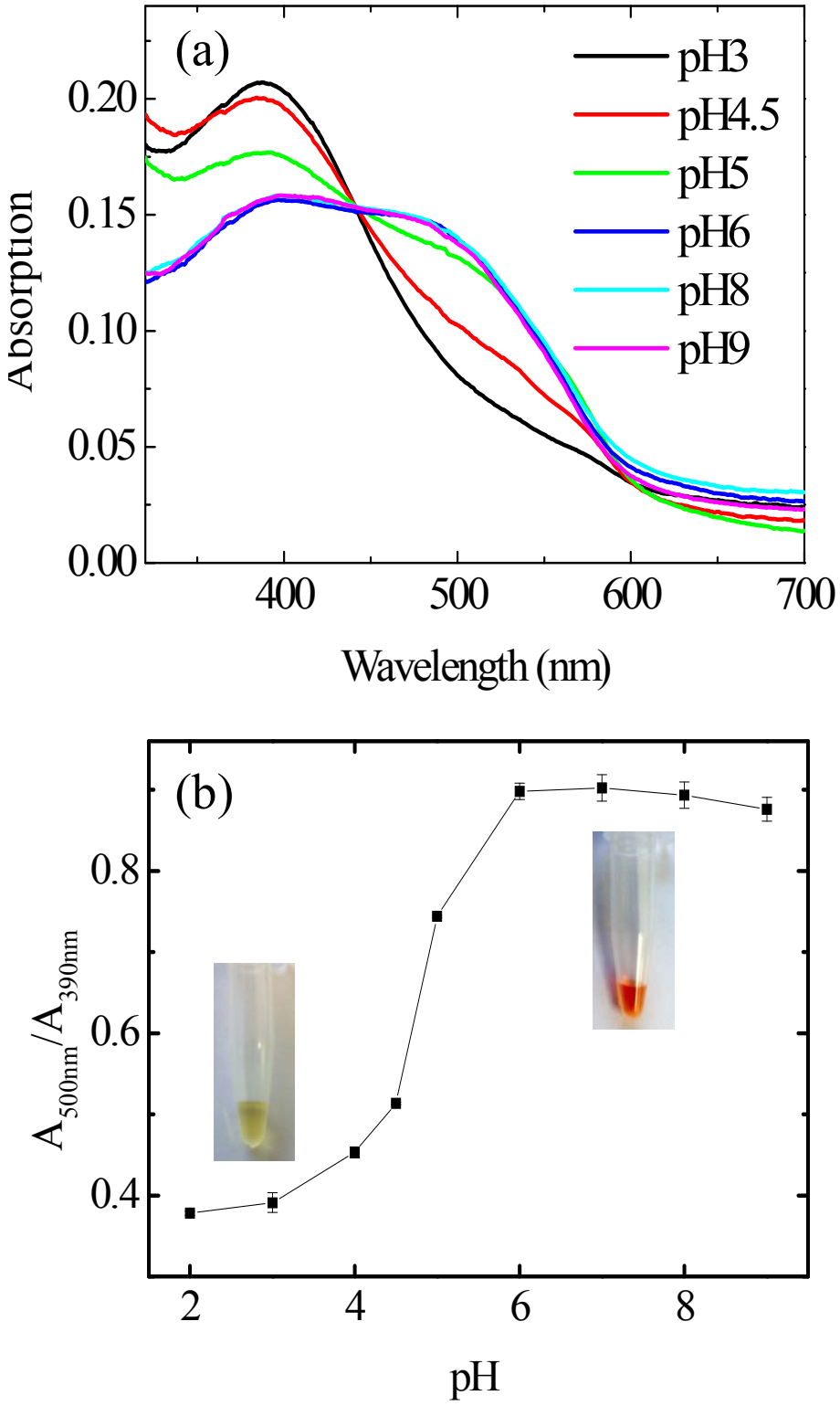

Figure 5.1. (a) The absorption spectra of i-DNA/PMNT complexes at different pH: [PMNT] =7.8*10^{-5}M; [i-DNA] =2*10^{-6}M. The pictures of the solutions at pH 4.5 and pH 8 are also shown in (b).

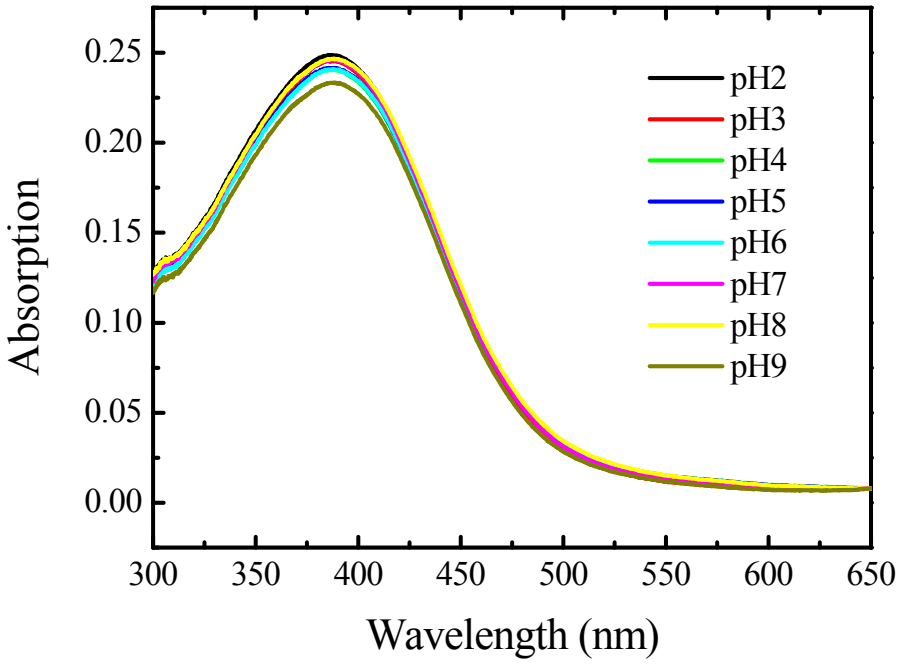

Figure 5.2. The absorption spectra of PMNT at different pH: [PMNT] =7.8*10^{-5}M.

The structures of the open and closed states were further confirmed by circular dichroism (CD) spectroscopy (Figure 5.3). At pH 4.5, the CD spectrum of the solution showed the distinct characteristic of the i-motif structure: a strong positive band near 287 nm, a smaller negative band near 255 nm, and a crossover around 265 nm, which is a characteristic of i-motif structure and is consistent with the previous reported CD spectra of the i-motif structure (9, 26). These results confirm that the system is in the closed state at pH 4.5. At pH 8, the CD spectrum showed an obvious change, with the maximum shifted towards around 275 nm, consistent with the unfolded, unstructured single-stranded DNA (21, 27-29). The results suggest that the DNA adopted the single-stranded open state at high pH conditions. CD spectrum of PMNT alone was also measured and no CD optical activity was observed in the same spectral range (220-320 nm), confirming that the observed CD signal of DNA/PMNT is indeed due

to the conformational change of i-DNA.

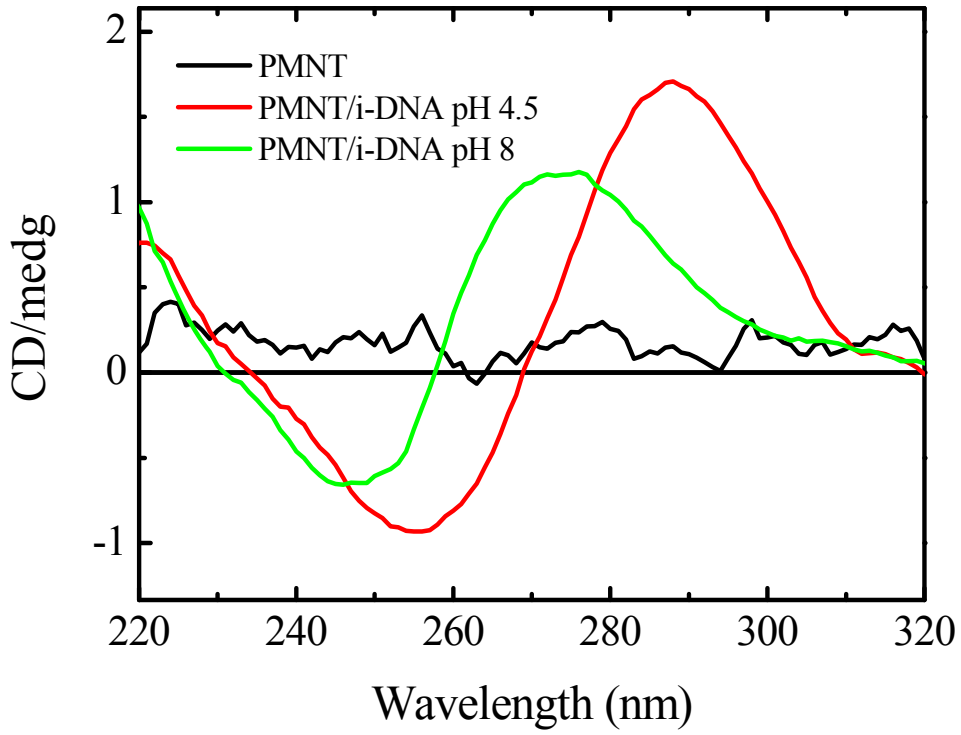

Figure 5.3. Circular dichroism spectra of PMNT alone, i-DNA/PMNT at pH 4.5 and 8 in solutions: [PMNT] =7.8*10^{-5}M; [i-DNA] = 2*10^{-6}M.

Based on this observation, PMNT can be used as a colorimetric probe to directly visualize the conformational switch of i-DNA. The conformational changes of i-DNA are companied by significant molecular motions, rotatory, stretching or even translatory motions. The conformational switch of i-DNA has thus been utilized to design many DNA based molecular or nanomachines (8, 13, 15, 16, 21). In the presence of PMNT, i-DNA and PMNT form a complex. The conformational change of i–DNA causes a corresponding change in the conformation of PMNT in the complex. This conformational change will cause a change in the appearance color of the PMNT solution, which can be directly visualized by naked eyes. The conformational switch of DNA could thus be conveniently monitored. This method is direct and simple. The

labeling of the DNA as required in many previous reports (8, 15, 16) is not needed, which greatly simplifies the protocols.

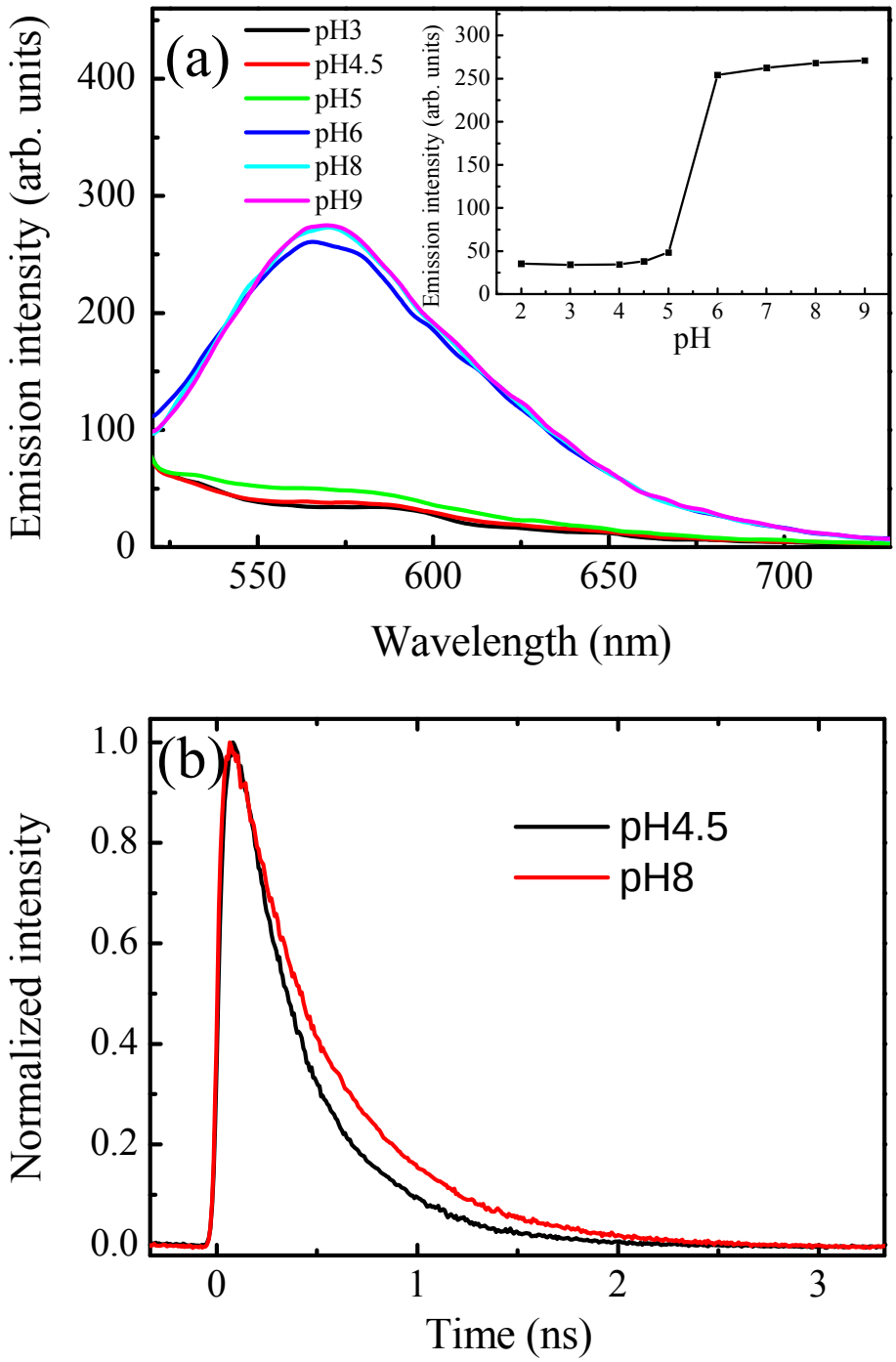

Figure 5.4. (a) The emission spectra of i-DNA/PMNT complexes at different pH: [PMNT] = $2.0*10^{-6}$M, [i-DNA] = $5.1*10^{-8}$M, λex = 500 nm; (b) Fluorescence lifetime measurements of i-DNA/PMNT complexes at pH 4.5 and 8, λex = 400 nm and λem = 580 nm.

The colorimetric detection method is simple and rapid, but the detection sensitivity is usually quite limited. The detection sensitivity could be further improved by using a fluorescence method. Figure 5.4 show the pH dependent emission spectra of i-DNA/PMNT complex under excitation at 500 nm. When the pH was 4.5 or below, the fluorescence intensity was weak. When the pH value was raised to 6 or above, the fluorescence intensity was found to increase significantly (up to 8 times). The transition point is at around pH 5.5, similar to that obtained from the absorption measurements. Two factors are responsible for the observed change in the emission intensity: change in the emission quantum yield and change in the absorbance at the excitation wavelength (500 nm). At a low pH, i–DNA is in a closed state, the PMNT will wrap around the compact i-motif structure, resulting in a twisting structure of PMNT. PMNT in this twisting structure has a relative low emission yield. While in a basic solution, i-DNA will take the open state. The binding of i–DNA with PMNT will cause a relatively rigid structure of PMNT, which will result in reduced aggregation effect and reduced non-radiative decay. The emission efficiency will thus be improved correspondingly. The change in the emission yield has also been confirmed by measuring their fluorescence lifetime at 580 nm upon excitation at 400 nm by using a time-correlated single photon counting (TCSPC) method. The emission lifetime of i-DNA/PMNT at pH 8 (~490 ps) is longer than that at pH 4.5 (~360 ps), suggesting an increased emission yield of PMNT in the complex as the pH increases. The change in the emission yield is only partially responsible for the observed emission intensity change. The increased emission is also partially due to increased

absorption of the complex at the excitation wavelength of 500 nm at high pH. As can be seen from Figure 5.1, the absorption spectrum of i-DNA/PMNT shifts towards red as the pH increases. The absorbance at 500 nm increases correspondingly, the PMNT thus can be excited more effectively and the emission intensity increases.

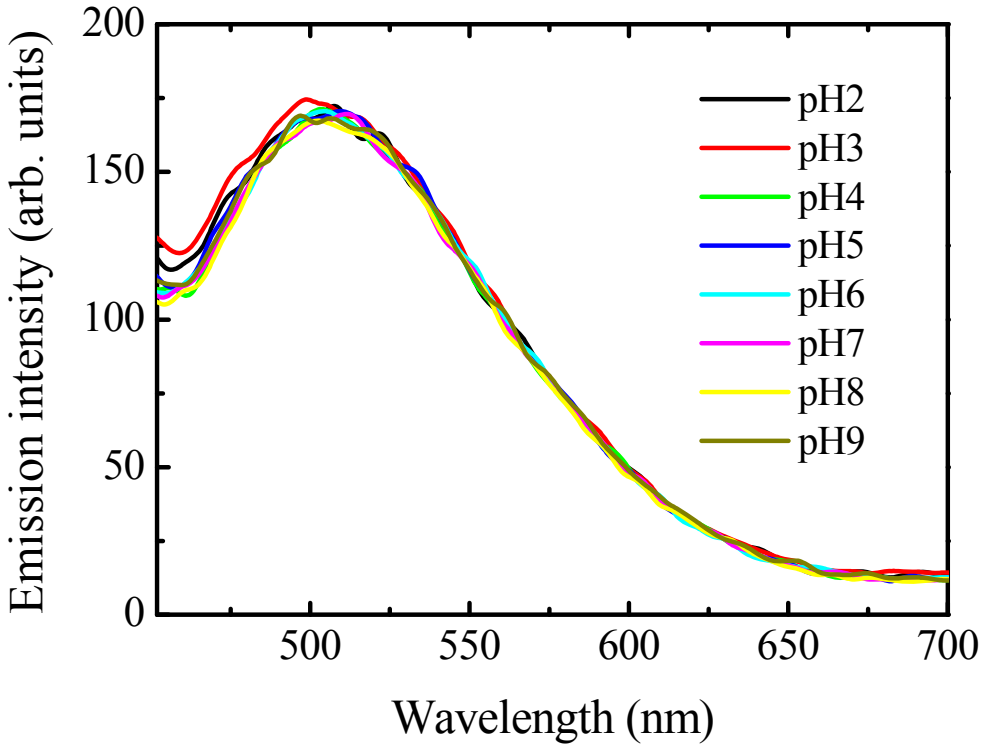

Figure 5.5. The emission spectra of PMNT at different pH: [PMNT] =2.0*10^{-6}M, λ_{ex} = 500 nm.

The fluorescence spectra of PMNT alone in the range of pH 2-9 have also been measured (Figure 5.5). The PMNT fluorescence was nearly insensitive to the pH change. Less than 10% variation of fluorescence intensity was observed in the pH range of 2-9. These results confirm that the observed dramatic change in the emission of i-DNA/PMNT complex is indeed caused by the conformational switch of i-DNA.

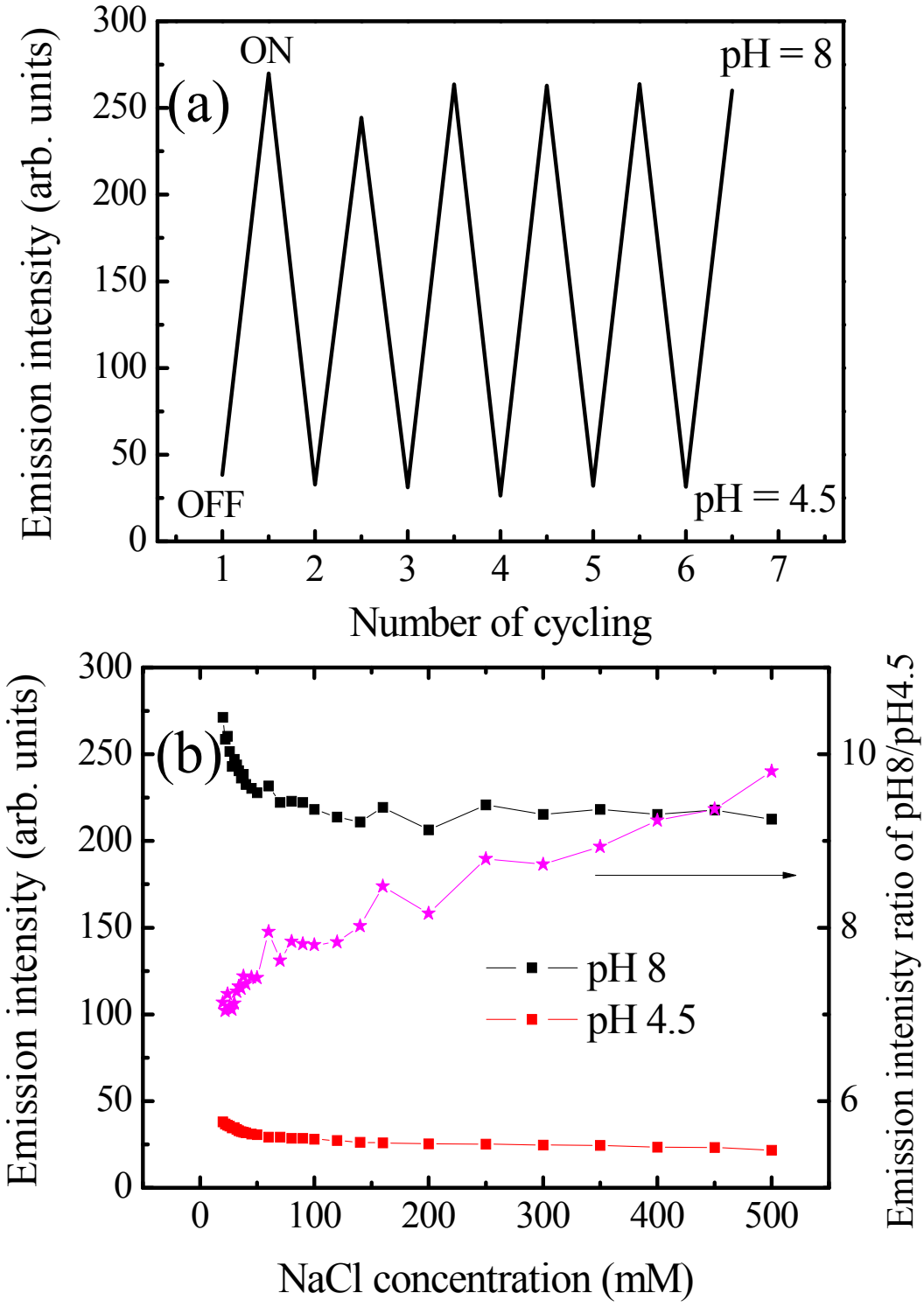

Figure 5.6. (a) Repeated opening and closing of the pH driven DNA conformational switch by alternating addition of HCl and NaOH. (b) The NaCl effect on the emission intensities of i-DNA/PMNT complex at pH 4.5 and 8: [PMNT] = $2.0*10^{-6}$M; [i-DNA] = $5.1*10^{-8}$M; The emission intensities were monitored at 580 nm; λex = 500 nm.

The pH dependent absorption and fluorescence intensity change of i-DNA/PMNT complexes could be utilized to directly monitor the conformational switch of i-DNA, The pH dependent optical property change of i-DNA/PMNT complexes could be utilized as an optical switch. The color or emission intensity could be switched by adjusting their environmental pH values. Because interconversion of the closed and open states of i-DNA could be mediated by their environmental pH, multiple cycling of the conformational switch can be carried out by alternating addition of HCl and NaOH. Figure 5.6 shows the cyclical changes in fluorescence emission resulting from controlled opening and closing of the system. The solutions were excited at 500 nm and the emissions were monitored at 580 nm. The emission was turned ON at pH 8 when the DNA was in an open state, and turned OFF at pH 4.5 when the DNA was in a closed state. The emission intensity remained almost the same after a few cycles, suggesting that the waste products (NaCl and H_2O) did not interfere with the molecular mechanism of the switch. This switch has many unique advantages. The waste products are NaCl and H_2O, which are nontoxic and environmentally friendly. The opening and closing processes are fast and can complete within ~5s, significantly faster than DNA nanodevices that employ hybridization mechanisms.

The performance of DNA based switch usually gradually degrades after a few cycles because of the waste product that might poison the system, which has been one of the obstacles for their potential applications (12). We have investigated the effect of NaCl on the emission intensity of our i-DNA/PMNT system. At pH 8, the emission

intensity of the complex initially decreases gradually by ~20% as the concentration of NaCl increases up to 0.1M, and then became constant as the NaCl concentration further increases (we measured up to 0.5 M in the experiments). At pH 4.5, the emission intensity of the complex continuously decreases as the concentration of NaCl increases. The emission intensity decreased by 26% for NaCl concentration of 0.1 M , and 45% for NaCl concentration of 0.5 M. Under all the concentrations, the emission intensity of pH 8 is much larger than that at pH 4.5 and the emission intensity ratio of pH8/pH4.5 increases as the NaCl concentration increases. As NaCl is the major product of the cycling process, this optical switch is environmentally friendly. The results suggest that the switch can undergo thousands of times without significant degradation.

5.4 Conclusion

In summary, we have demonstrated that optical properties of an i-DNA/PMNT complex were strongly dependent on the environmental pH. The dramatic optical property change at different pH is due to pH driven conformational switch of i-DNA. In response, the conformation of PMNT that forms a complex with i-DNA changes correspondingly, resulting in a different appearance color and dramatic change in its emission intensity. PMNT could thus be utilized as an optical probe to visualize the conformational switch of i-DNA. This method is label free, simple and direct. The conformational switch of i-DNA could even be directly visualized by naked eyes without the need of any sophisticated instrumentation. In addition, the waste products

are nontoxic to the system. This i-DNA/PMNT complex could act as an environmentally friendly optical switch with a fast response, which could be reversibly cycled many times by adjusting the pH.

5.5 References

1. Chen, J. H. & Seeman, N. C. (1991) *Nature* **350,** 631-633.

2. Mirkin, C. A., Letsinger, R. L., Mucic, R. C. & Storhoff, J. J. (1996) *Nature* **382,** 607-609.

3. Seeman, N. C. (2003) *Nature* **421,** 427-431.

4. Alberti, P., Bourdoncle, A., Sacca, B., Lacroix, L. & Mergny, J. L. (2006) *Organic & Biomolecular Chemistry* **4,** 3383-3391.

5. Alberti, P. & Mergny, J. L. (2003) *Proceedings of the National Academy of Sciences of the United States of America* **100,** 1569-1573.

6. Bath, J. & Turberfield, A. J. (2007) *Nature Nanotechnology* **2,** 275-284.

7. Liang, X. G., Nishioka, H., Takenaka, N. & Asanuma, H. (2008) *Chembiochem* **9,** 702-705.

8. Liu, D. S. & Balasubramanian, S. (2003) *Angewandte Chemie-International Edition* **42,** 5734-5736.

9. Liu, H. J., Zhou, Y. C., Yang, Y., Wang, W. X., Qu, L., Chen, C., Liu, D. S., Zhang, D. Q. & Zhu, D. B. (2008) *Journal of Physical Chemistry B* **112,** 6893-6896.

10. Mao, C. D., Sun, W. Q., Shen, Z. Y. & Seeman, N. C. (1999) *Nature* **397,** 144-146.

11. Niemeyer, C. M. & Adler, M. (2002) *Angewandte Chemie-International Edition* **41,** 3779-3783.

12. Yurke, B., Turberfield, A. J., Mills, A. P., Simmel, F. C. & Neumann, J. L.

(2000) *Nature* **406,** 605-608.

13. Sharma, J., Chhabra, R., Yan, H. & Liu, Y. (2007) *Chemical Communications***,** 477-479.

14. Wang, W. X., Yang, Y., Cheng, E. J., Zhao, M. C., Meng, H. F., Liu, D. S. & Zhou, D. J. (2009) *Chemical Communications***,** 824-826.

15. Zhao, C., Song, Y. J., Ren, J. S. & Qu, X. G. (2009) *Biomaterials* **30,** 1739-1745.

16. Liedl, T. & Simmel, F. C. (2005) *Nano Letters* **5,** 1894-1898.

17. Liedl, T., Olapinski, M. & Simmel, F. C. (2006) *Angewandte Chemie-International Edition* **45,** 5007-5010.

18. Gehring, K., Leroy, J. L. & Gueron, M. (1993) *Nature* **363,** 561-565.

19. Chen, Y., Wang, M. S. & Mao, C. D. (2004) *Angewandte Chemie-International Edition* **43,** 3554-3557.

20. Dittmer, W. U., Kempter, S., Radler, J. O. & Simmel, F. C. (2005) *Small* **1,** 709-712.

21. Liu, H. J., Xu, Y., Li, F. Y., Yang, Y., Wang, W. X., Song, Y. L. & Liu, D. S. (2007) *Angewandte Chemie-International Edition* **46,** 2515-2517.

22. Ho, H. A., Boissinot, M., Bergeron, M. G., Corbeil, G., Dore, K., Boudreau, D. & Leclerc, M. (2002) *Angewandte Chemie-International Edition* **41,** 1548-1551.

23. Leclerc, M. (1999) *Advanced Materials* **11,** 1491-1498.

24. Ho, H. A. & Leclerc, M. (2004) *Journal of the American Chemical Society*

126, 1384-1387.

25. Tang, Y. L., Feng, F. D., He, F., Wang, S., Li, Y. L. & Zhu, D. B. (2006) *Journal of the American Chemical Society* **128,** 14972-14976.

26. Liu, X. F., Tang, Y. L., Wang, L. H., Zhang, J., Song, S. P., Fan, C. H. & Wang, S. (2007) *Advanced Materials* **19,** 1471-1474.

27. Mathur, V., Verma, A., Maiti, S. & Chowdhury, S. (2004) *Biochemical and Biophysical Research Communications* **320,** 1220-1227.

28. Xu, Y. & Sugiyama, H. (2006) *Nucleic Acids Research* **34,** 949-954.

29. Manzini, G., Yathindra, N. & Xodo, L. E. (1994) *Nucleic Acids Research* **22,** 4634-4640.

Chapter 6

Label-free Nuclease Assay using Conjugated Polymer and DNA/Intercalating Dye Complexes

6.1. Introduction

The DNA cleavage catalyzed by nucleases are involved in many important biological processes such as replication, recombination and repair (1, 2). These cleavage reactions are also being applied in various biotechnology tools in polymerase chain reaction (PCR) assays, gene mapping and molecular cloning (3). Traditional methods such as gel electrophoresis, high-performance liquid chromatography (HPLC), and enzyme-linked immunosorbent assay (ELISA) have been established for nuclease assay (4-6). However, these methods suffer from drawbacks such as being time-consuming, laborious, discontinuous and requiring substrate to be labeled.

To circumvent these limitations, nuclease assays based on fluorescence techniques have been developed in the past decade. For example, assays based on molecular beacons (7) and "molecular break light" probes (8) have been developed for continuous assay of DNA cleavage by S1 nuclease. However, in these studies, the sensing was based on fluorescence intensity measurements which are easily affected

by external nonspecific events such as localization of the probes, changes in environment of the probes (such as pH, temperature and polarity) (9, 10). In this respect, nuclease assay based on FRET technique can provide us a ratiometric fluorescence approach, in which the fluorescence intensities at two wavelengths are recorded and their ratios are calculated. This technique will help to reduce the influence of nonspecific events and give better precision.

Cationic conjugated polymers (CPs) can coordinate the action of a large number of absorbing units with efficient intrachain and interchain energy-transfer mechanisms (11, 12). The transfer of excitation energy along the backbone of CP to an energy acceptor leads to fluorescence signal amplifications (13). Therefore, the use of CPs as chemical or biological sensing elements has received intense research interest, especially in sensitive optical detection of biomolecules like nucleic acids and proteins (14-19). Recently, Wang et al have reported calorimetric and fluorescence methods based on FRET using cationic conjugated polymers/DNA complexes for amplified fluorescence assay of nucleases (20, 21). Although these assay methods are proven to be reliable, sensitive and convenient, they need to use chromophore-labeled DNA.

Herein, we demonstrate a new technique to assay nuclease based on CPs/DNA/intercalating dye system. This system can achieve a label-free platform for monitoring nuclease activity by using DNA intercalators. The intercalating dye used is thiazole orange (TO). TO is an unsymmetrical cyanine dye with benzothiazole and

quinoline moieties linked by a methenyl bridge (shown in Table 6.1). The fluorescence of TO itself is very weak in aqueous solution. The fluorescence intensity of TO will be significantly enhanced upon binding to DNA by inserting the aromatic moieties between the DNA bases. This enhancement in fluorescence emission is due to the restriction of rotational motion around the methenyl bridge between the aromatic moieties which closes a channel for non-radiative decay (22).

6.2 Experimental

6.2.1 Materials and Sample Preparation.

Table 6.1 Molecular structure of PFP, TO and sequences of ssDNA.

PFP	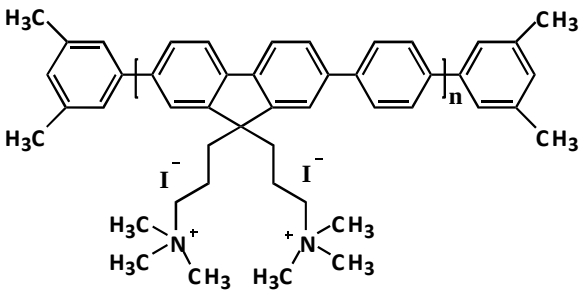
TO	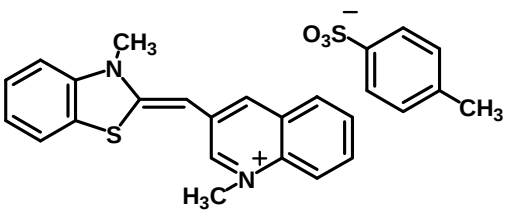
DNA1 (8-mer)	TAGCTAGC
DNA2 (12-mer)	TAGCTAGCTAGC
DNA3 (20-mer)	TAGCTAGCTAGCTAGC TAGC
DNA4 (32-mer)	TAGCTAGCTAGCTAGC TAGCTAGCTAGCTAGC

All DNA strand, TO and S1 nuclease enzyme were obtained from Sigma-Aldrich. PFP was purchased from the American dye source.

TO/DNA complexes were prepared in S1 nuclease buffer solution comprising of 2mM CH_3COONa, 15mM NaCl, 0.1mM $ZnSO_4$ at pH 4.6. In order to reduce the complication arising from dye aggregation that may interfere with the binding of the dye to the nuclei acid (23), the final concentration of TO was kept at a very dilute concentrations of 10^{-7}M for all measurements. PFP concentrations are in terms of repeating units (RU).

6.2.2 UV-Vis and FRET Experiment.

UV-Vis absorption spectra were measured by using a SHIMADZU UV-2450 spectrophotometer, and fluorescence measurements were done on a Perkin-Elmer fluoremeter with temperature control system. The concentration of DNA was determined by measuring its absorbance at 260 nm in a 200 μL quartz cuvette.

6.3 Results and Discussion

The assay strategy for enzymatic cleavage of ssDNA is illustrated in Scheme 6.1. In the absence of PFP, ssDNA exists as random coil, whereby TO molecules might bind to the DNA strand. Upon addition of PFP, the positively-charged PFP and the negatively-charged DNA is in close proximity due to electrostatic interactions, thus allowing FRET from PFP to TO. Therefore, fluorescence of PFP will be quenched and emission of TO will increase. When the ssDNA is cleaved by S1

nuclease into small fragments, the distance between PFP and TO will increase due to the relatively weak electrostatic interactions of the DNA fragments with PFP. Therefore, FRET between PFP and TO become less efficient. In this case, emission increase of PFP and emission decrease of TO occur. Thus the cleavage of DNA by S1 nuclease can be monitored by fluorescence spectra by observing PFP or TO emission changes in aqueous solution.

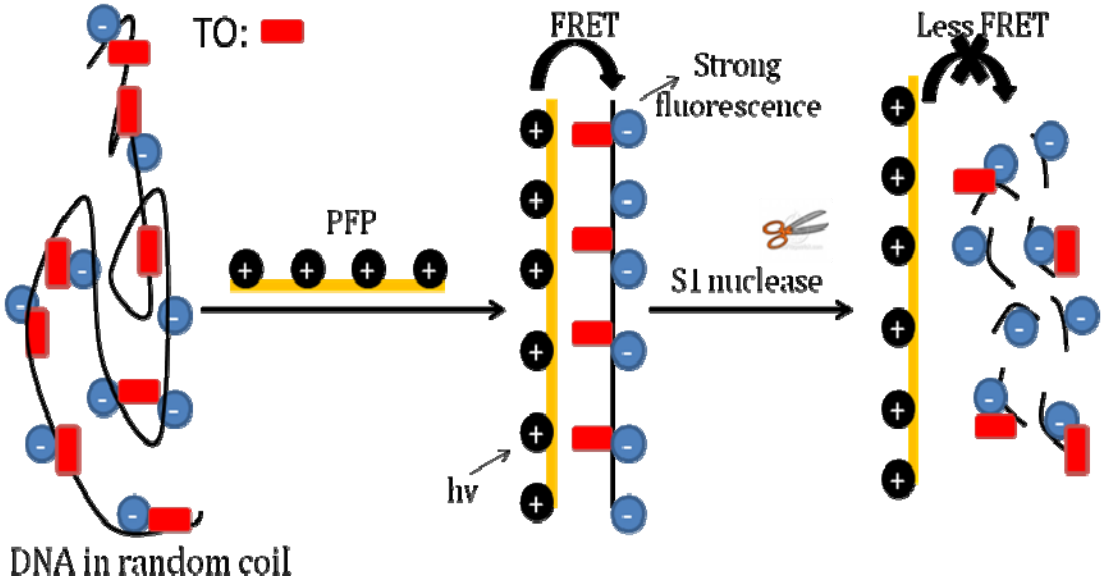

Scheme 6.1: Schematic illustration of the strategy for label-free nuclease assay using PFP and thiazole orange (TO)-DNA complex.

6.3.1 TO as fluorescent probe

In the preliminary investigation, the four ssDNA with different length, varying from 8- to 32-mer, were employed to investigate the influences of the length of DNA on the fluorescence enhancement of TO. Figure 6.1A shows the fluorescence intensity of TO/DNA complex at 530nm for four ssDNA samples at different base concentration. Normalized fluorescence intensity of TO increases as DNA bases concentration

increases. As the length of ssDNA increases, the fluorescence enhancement of TO becomes greater. The fluorescence of TO is enhanced by up to 16.5 times when binding to DNA_4 (32-mer), followed by DNA_3 (20-mer) for 13.5 times and DNA_2 (12-mer) for 4.3 times. There was little fluorescence enhancement for DNA_1 (8-mer) which is the shortest DNA.

To better compare the difference of fluorescence of TO when intercalated with four ssDNAs, the ratio of fluorescence intensity of TO/DNA_4, TO/DNA_3 and TO/DNA_2 against TO/DNA_1 is shown in Figure 6.1B. There was a highest 12-fold increase in TO fluorescence intensity for DNA_4, 10-fold increase for DNA_3 and 3.2-fold increase for DNA_2 as compared with TO/DNA_1. The result shows that longer ssDNA results in more significant fluorescence increase. It is expected that even larger fluorescence enhancement will result if TO is bind to long ssDNA(>32-mer) under the same conditions. These results can be understood that longer DNA provides more negative binding sites and stronger binding interactions with positively-charged TO molecules, leading to larger enhancement in emission of TO.

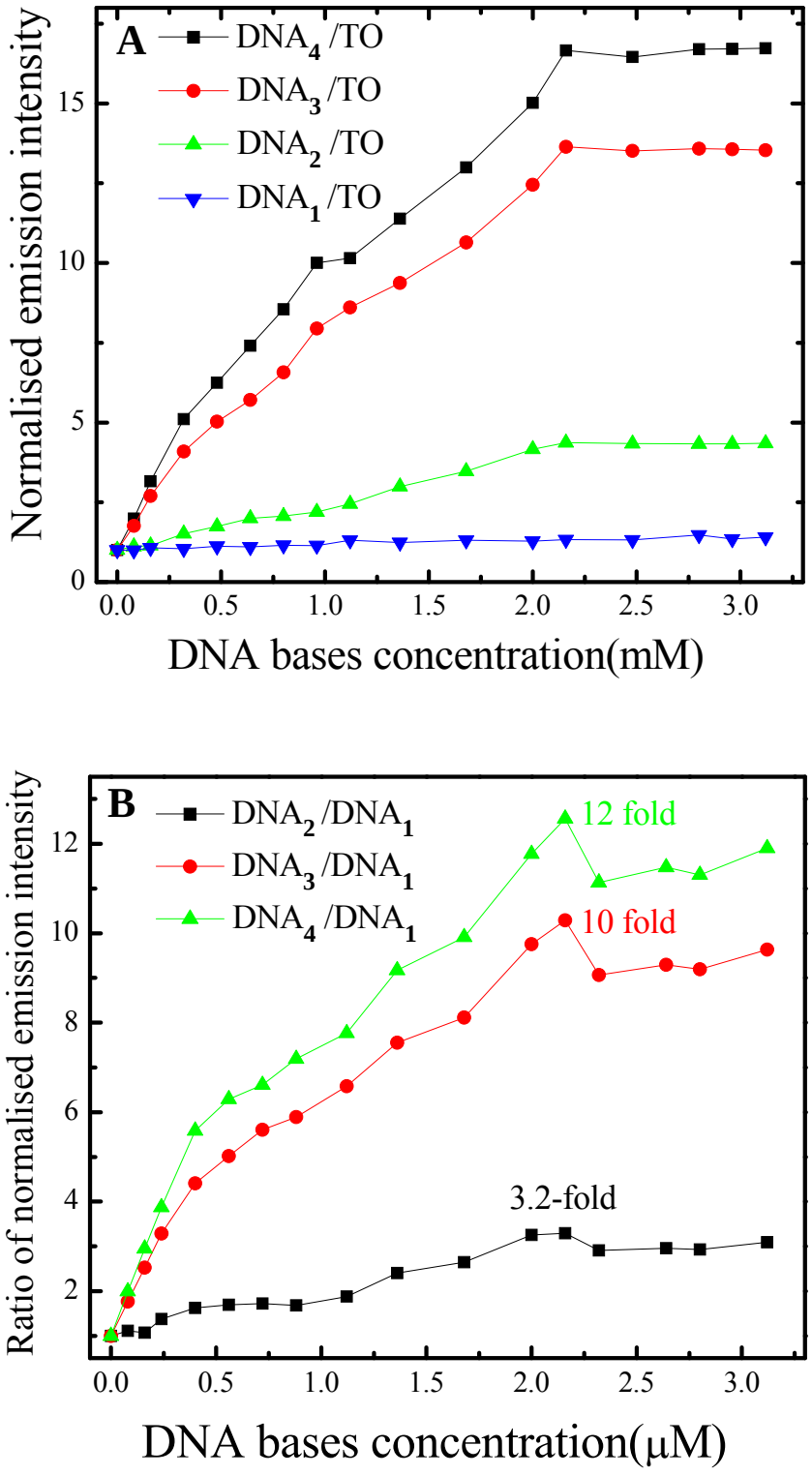

Figure 6.1: (A) Normalized fluorescence intensity of DNA/TO at 530nm at different DNA base concentrations. **(B)** Ratio of normalized fluorescence intensity of TO with DNA_2, DNA_3 and DNA_4 compared with DNA_1 /TO, [TO] = $5*10^{-8}$ M, λ_{ex}=500 nm. Measurements were conducted in 2mM CH_3COONa, 15mM NaCl, 0.1mM $ZnSO_4$, pH 4.6, 37°C.

6.3.2 S1 nuclease Assay using TO-DNA

The S1 nuclease is a single strand DNA-specific nuclease, which exhibits endo- and exolytic hydrolytic activity for the phosphodiester bonds of ssDNA or RNA and produces mono- or oligonucleotide fragments (24-26).

The observation of different fluorescence enhancement of TO binding to the different lengths of ssDNA, which can thus be utilized for real time monitoring of the S1 nuclease cleavage assay by monitoring the change in fluorescence intensity of TO at 530 nm. Figure 6.2A shows the fluorescence spectra obtained at different time intervals upon addition of S1 nuclease to a fixed concentration of TO-DNA complex. The cleavage reaction was monitored for 42 minutes upon addition of S1 nuclease. The fluorescence intensity of TO at 530 nm dropped by about 43% as shown in Figure 6.2B. The cleavage reaction could thus be monitored in real time by direct monitoring of TO emission.

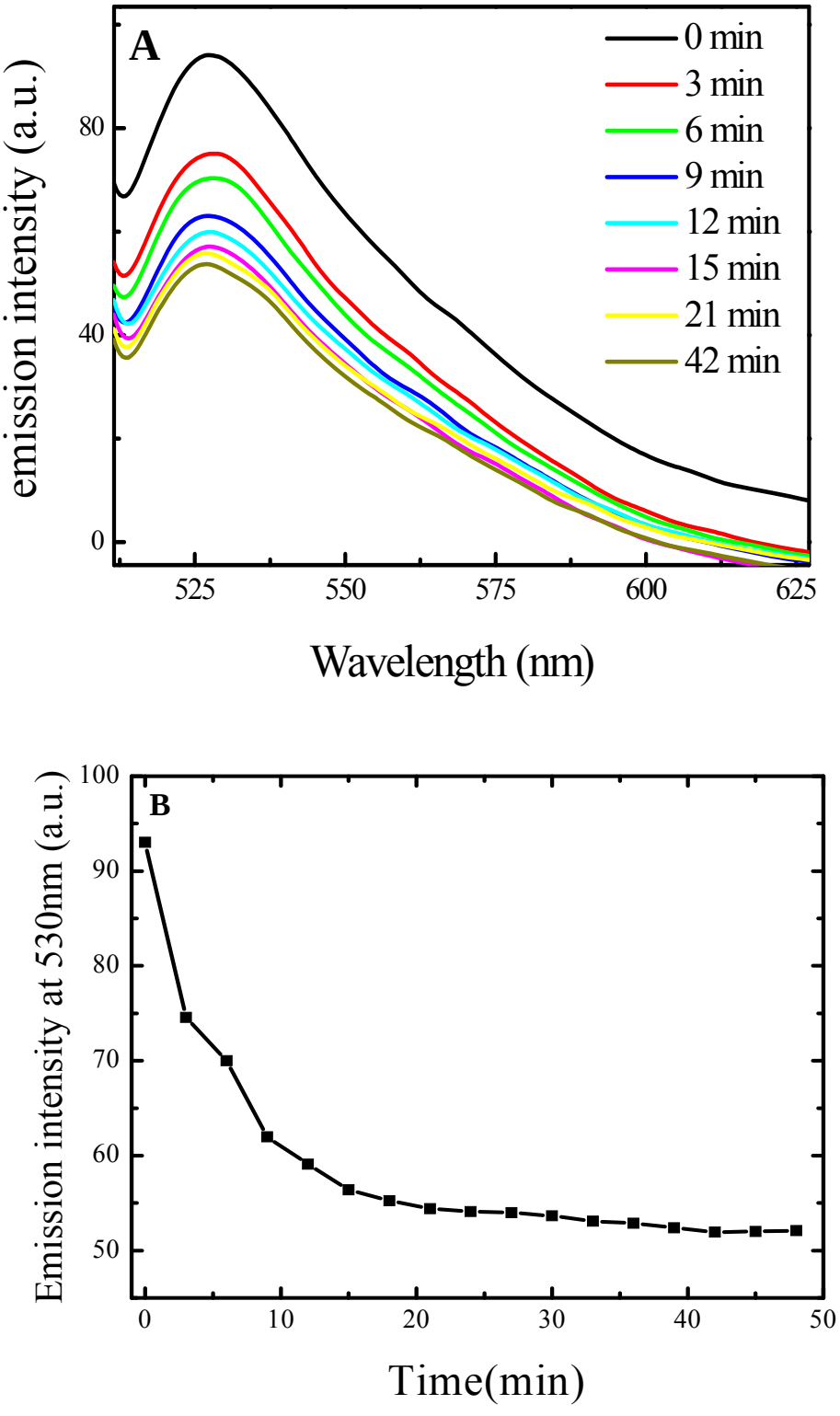

Figure 6.2: (A) Fluorescence spectra of TO-DNA_4 upon addition of S1 nuclease at different time interval. **(B)** Fluorescence intensity at 530nm against time. Conditions: [TO] = 5x 10^{-8}M, [DNA_4] = 6.75x 10^{-8}M, [S1 nuclease] = 2X10^{-3} U μL^{-1}, λ_{ex}= 485nm. Measurements were conducted in 2 mM CH_3COONa, 15 mM NaCl, 0.1 mM $ZnSO_4$, pH 4.6, 37 °C.

6.3.3 S1 nuclease Assay using PFP/TO-DNA

Figure 6.3A shows the fluorescence spectra obtained at direct excitation of TO at 485 nm in the present of PFP during the cleavage of DNA_4. The fluorescence intensity at 530 nm is gradually decreased as the reaction time increased. Compared with the DNA_4 cleavage reaction monitored by TO-DNA only (Figure 6.2), the drop of the fluorescence intensity at 530 nm is similar (the drop is about 43%). This result indicates that the activity of S1 nuclease is not affected when PFP is added. Conjugated polymers can offer signal amplification by FRET. As shown in Figure 6.3B, the emission intensity of PFP/TO-DNA could be enhanced by up to 7.6 times through FRET under excitation at 380 nm compared to that when TO-DNA was directly excited at 485 nm. Use of conjugated polymers is expected to enhance the detection sensitivity of the scheme. Figure 6.3C shows the fluorescence spectra using FRET assay during the S1 nuclease cleavage of DNA_4. The initial solution of PFP/TO-DNA_4 shows intense TO emission at 530 nm due to FRET from PFP to TO. Upon addition of S1 nuclease to the PFP/TO-DNA complex, the emission intensity of PFP at 425 nm gradually increased, while that of TO gradually decrease over the incubation time from 0 to 42 minutes. The fluorescence intensity at 530 nm was found to decrease by 90% (Figure 6.3C inset), which suggest that the use of conjugated polymers not only increases the amplitude of the emission signal, but also enhance relative change in the emission signal after addition of S1 nuclease. The reasons of the observed fluorescence change are: 1) DNA is cleaved into smaller fragments by the nuclease, the binding interactions between the DNA and TO become weaker and

emission yield of TO decreases. 2) The distance between PFP and TO becomes larger because of weaker interactions between PFP and DNA/TO as DNA was cleaved into small fragments.

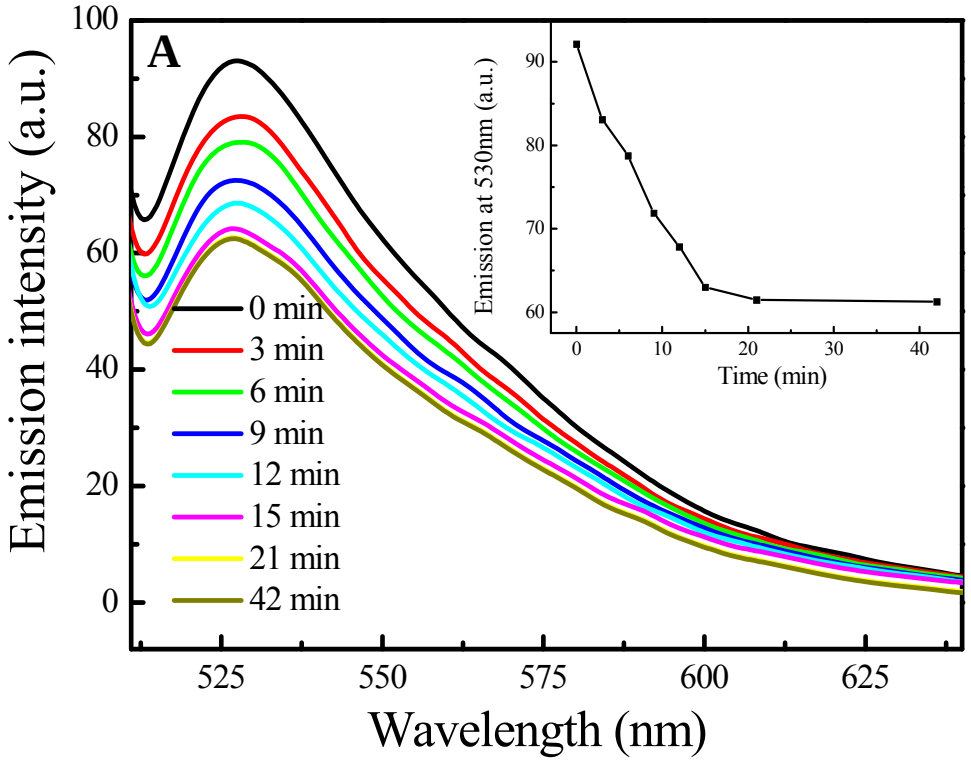

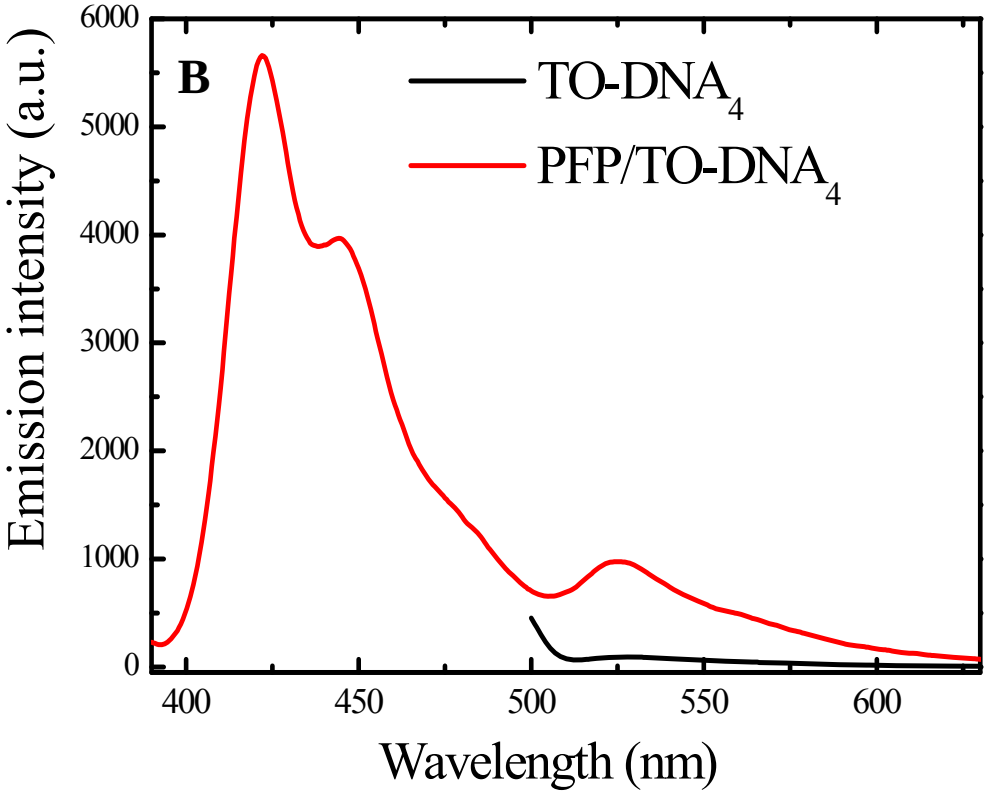
B
TO-DNA4
PFP/TO-DNA4
Emission intensity (a.u.)
Wavelength (nm)
0
1000
2000
3000
4000
5000
6000
400
450
500
550
600

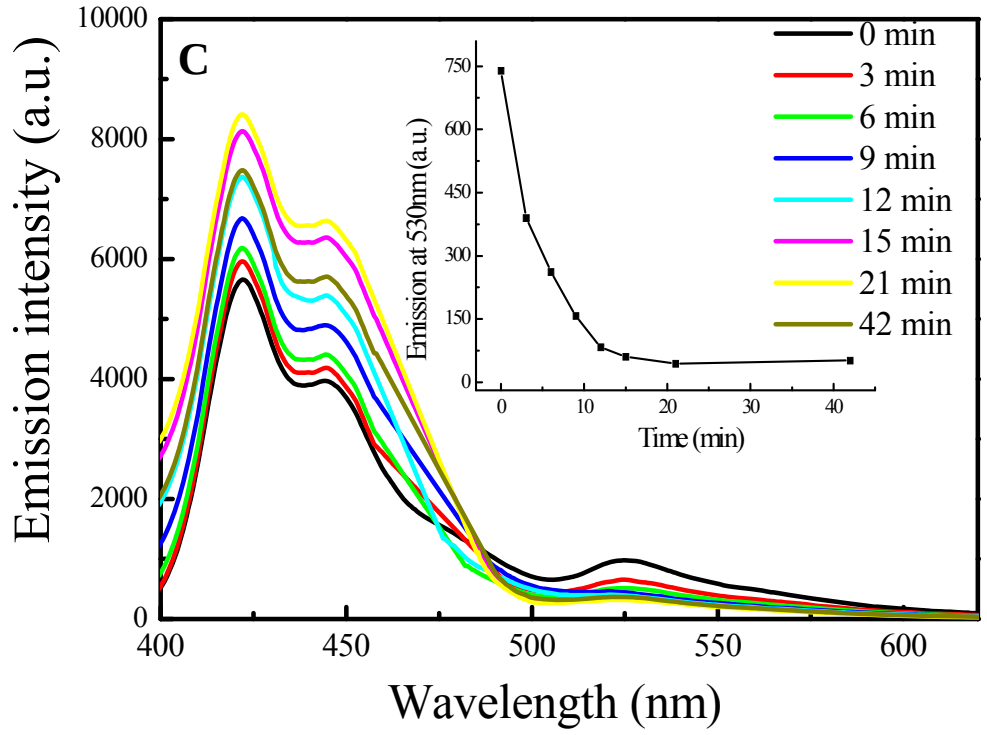
C
0 min
3 min
6 min
9 min
12 min
15 min
21 min
42 min
Emission at 530nm (a.u.)
Time (min)
Emission intensity (a.u.)
Wavelength (nm)
0
2000
4000
6000
8000
10000
400
450
500
550
600

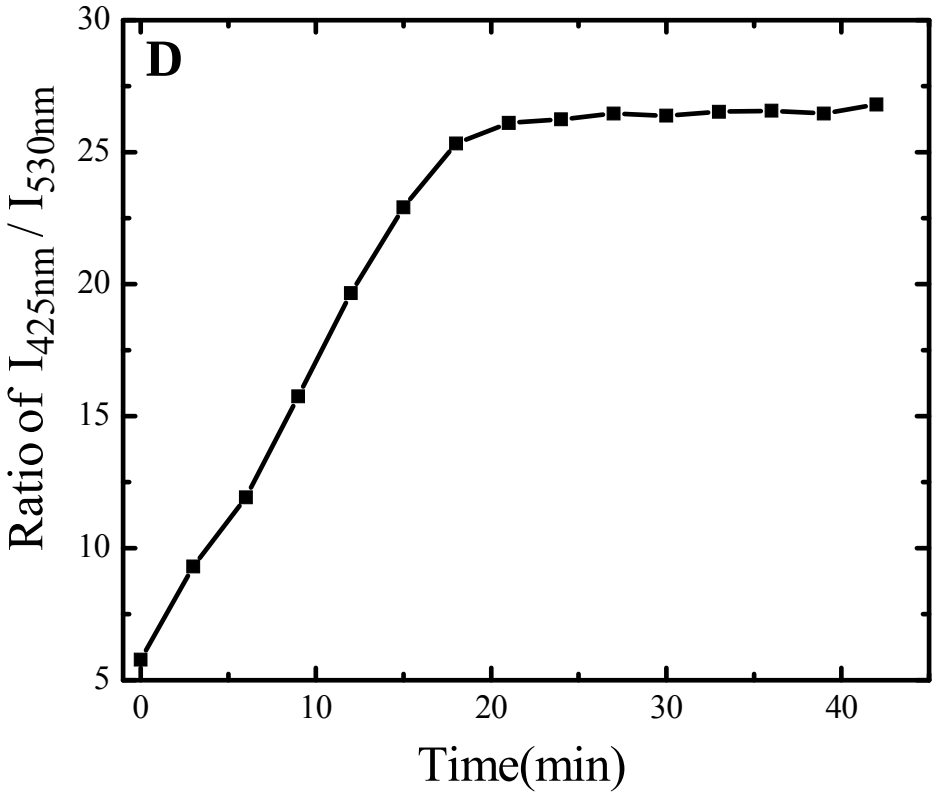

Figure 6.3: (A) Emission spectra upon addition of S1 nuclease at different time intervals. λ_{ex}= 485 nm. **(B)** Emission spectra of PFP/TO-DNA (λ_{ex}= 380 nm) and TO-DNA. (λ_{ex}= 485 nm) **(C)** Emission spectra upon addition of S1 nuclease at different time intervals. λ_{ex}= 380 nm. Inset is the emission change at 530nm. **(D)** Ratio of emission at the wavelengths 425 nm / 530 nm (I_{425nm}/I_{530nm}) versus digestion time of DNA_4 by S1 nuclease. Conditions: [TO] = $5x10^{-8}$ M, [DNA_4] = $6.75x\ 10^{-8}$M, [PFP] = 1.4μM, [S1 nuclease] = $2.62x10^{-4}$ U μL^{-1}. Measurements were conducted in 2mM CH_3COONa, 15mM NaCl, 0.1mM $ZnSO_4$, pH 4.6, 37 °C.

FRET between PFP and TO will result in simultaneous changes in the fluorescence intensity at the two wavelengths of 425 nm and 530 nm as the digestion of DNA_4 by S1 nuclease occurs. The ratio of emission intensity at 425 nm and 530 nm (I_{425nm}/I_{530nm}) is associated with the population of cleaved DNA(20) and can be studied as a function of incubation time. Figure 6.3D shows the ratio of I_{425nm}/I_{530nm} increase as the cleavages of DNA4 occurs and reach a plateau after 24 minutes,

indicating that the digestion of DNA_4 is nearly completed. The initial digestion rate can be measured from the gradient of the linear portion of the time curve, and can then be used to determine enzyme activity in the cleavage reaction.

Compared to the use of TO as the direct reporter to assay S1 nuclease cleavage of ssDNA, the advantages of using conjugated polymer PFP for the nuclease assay are obvious. First, the emission of TO at 530nm is enhanced, giving an improved detection sensitivity during the cleavage process. Second, it provides us with a ratiometric way to assay the cleavage reaction using emission ratios (I_{425nm}/I_{530nm}) instead of only monitoring the drop in fluorescence intensity of TO during the cleavage reaction. The assay involves FRET between PFP and TO. Thus, intervening solvents or any macromolecules would have less effect on the energy transfer efficiency, which depends primarily on PFP-TO distance.

6.3.4 Optimization of the experimental conditions

6.3.4.1 Optimizing zinc ion concentration

To obtain the optimum condition for this assay, the effect of Zn^{2+} concentration has been investigated. Zn^{2+} is an important coenzyme for S1 nuclease activity and its concentration may affect the rate of the cleavage reaction (27). Figure 6.4A shows the emission ratio I_{425nm}/I_{530nm} at each Zn^{2+} concentration. Then the initial digestion rate at each Zn^{2+} concentration is calculated from the rate of change of I_{425nm}/I_{530nm} at the first three minute portion of the I_{425nm}/I_{530nm} plot and the initial digestion rate against different Zn^{2+} concentrations is shown in Figure 6.4B. From Figure 6.4B, the initial

rate of DNA_4 cleavage was at the maximum at the Zn^{2+} concentration of 1.0 mM and then declined as the concentration of Zn^{2+} increases. No enzyme activity was observed when the concentration of Zn^{2+} was zero, as indicated by the observation that the emission ratio I_{425nm}/I_{530nm} remained almost constant. Therefore, 1.0 mM of Zn^{2+} was used for the buffer solution for S1 nuclease reaction hereafter.

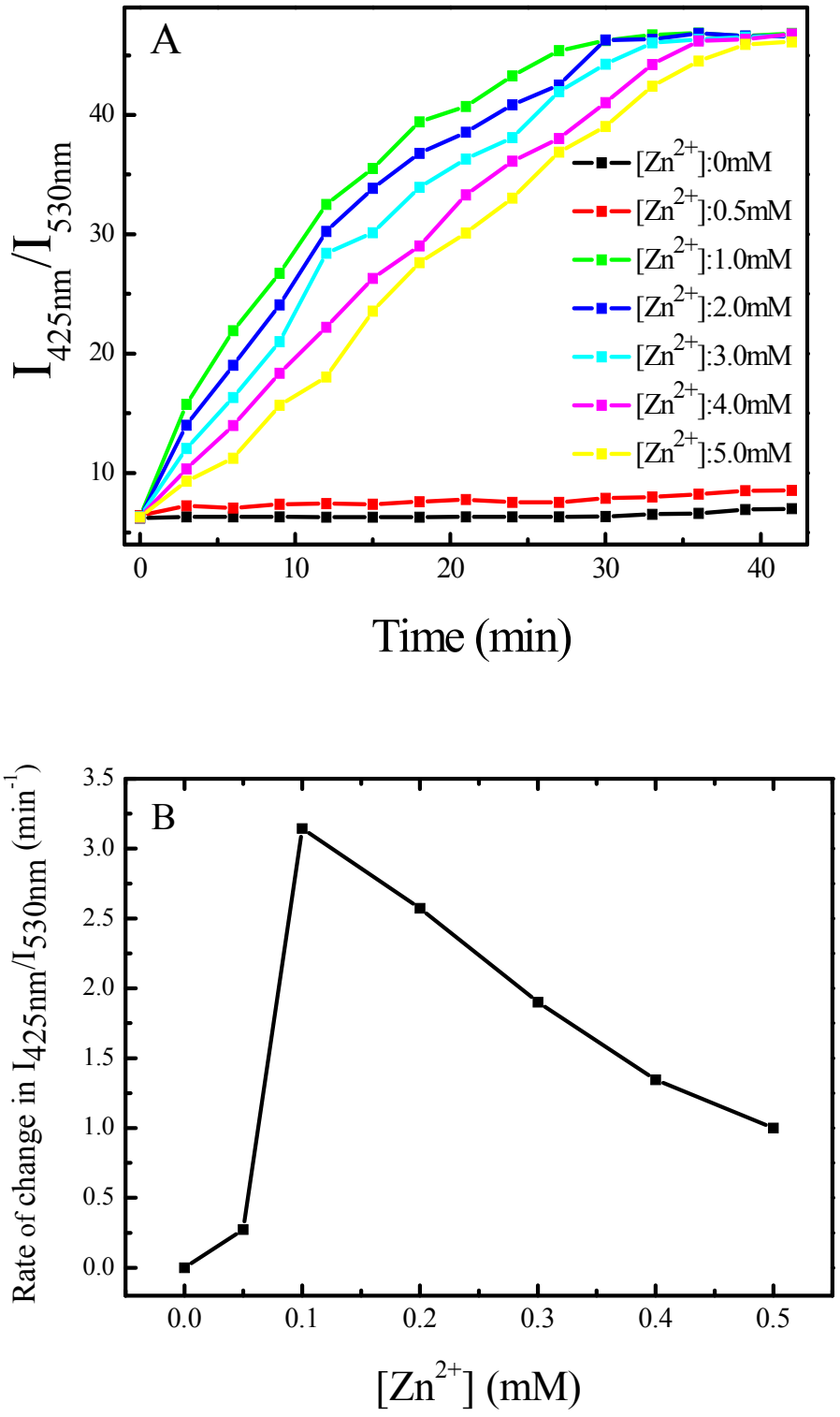

Figure 6.4: (A) Ratio of emission intensity at the wavelength 425nm/530 nm at different zinc concentration at regular time interval. **(B)** Initial rate at different Zn^{2+} concentrations. Conditions: [TO] = $5x10^{-8}$ M, [DNA_4] = $6.75x10^{-8}$ M, [PFP] = 1.4 µM, [S1 nuclease] = $2X10^{-3}$ U μL^{-1}. Measurements were conducted in 2mM CH_3COONa, 15mM NaCl, pH = 4.6, T = 37°C.

6.3.4.2 Varying the S1 nuclease concentration

To demonstrate the applicability of PFP/TO-DNA complex in monitoring the nuclease activity, the ratio of emission at 425 nm and 530 nm (I_{425nm}/I_{530nm}) as a function of nuclease concentration were studied. Figure 6.5A shows the time curves of DNA_4 digestion reactions at a fixed concentration of TO-DNA_4 with various S1 nuclease concentrations ranging from 0.262 mU/μL to 2.00 mU/μL. It is found that the ratio values do not change any more after 33 minutes, which indicates that the digestion of DNA_4 is nearly completed.

Increasing the amount of S1 nuclease gives rise to faster initial cleavage rate, which is expected since greater concentration of S1 nuclease cleaves DNA_4 more rapidly. The initial cleavage rate at each S1 nuclease concentration is calculated from the rate of change of emission ratio at 425 nm and 530 nm (I_{425nm}/I_{530nm}) for the first three minutes of the cleavage reaction. Figure 6.5B shows initial rate against S1 nuclease concentration. There is a good linear relationship (R^2= 0.9461) between initial digestion rate and enzyme concentration. Reaction rate increases with increasing enzyme concentration and can be monitored in real time. This indicates that the cleavage reaction is 1st order with respect to S1 nuclease concentration, which is consistent for the general model for enzyme-catalyzed reaction (28).

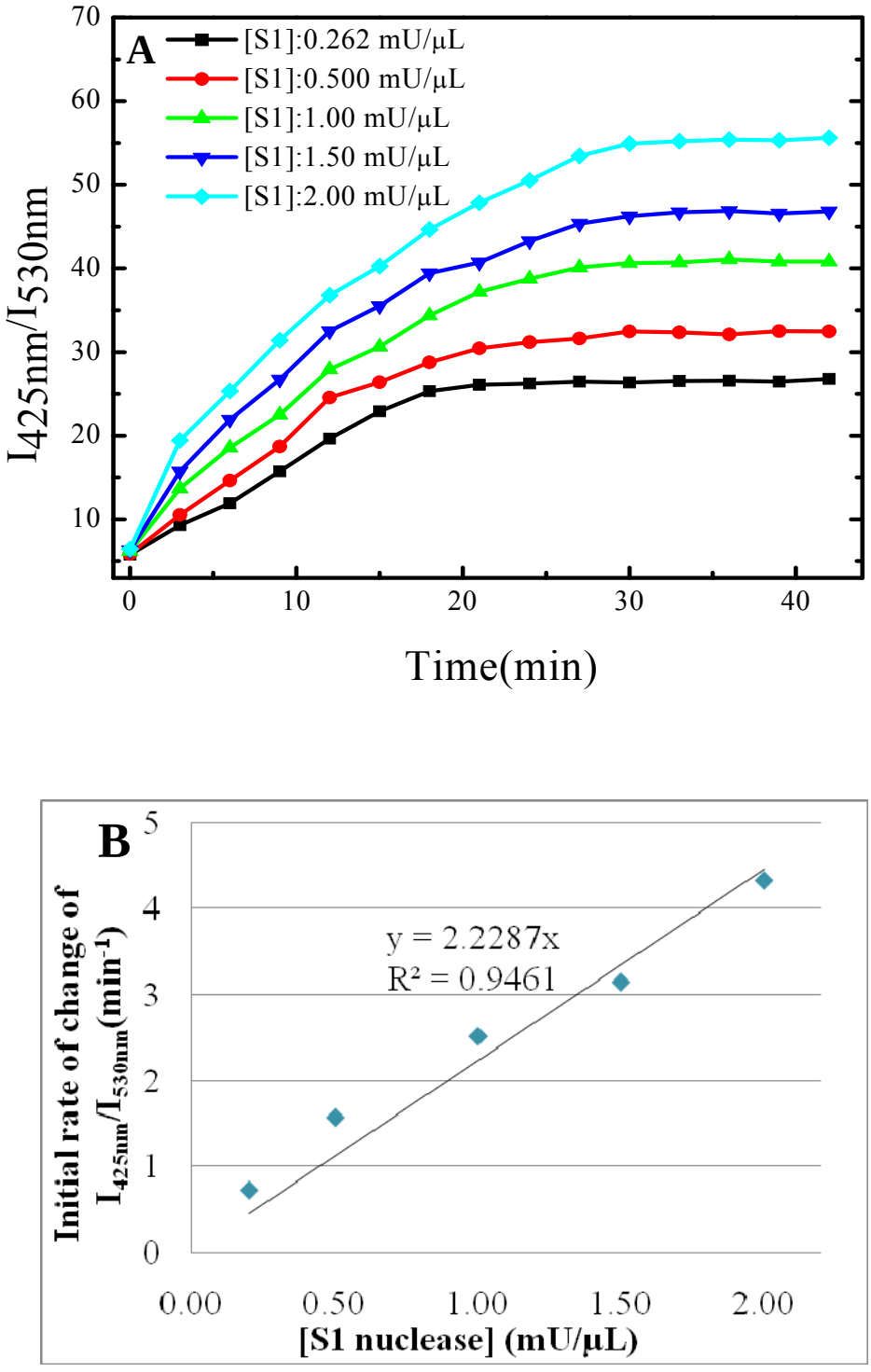

Figure 6.5: (A) Ratio of emission intensity at the wavelength 425nm/530 nm at different S1 nuclease concentrations. **(B)** Initial rate at different S1 nuclease concentrations. Conditions: [TO] = $5*10^{-8}$ M, [DNA_4]= $6.75*10^{-8}$M, [PFP]= 1.4µM. Measurements were conducted in 2 mM CH_3COONa, 15 mM NaCl, 0.1 mM $ZnSO_4$, pH 4.6, 37°C.

6.4 Conclusion

In conclusion, we have demonstrated a label-free method for the detection of S1 nuclease cleavage of single-stranded DNA based on CPs/DNA/intercalating dye system. This assay method relies on the optical amplification properties via efficient FRET from the conjugated polymer PFP to the DNA intercalating dye TO. Compared with the previous reports where DNA substrate needs to be labeled with the fluorophores, our assay technique is simple and convenient. It provides a "mix-and-detect" protocol that allows for homogeneous and rapid detection. Most importantly, as compared to the use of TO as direct reporter for the nuclease assay, the simultaneous changes in the fluorescence intensity of PFP and TO offers a ratiometric fluorescence measurements of the cleavage reaction, which is more accurate and can reduce any external nonspecific events. We expect that this assay strategy will have important applications in many fields such as drug discovery, DNA genomics and the study of biological processes.

6.5 References

1. Gite, S. U. & Shankar, V. (1995) *Critical Reviews in Microbiology* **21**, 101-122.
2. Roberts, R. J. (1990) *Nucleic Acids Research* **18**, 2331-2365.
3. Ma, M., Benimetskaya, L., Lebedeva, I., Dignam, J., Takle, G. & Stein, C. A. (2000) *Nature Biotechnology* **18**, 58-61.
4. Alves, J., Ruter, T., Geiger, R., Fliess, A., Maass, G. & Pingoud, A. (1989) *Biochemistry* **28**, 2678-2684.
5. Jeltsch, A., Fritz, A., Alves, J., Wolfes, H. & Pingoud, A. (1993) *Analytical Biochemistry* **213**, 234-240.
6. McLaughlin, L. W., Benseler, F., Graeser, E., Piel, N. & Scholtissek, S. (1987) *Biochemistry* **26**, 7238-7245.
7. Li, J. J., Geyer, R. & H., T. W. (2002) *Nucleic Acids Research* **28**, e52.
8. Biggins, J. B., Prudent, J. R., Marshall, D. J., Ruppen, M. & Thorson, J. S. (2000) *Proceedings of the National Academy of Sciences of the United States of America* **97**, 13537-13542.
9. Takakusa, H., Kikuchi, K., Urano, Y., Kojima, H. & Nagano, T. (2003) *Chemistry-a European Journal* **9**, 1479-1485.
10. Lakowicz, J. R. (2006) *Principles of Fluorescence Spectroscopy* (Springer-Verlag Berlin Heidelberg.)
11. Liu, Y., Ogawa, K. & Schanze, K. S. (2009) *Journal of Photochemistry and Photobiology C-Photochemistry Reviews* **10**, 173-190.

12. Thomas, S. W., Joly, G. D. & Swager, T. M. (2007) *Chemical Reviews* **107**, 1339-1386.

13. Liu, B. & Bazan, G. C. (2007) *Macromolecular Rapid Communications* **28**, 1804-1808.

14. Achyuthan, K. E., Bergstedt, T. S., Chen, L., Jones, R. M., Kumaraswamy, S., Kushon, S. A., Ley, K. D., Lu, L., McBranch, D., Mukundan, H., Rininsland, F., Shi, X., Xia, W. & Whitten, D. G. (2005) *Journal of Materials Chemistry* **15**, 2648-2656.

15. Gaylord, B. S., Heeger, A. J. & Bazan, G. C. (2003) *Journal of the American Chemical Society* **125**, 896-900.

16. Ho, H. A., Dore, K., Boissinot, M., Bergeron, M. G., Tanguay, R. M., Boudreau, D. & Leclerc, M. (2005) *Journal of the American Chemical Society* **127**, 12673-12676.

17. Kumaraswamy, S., Bergstedt, T., Shi, X. B., Rininsland, F., Kushon, S., Xia, W. S., Ley, K., Achyuthan, K., McBranch, D. & Whitten, D. (2004) *Proceedings of the National Academy of Sciences of the United States of America* **101**, 7511-7515.

18. Pinto, M. R. & Schanze, K. S. (2004) *Proceedings of the National Academy of Sciences of the United States of America* **101**, 7505-7510.

19. Wang, D. L., Gong, X., Heeger, P. S., Rininsland, F., Bazan, G. C. & Heeger, A. J. (2002) *Proceedings of the National Academy of Sciences of the United States of America* **99**, 49-53.

20. Feng, F. D., Tang, Y. L., He, F., Yu, M. H., Duan, X. R., Wang, S., Li, Y. H. & Zhu, D. B. (2007) *Advanced Materials* **19**, 3490-3495.

21. Tang, Y. L., Feng, F. D., He, F., Wang, S., Li, Y. L. & Zhu, D. B. (2006) *Journal of the American Chemical Society* **128**, 14972-14976.

22. Nygren, J., Svanvik, N. & Kubista, M. (1998) *Biopolymers* **46**, 39-51.

23. Biver, T., Boggioni, A., Secco, F., Turriani, E., Venturini, M. & Yarnaoluk, S. (2007) *Archives of Biochemistry and Biophysics* **465**, 90-100.

24. Beard, P., Morrow, J. F. & Berg, P. (1973) *Journal of Virology* **12**, 1303-1313.

25. Harada, F. & Dahlberg, J. E. (1975) *Nucleic Acids Research* **2**, 865-871.

26. Oleson, A. E. & Sasakuma, M. (1980) *Archives of Biochemistry and Biophysics* **204**, 361-370.

27. Desai, N. A. & Shankar, V. (2003) *Fems Microbiology Reviews* **26**, 457-491.

28. Lehninger, A. L., Nelson, D. L. & Cox, M. M. (2005) *Lehninger principles of biochemistry* (W. H. Freeman.)

Chapter 7

Conclusion and Outlook

Conjugated polymers are characterized by a backbone with a delocalized electronic structure and known to provide an advantage of collective optical response. The electronic structure of the CPs can coordinates the action of a large number of absorbing units compared to small molecule counterparts. The excitation energy can migrate along the whole polymer backbone and transferring to a lower energy acceptor over long distance and results in an amplified fluorescent signals. CPs are also known to have large two-photon absorption cross sections compared to the small molecule counterpart. We have investigated enhanced two-photon excitation fluorescence of DNA intercalator by fluorescence resonance energy transfer using two different conjugated polymers. CPs can be utilized to act as a two-photon excitation light harvesting complex and transfer the harvested energy to the drug molecules, which can significantly enhance the drug efficiency in two-photon excitation phototherapy.

CPs can be used as the optical platforms to develop highly sensitive chemical and biological sensors. By using CPs and a DNA intercalator, a scheme for label free DNA sequence detection was introduced in this thesis. The detection sensitivity could be significantly improved through FRET from CPs, taking advantage of its optical

amplification effects. And the selectivity has also been significantly improved. The single nucleotide mismatch detection can be detected even at the room temperature. Here we also present a practical scheme for highly sensitive and selective detection of mercury ions by using a combination of oligonucleotides, DNA intercalator dye and CPs. The limit of detection is sub-nM using this method. Our scheme could also be used as a two-photon sensor for detection of mercury ions deep into the biological environments with high sensitivity.

We have also developed a label free method using a water soluble polythiophene derivative PMNT to visualize the conformational switch of i-motif DNA driven by the environmental pH change. The DNA conformational switch was companied by a color change, which can be directly visualized by naked eyes. Our scheme has many advantages compared with the DNA based nanodevices driven by DNA/RNA strands, acids/bases, enzymes and light. This i-DNA/PMNT complex could act as an environmentally friendly optical switch with a fast response.

Traditional methods for S1 nuclease assay have many drawbacks such as being time-consuming, laborious and require substrate to be labeled. here we demonstrated a label-free method for the S1 nuclease cleavage of single-stranded DNA based on CPs/DNA/intercalating dye system based on FRET. This method overcomes the limitation of the traditional methods. S1 nuclease assay based on FRET technique can provide us with a ratiometric fluorescence approach.

In conclusion, different schemes have been proposed in this work to detect

DNA, mercury ions, DNA conformational change and S1 nuclease using conjugated polymers. The CPs can form complexes with oppositely charged molecules through electrostatic interactions. These methods are label free, low cost and simple. All the detections are highly sensitive by taking advantage of the optical amplification property of conjugated polymers.

CPs have been widely used as optical platform for detection of chemical and biological species over the past decades. In the future, the application of CPs could be extended to the fluorescence imaging in vivo and in cell level, disease diagnostics and be incorporated into the characterization protocols in molecular biology laboratories. CPs could also be used on solid matrixes, such as chips, microgels or silica particles to meet the requirement for high throughput assay.